Kobe University Repository : Kernel

PDF issue: 2024-12-30

Study on Combustion and Exhaust Gas Emissions of Jatropha Oil Emulsion Fueled Diesel Engine

NGUYEN KIM BAO

(Degree)
博士（工学）

(Date of Degree)
2015-03-25

(Date of Publication)
2016-03-01

(Resource Type)
doctoral thesis

(Report Number)
甲第6338号

(URL)
https://hdl.handle.net/20.500.14094/D1006338

※ 当コンテンツは神戸大学の学術成果です。無断複製・不正使用等を禁じます。著作権法で認められている範囲内で、適切にご利用ください。

Doctoral Dissertation

Study on Combustion and Exhaust Gas Emissions of Jatropha Oil Emulsion Fueled Diesel Engine

(ジャトロファ油エマルジョン燃料を用いた
ディーゼルエンジンの燃焼と排ガス性能に関する研究)

January, 2015

Graduate School of Maritime Sciences
Kobe University

NGUYEN KIM BAO

Acknowledgements

This research would not be completed without the blessing of my previous generations, I pray to them for giving me health during study in here. First of all, I would like to express my deep gratitude to my supervisor, Professor Tomohisa DAN, who always take care, provide me suggestion and guidance, and support me in academic activities and daily life as well!

I would like to thank some professors who taught me in here including Prof. Katsuya FUKUDA, Prof. QiuSheng LIU, Prof. Hirotsugu FUJITA, Prof. Shigeaki SHIOTANI, and Prof. Makoto UCHIDA. Moreover, I would like to thank all staffs at Student and Academic section office, and KALCS, especially Ms. NAKAO, and Mr. Don who have been kindly supported me since enrollment, and English proof reading for paper publication, respectively.

Special thanks for Vietnam Government and the Staffs at there who support me financial for 3 years when I have been studied at Kobe University. It is my pleasure to thank to my lecturer, Dr. Tran Hong Ha who recommended me to my Supervisor. I would like to express my thanks to technician, Mr. ASANO, and all my Lab-mates who helped, collaborated with me in the experiments and academic exchange! I also want to deeply thank my senior, Dr. Nguyen Ngoc Hai; my junior, Ms. Tran Thi Anh Tam, Ph.D student at Faculty of Maritime Sciences, who have academic exchanges to me during this period.

Finally, I would like to express my deep gratitude to my parents; my wife, Ms. Nguyen Thi Thu; my son, Nguyen Bao Phuc; and all my sisters, and brothers for their love, and patience!

January, 2015

Nguyen Kim Bao

Abstract

Jatropha oil was identified as a leading candidate for an alternative fuel among various non-edible vegetable oil. However, it was revealed that the combustion of Jatropha oil in diesel engine resulted in higher particulate, CO, and HC. Additionally, some operational problems such as injector coking, severe engine deposits, gum formation, and oil thickening were reported in long term test. This is resulted from the high viscosity, poor volatility, large molecular weight and bulky molecular structure of the fuel. Therefore, the combustion of Jatropha should be improved by investigation some methods.

In this study, diesel engines fueled with Jatropha based fuel were studied with double injections, or Jatropha water emulsion with double injection, or Jatropha hydrogen peroxide emulsion. The experiments were conducted on high-speed, four-stroke, direct injection diesel engines. To study effect of double injections, a common rail fuel system diesel engine modified from mechanical fuel system were used. For the Jatropha hydrogen peroxide emulsion fuel, I used a mechanical fuel system diesel engine. The modified common rail diesel engine, however, remains mechanical injector that injects fuel into the combustion chamber. The contents of the dissertation are included as follows:

Chapter 1, I present the considerations of environmental and social issues including greenhouse gases emission and global climate change; some common air pollutants; global fuel production and consumption; Fuel pricing

trend. Besides this, the fundamentals of diesel engine emissions are also introduced for briefly understanding. Furthermore, research backgrounds including information of Jatropha oil in general and literature review are given.

Chapter 2 includes research objective, theoretical considerations and infrastructure of the research. In the research objective I present briefly the purpose of each sub-study. Then, the method of calculation some parameters is described in theoretical considerations. Finally, the information of apparatus and devices using to conduct the experiments are presented in the last section.

In chapter 3, I presented the combustion, performance and emissions characteristics of diesel engine fueled with neat Jatropha oil with double injections. In this chapter, the timings of double injections in term of main-injection and after-injection were varied to verify the optimum timings of the engine fueled with neat Jatropha oil. After finding the optimum timing for double injections, I changed the injection quantity the after-injection of double injections to test the engine. The results are briefly summarized as follows.

1. Effect of double injection timings

i. Retarded double timings significantly reduced the peaks of combustion pressure, peaks of HRR, and shifted the combustion to the later phase. Late double timings increased HRR at the later combustion stage.

ii. There was slight reduction of ID for retarded double timings at low load; ID increased slightly at 6.0 kW due to imperfect gas exchange. Optimum double injection timings for BTE were between m-11,a+1.5 and m-13,a-0.5.

iii. Emissions of CO_2, CO, HC, Smoke and dust were lower at timings between m-11,a+1.5 and m-13,a-0.5. Late double timings significantly reduced emissions of NOx.

Overall, the optimum injection timings for combustion, performance, and emissions were between m-11,a+1.5 and m-13,a-0.5.

2. Effect of amount of after-injection

Timing of m-11,a+1.5 was tested with small and large amounts of after-injection. I found a considerably influence to the combustion, performance and emissions.

i. Peaks of cylinder pressure and HRR were remarkably reduced with m-11,a+1.5-L at 3.0 and 4.5 kW. Otherwise, they were comparable at 6.0 kW with a minor reduction of peak HRR with m-11,a+1.5-L.

ii. When compared with m-11,a+1.5-S, the injection pattern of m-11,a+1.5-L reduced BTE especially at higher engine loads.

iii. For m-11,a+1.5-S, reduction of emissions of CO_2, CO, smoke and dust concentration was observed, while it increased emissions of NOx, and HC.

In chapter 4, I used the Jatropha water emulsion fuel and double injections to investigate the combustion, performance, and emissions characteristics of diesel engine. Jatropha water emulsion was created by mixing 10% of water

with Jatropha. The engine was fed with LO, and JO with single injection at the injection timing set by the engine Maker of -17 deg. CA. ATDC for baseline data. To investigate the effect of injection pattern and the JWE, the first injection was kept at -23 deg. CA ATDC and the second injection was set at 0, +3, +6 deg. ATDC for double injection mode. After a preliminary investigation for the lowest smoke opacity, the optimum timing of second injection was chosen to conduct experiments for measurement of dust, soluble and in-soluble organic fraction with different injection quantities in the second injection (hereafter called small and large). The main results are summarized as follows:

1- Large amount of fuel in the second injection in injection patterns such as JWE-23/0 and JWE-23/+3-large dramatically reduced the peaks of in-cylinder pressure; suddenly reduced the peak of HRR; and increased significantly the ignition delay, combustion duration, and shifted the combustion center toward the later stage. For small amount of fuel in the second injection such as JWE-23/+3-small and JWE-23/+6, the peaks of the in-cylinder pressures were higher, while, other parameters had the same tendency with lower intensity when compared with those of the LO.

2- Large amount of fuel in the second injection dramatically reduced the in-cylinder temperatures, increased the exhaust gas temperatures, and lowered the BTE in comparison with those of the JO. The opposite occurred when small second injection amount was used as in JWE-23/+3-small and

JWE-23/+6. I also found that when using the JWE-23/+3-small the BTE was higher than that of the JO.

3- The emulsion fuel and double injection increased CO_2, CO, and HC emissions when compared with those of the LO. However, in comparison with those of the JO, the large second injection quantity such as the JWE-23/+3-large reduced the HC emissions. NOx emissions were related to the combustion characteristics of the engine with different injection patterns. The emulsion fuel, and double injection patterns reduced NOx emissions when compared with those of the LO. Large second injection amount such as the JWE-23/0 and JWE-23/+3-large significantly reduced the NOx emissions.

4- In three timing tests, the JWE-26/+3 reduced smoke opacity when using JWE and double injection. The ISF was the main element, while the SOF was a minor element of the dust. Large second injection amount increased the ISF and dust concentration much more than a small second injection amount.

In chapter 5, combustion, performance, and emisions of a direct injection diesel engine fueled with Jatropha hydrogen peroxide emulsion was investigated. To make this investigation, a diesel engine with mechanical fuel injection system was used to supply Jatropha hydrogen peroxide emulsion to the combustion chamber of the engine. Hydrogen peroxide in a solution of water at a concentration of 30% was used for making the emulsions. Mixtures of Jatropha oil with solutions of hydrogen peroxide

were created according to the Jatropha oil mass with mixing ratios of 5%, 10% and 15% (hereafter so-called JHE5%, JHE10%, and JHE15%). The experimental results are featured following:

1- The engine has operated experimentally on the Jatropha hydrogen peroxide emulsion up to the 15% mixing ratio. The combustion of the emulsified fuels shifted to the earlier stage and extended to the later stage. The peak of the heat release rate was reduced with emulsified fuels and there was a large magnitude of oscillation in the heat release rate in the diffusion combustion phase. The heat release rate in the late combustion stage for the emulsified fuels was higher than those of the Jatropha oil and light oil, and the cumulative heat release for the emulsified fuel was also higher.

2- In-cylinder and exhaust gas temperatures were higher especially for the JHE5% and JHE15% as compared to those of the Jatropha and light oil. The JHE15% improved brake thermal efficiency of the engine in most cases as compared to other emulsion fuels and Jatropha oil.

3- The JHE5% and JHE15% reduced CO_2 and NOx emissions, while, they also reduced CO emissions at low and medium loads. The emulsion fuels increased HC emissions. At medium and high power conditions, dust and ISF concentration were significantly reduced by the emulsion fuel, especially for the JHE10% and JHE15%. Overall, this study found that the optimum mixing ratio of hydrogen peroxide to improve combustion, performance and emissions in diesel engine was 15%.

Chapter 6, conclusions summary of the results of the study. It contains the main method, procedures, and results of each sub-study in each chapter.

Table of Contents

List of Figures

List of Abbreviations and symbols

ATDC	Crank angle after top dead center
BTE	Brake thermal efficiency
C (s)	Solid carbon
CFCs	Chlorofluorocarbons
CH_4	Methane
CO	Carbon monoxide
CO_2	Carbon dioxides
CxHy	Hydrocarbon
d	diameter of orifice
ECU	Electronic control unit
EOC	End of combustion
EPA	Environmental Protection Agency
GHGs	Greenhouse gases
H	Monatomic Hydrogen
H_2O	Water molecule
H_2O_2	Hydrogen peroxide
HC	Unburned hydrocarbon
HCFCs	Hydrochlorofluorocarbons
HFCs	Hydrofluorocarbons
HR	Net cumulative heat release
HRR	Heat release rate
ID	Ignition delay
IQ	Intelligence quotient
ISF	In-soluble organic fraction
JHE	Jatropha hydrogen peroxide emulsion
JO	Jatropha oil

JWE	Jatropha water emulsion
LO	Light oil
N	Monatomic Nitrogen
N_2	Atomic Nitrogen
N_2O	Nitrous oxide
NO	Nitric oxide
NO_2	Nitrogen dioxide
NOx	Nitrogen oxides
Ø	Air-fuel ratio, relative humidity
O	Monatomic Oxygen
O_2	Oxygen
O_3	Ozone
OH	Hydroxyl radical
OPEC	Organization of the Petroleum Exporting Countries
Pb	Lead
PC	Personal computer
PFCs	Perfluorocarbons
PM	Particulate matter
ppmv	volume part per million
SF_6	sulfur hexafluoride
SO_2	Sulfur dioxide
SOF	Soluble organic fraction
SOx	Sulfur oxides
TDC	Top dead center
VOC	Volatile organic compounds
dQ_{ht}/dt	Rate heat transfer to the wall
dQ_{ch}/dt	Gross heat release
dQ_n/dt	Net heat release rate

$\dot{m}_i$	Mass flow rate at location *i*
h_i	Enthalpy of flux *i*
D_t	Diameter of charge tube on surge air tank
G_F	Fuel flow rate
G_a	Intake air flow rate
$G_{exhaust}$	Exhaust gas flow rate
H_a	Absolute humidity of air
N_e	Engine power
P_0	Atmospheric pressure
P_a	Saturate vapor pressure
P_b	Atmospheric pressure
R_a	Relative humidity of air
T_a	Temperature of air
dQ/dt	Heat transfer rate
$p(dV/dt)$	Rate of work transfer
t_0	Ambient air temperature
c_p	Specific heat (constant pressure)
c_v	Specific heat (constant volume)
γ_1	Density of air before orifice
ΔP	Pressure difference between orifice
F	Saturate vapor pressure
$GASx$	Exhaust gas emission
R	Constant
T	Temperature
U	Constant factor, Energy of the system
V	Volume
$conc$	Concentration of exhaust gas

m	Mass
m-11,a+1.5	Main-injection at 11 degree crank angle before top dead center, afte-injection at 1.5 degree after top dead center (other injection patterns are similar with this denotation)
m-11,a+1.5-S	Main injection at 11 degree crank angle before top dead center, after injection at 1.5 degree after top dead center with small after-injection amount
m-11,a+1.5-L	Main injection at 11 degree crank angle before top dead center, after injection at 1.5 degree after top dead center with large after-injection amount
p	Pressure
α	Flow rate coefficient
γ	Ratio of specific heats
ξ	Adjustment coefficient of compressed air
t	room air temperature

Chapter 1 Introduction

1. 1 Environmental and social considerations

Transportation plays important role in human activity which enhances development of commercial, tourist, and economy between nations, areas all over the world. Besides sea and airlines transport, the road traffic is a major factor contribute to global warming due to greenhouse gas which emits whenever using internal combustion engines. Even greenhouse gas from sea transport is lower than others due to its energy effective form of transport. However, sea transport has been facing this problem when global warming is becoming more urgent. Moreover, the avoidable harmful emissions of the fossil fuel using diesel engines such as NOx, SOx, and particulate which can lead to serious environmental and health issues.

Use of biofuels can reduce these emissions, but the combustion of carbon-based material such as biofuels will always lead to some level of emissions. For instance, the reactant for fuel combustion is air, which consists of 79 % Nitrogen and 21 % Oxygen, leading to NOx-emissions from combustion.

A number of very complicated reactions and the products formed in combustion depend on many factors. The quality of the fuel-air mixture forming in the combustion chamber can regulate the reactions occurring with fuel burning. Ideally, for completed combustion, there is no carbon monoxide (CO) or

unburned-hydrocarbons (HC), unfortunately this increase NOx emissions which is strongly influenced by the combustion temperature.

1. 1. 1 Greenhouse gas and the change of global climate

1. 1. 1. 1 Emissions of greenhouse gas

Greenhouse gases

Greenhouse gases (GHGs) are gaseous in the atmosphere originating naturally or due to the human activity those absorb and emit infrared radiation emitting from surface of the earth, clouds, and the atmosphere [1]. Primary greenhouse gases in the atmosphere include carbon dioxide (CO_2), water vapor (H_2O), nitrous oxide (N_2O), methane (CH_4), and ozone (O_3). Besides these, hydrofluorocarbons (HFCs), perfluorocarbons (PFCs), and sulfur hexafluoride (SF6) were considered as greenhouse gases by the Kyoto Protocol.

Global GHG emissions by gas

The main GHGs including CO_2, CH_4, N_2O, and some others directly originate from human's activity. Figure 1-1 shows the component of global GHG emissions by gas**.**

Carbon dioxide (CO_2)

CO is the principal greenhouse gas contributing to recent change of climate. It is a partial carbon-cycle naturally absorbed and released through the respiration of animal and plant, the exchange of ocean and atmosphere, and volcanic eruptions. Burning of fossil fuels and changes in land use, especially involves deforestation, are human activities those release large amounts of CO_2

to the atmosphere raising its concentrations. However, CO_2 can be removed from the atmosphere by reforestation, and other activities [3].

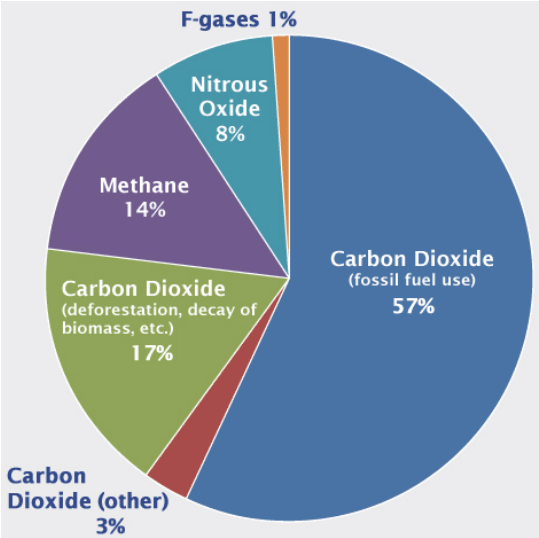

Figure 1-1 Global greenhouse gas emissions [2]

In the distant past, large amounts of CO_2 emitted from volcanic eruptions. However, each year, over 30 billion tons of CO_2 are being released by human activities those are more than 135 times as much CO_2 as volcanoes, the United States Geological Survey reported. Figure 1-2 indicates that the concentration of CO_2 in the atmospheric has increased almost 40% from approximately 280 ppmv since pre-industrial times to 390 ppmv in 2010.

Sources of CO_2 emission comes from: **electricity** generated by the combustion of fossil fuels; **transportation** by the combustion of diesel and gasoline to transport passengers and goods; and **industry** through combustion such as the

production of metals or chemical reactions that do not involve combustion as production of cement, and chemicals [4].

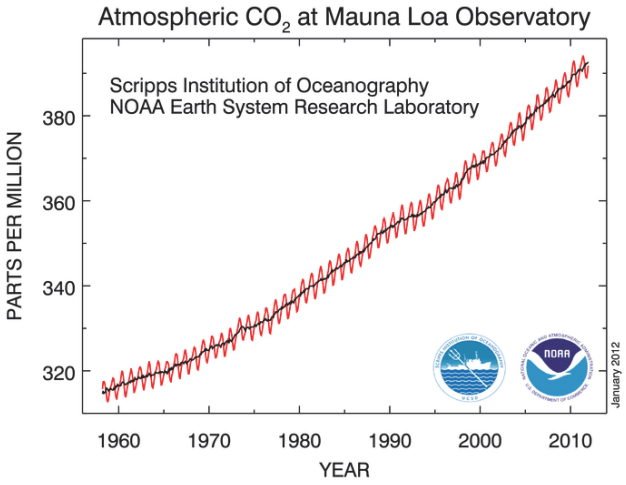

Figure 1-2 Carbon dioxide concentration has risen from 1958 to 2010 [3]

Methane (CH_4)

Methane (CH_4) is classified as the second grade of the most prevalent GHG releasing by human. It is naturally produced or due to the activities of human including agricultural activities, natural wetlands, and the extraction or transportation of fossil fuel. Globally, human activities release over 60% of total emission of CH_4 [5]. During most of the 20th century, the concentrations of CH_4 sharply increased as a result of human activities. Now, they are more than two-and- half times higher when compared to the levels in pre-industrial period. Recently, theirs increment considerably have slowed [3]. In the atmosphere, the lifetime of CH_4 is much shorter than that of CO_2, while methane trapes radiation more efficiently than CO_2. Over a period of 100-year,

the influence of CH_4 on climate change was reported over 20 times higher than CO_2. Methane is released from in some sources: (***i***) **industry** such as processing, production, storage, transmission, and distribution process of ***natural gas*** and ***petroleum*** releasing the largest source of CH_4 emissions; (***ii***) **agriculture** through the digestive process of animals and their manure storage; ***(iii***) **waste** by the decomposition of the waste in landfills and the treatment of wastewater. Moreover, it comes from natural sources such as decomposition of organic materials in the absence of oxygen wetlands, wildfires, volcanoes, oceans [5].

Nitrous oxide (N_2O)

Nitrous oxide is mainly generated by agricultural and biological activities. Besides, N_2O is also produced by burning the fuel and other processes. Since the end of the 20th century, N_2O concentrations have rapidly increased [3]. In the atmosphere, nitrous oxide remains around 120 years before being destroyed or removed. On the mass unit, 300 times is effect of N_2O on global warming over carbon dioxide. Globally, human activities approximately result in 40% total N_2O emissions [5]. The sources emitting nitrous oxide including: ***(i)*** **agriculture** when using synthetic fertilizers or releasing from animal's urine and manure); ***(ii)*** **transportation** when fuel burning in engine-driven-vehicles; and ***(iii)*** **industry** to make fibers such as nylon and other synthetic products, or synthetic fertilizer when nitric/adipic acids are necessary[6].

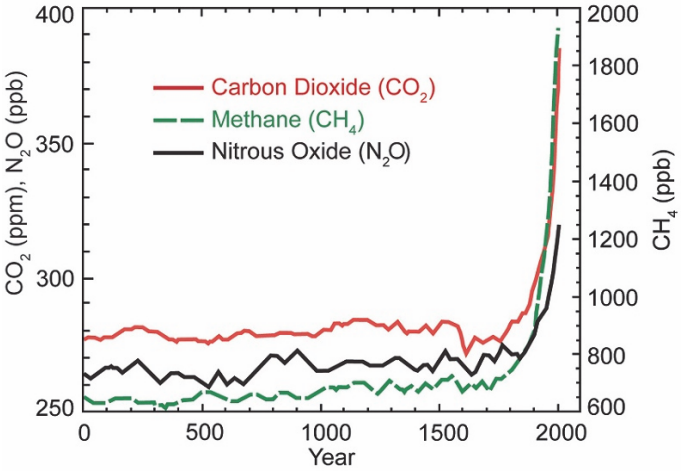

Figure 1-3 Atmosphere GHG concentrations over 2000 years [3]

Fig. 1-3 shows the change of three main GHGs over 2000-year period.

Other Greenhouse Gases

There are some other GHG rather than main GHG listed above, they are [3]:

- Vapor of water is one plentiful GHG and also has large contribution to the natural greenhouse effect in spite of its short lifetime in the atmosphere. Global water vapor concentration is controlled by temperature which affect to the evaporation and condensation rates. Thus, the water vapor concentration is not significantly resulted from direct emissions of human.
- Ozone (O_3) is a formidable GHG despite its short lifetime it the atmosphere. Ozone is resulted from chemical reactions due to the emissions of nitrogen oxides and volatile organic compounds exhausted from power plants, automobiles, and other industrial or commercial sources under the sunlight.
- F-gases consist of chlorofluorocarbons (CFCs), hydrochlorofluorocarbons (HCFCs), hydrofluorocarbons (HFCs), perfluorocarbons (PFCs), and sulfur

hexafluoride (SF6) those using in foaming agents, coolants, solvents, fire extinguishers, aerosol propellants, and pesticides. Unlike O_3 and water vapor, these F-gases will affect the climate for many decades due to theirs long lifetime in the atmosphere.

Global GHG emissions by source

Economic activities can lead to the production of global GHG emissions. Figure 1-4 shows the component of global GHG emissions by source.

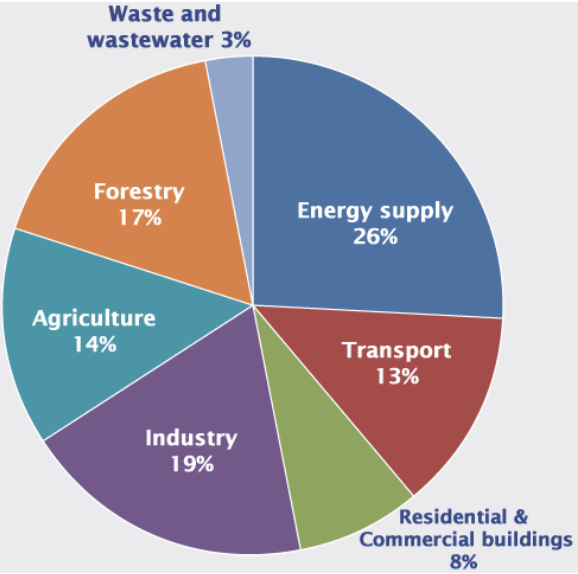

Figure 1-4 Emissions of global GHG by source [2]

By energy supply (26%) – the largest single source of global GHG emissions is resulted from burning of fossil fuels such as coal, oil, and natural gas for electricity and heating.

From industry (19%) – fossil fuel burning for energy at industrial facilities primarily produces GHG emissions. Besides, industrial processes in metallurgical, chemical, and mineral transformation also create GHG.

By land use and change, and forestry (17%) – GHG in this sector primarily comprise CO_2 releasing from agricultural land clearing, deforestation, and peat soils firing or decay. CO_2 removal by ecosystems from the atmosphere is not included in this estimate.

From agriculture (14%) – GHG in this sector mostly comes from the production of livestock, and rice; burning biomass; and the agricultural soils management.

By transportation (13%) – GHG released from burning fossil fuels for mean transportation such as rail, road, marine, and air. Globally, almost energy for transportation (95%) largely generated by burning petroleum such as diesel oil and gasoline.

From commercial and residential buildings (8%) – GHG from buildings resulted from generation of energy and burning fuels for heating or cooking.

From waste and wastewater (3%) – this sector, methane released from landfill is the largest GHG source, followed by methane generated by wastewater and nitrous oxide. The burning of waste products such as synthetic textiles and plastics with fossil fuels also create minor CO_2.

GHG emissions estimated by country

China, the United States, the European Union, India, the Russian Federation, Japan, and Canada were the top countries releasing carbon dioxide. These include emissions of CO_2 due to burning fossil fuel, cement production, as well

as gas flaring. Fig. 1-5 shows the component of the global emission of CO_2 by country.

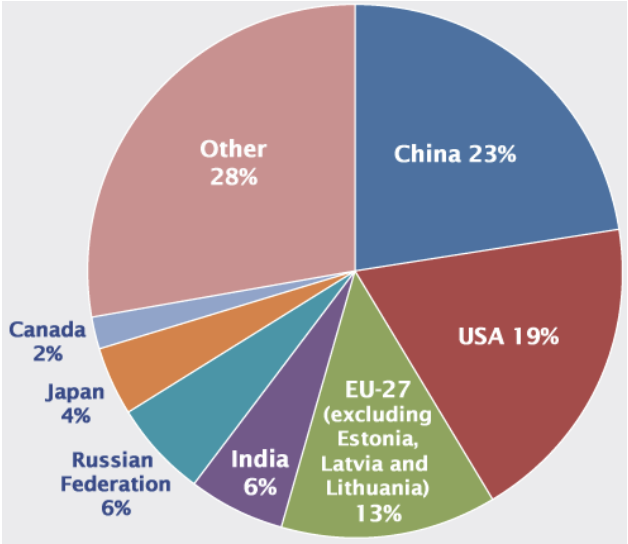

Figure 1-5 Global CO_2 emissions from fossil fuels burning and industry [2]

Consequences of global warming

Greenhouse gases have been leading to global warming. According to the National Oceanic and Atmospheric Administration of the U.S., the warmest global surface temperatures were recorded in 2005. During the 21st century, the earth temperature could additionally raise by 7.2 ^oF if we do not mitigate emissions from burning oil and coal. The rise of temperature will leading to the effects on climate change and on all living. The effect of the global warming can list down following:

(i) Weather patterns

- **More dangerous and powerful typhoon:** stronger and more harmful tropical storms can be resulted from more energy supplied by warmer ocean

water. Even with the same intensity, but the prospective storms will damage more seriously with higher sea level making flood, and erosion [7].

- **Wildfire and drought:** higher temperatures can raise drought probability. Drought conditions become worse when greater evaporation with higher temperatures, especially in summer and autumn, increasing the danger of wildfires [7].
- **Intense rainstorms:** some areas, heavier rainfall can be resulted due to **w**armer temperatures climate. Many communities will be putted at risk for severe damage from floods when heavy rainstorms frequently appear when climate change [7].

(ii) Health

- **Deadly heat waves:** it is said that, a larger number of deaths related to more frequent and severe heat waves would be. In 2003, 70000 European lives were claimed by extreme heat waves. Nearly 15000 French people died in two weeks due to soaring temperatures up to 104 ^{o}F. In July 2006, there were over 140 deaths in North America even who owned air conditioners due to the severe heat wave. In 1995, heat wave in Chicago induced 739 deaths in one week [8].
- **Bad air, allergy and asthma:** asthma and pollen allergies would be intensified due to an increase in smog pollution resulted from global warming. Over 100 million Americans were affected by worse local air quality owing to hotter conditions. Asthma and allergies and would become worse with the

growth of ragweed pollen as a result of higher level of carbon dioxide. Globally, the number of people suffering from asthma and pollen allergy has increased since some last decades. Pollen can interact with exhaust particles released from diesel engines, and consequently they can be deeply delivered into the lung. Ozone smog at the ground level increases with an increase in temperatures potentially threatening the asthmatics [8].

- **Food, infectious disease, and waterborne illness outbreaks:** outbreaks of infections like dengue fever, malaria, encephalitis, and diarrheal illnesses have been resulted from the disruption of ecosystem, the elevating temperatures, and the alternating drought and flood periods [8].
- **Dangerous weather events:** more humidity as a result of a warmer atmosphere contributes to more extreme weather events. In hurricane Katrina in 2005, 1.7 million people were forced into evacuation along with deaths and long term health problems for 200000 residents in New Orleans. The homes of 300000 residents in California were threatened by flood as a result of a combination of increased rainstorms, rising sea levels, and reduced snowfall. Additionally, drinking water of 24 million people was potentially contaminated. Drought and floods alternating have resulted in shortages of water and food, malnutrition, and migrations, consequently, international conflict. Globally, by 2010, fifty million "environmental refugees" were estimated as consequence of desertification, sea levels rising, river flooding, and depleted aquifers [8].

(iii) Wildlife

- **Ecosystems shifts and species die-off:** the disruption of ecosystem is attributed to global temperatures rise, pushing unadaptable species to extinction. By 2050, over 1 million species will be obliterated if the current situation of global warming continues [9].

Nearly 2000 plants and animals species have moved with a rate of 3.8 miles per decade toward the poles. Similarly, in the last half of the 20th century, 20 feet per decade was rate of vertically movement of species in alpine areas. If global temperature increases by more than 2.7 to 4.5 ^{o}F, approximately 20 to 30% of species of plants and animals are likely at increased extinction risk [9].

By mid-century, two-thirds the polar bear worldwide was predicted being extinct due to the ice in the Arctic melting down. The coastline life at sea in California is shifting northward, probably due to temperatures rise. Populations of Antarctic penguin have shrunk by 33% since last 25 years as a result of declination in habitat of winter sea ice [9].

Species with hard calcium carbonate shells such as coral reefs, which are vital to ocean ecosystems, are vulnerable with more acidic ocean induced by discharge of carbon dioxide emissions. An increase in ocean temperatures of 3.6 ^{o}F will destroy 97 % coral reefs worldwide [9].

(iiii) Glaciers and sea levels

- **Melting glaciers, early ice thaw:** melting speed of ice caps and glaciers increase with an increase of global temperature. Consequently this early melt down the ice on lakes and rivers [10].

- **Rising sea-level:** melting mountain glaciers and ice caps in west Antarctic along with thermal and expansion of the oceans are expected to raise level of sea. This may lose the islands and coastal wetlands and increase risk of flooding in coastal areas. The low-lying coastal regions such as the Chesapeake Bay and the Gulf of Mexico are potentially vulnerable [10].

1. 1. 1. 2 Global climate changes

The balance energy between the one entering and the leaving determines the Earth's temperature. The coming sunlight can be either absorbed or reflected by the Earth's surface. The Earth warms when the sunlight is absorbed, and it releases some of heat energy so-called infrared radiation back into the atmosphere. The Earth does not warm when coming sunlight energy is reflected back. The Earth cools when energy is released back into the atmosphere. Many factors those can change this balance of energy [3]:

- Variation in the greenhouse effect affecting to the retained heat of the atmosphere;
- Changes in reaching energy from the sun;
- Variation in the reflectivity of the Earth's surface and atmosphere.

Greenhouse gases (GHGs) like a blanket when preventing or slowing heat loss to the space, making the Earth warmer. This is commonly understood as the "greenhouse effect".

It is said that the Earth is warming with an increase of temperature of 1.4°F over the past century. Probably, additional increment of 2 to 11.5 °F will be for next hundred years [11]. Large and potentially dangerous climate changes may result from small changes in temperature.

The consequences of climate changes such as the changes in rainfall induce more droughts or floods, intense rain, along with severe and more frequent heat waves. Moreover, some phenomenon accompanied with climate changes including warmer and more acidic oceans, shrunk glaciers, melted ice caps, and raised sea levels.

GHGs including large amounts of CO_2 and others released in to the space have been likely attributed to the most climate changes. Major GHGs induced by burning fossil fuels to generate energy. Besides, they also come from industry, deforestation, and agriculture [11].

The greenhouse effect is essential for the Earth's life. However, the buildup of GHGs can make climate changes resulting in detrimental influences to communities and ecosystems. Some areas are forecasted under impacts of the global climate changes as follows [12]:

- **North America:** snowpack decreased in the western mountains; some regions, rainfall increased 5-20%; in cities, heat waves increased in frequency, duration, and intensity.
- **Latin America:** in eastern Amazon, tropical forest gradually replaced by savanna; in many tropical areas, significant risk in loss of biodiversity via extinction of species; availability of water human's activities significantly changes.
- **Europe:** flash floods risk increased; coastal flooding frequently occurred, rise of sea-level and storms increased erosion; retreated glacial in mountains; decreased cover snow and tourism in winter; species extensively lost; in southern Europe, reduced crop yields.
- **Africa:** by 2020, about 75 to 250 million people will be exposed to lack of water, up to 50% of rain-fed agriculture yields could be cut in some areas; agricultural production can be extremely damaged.
- **Asia:** availability of fresh water projected to reduce in most Asia by the 2050s; increased risk of coastal flooding; increased death rate due to disease related to droughts and floods in some areas.

1. 1. 2 Common air pollutants

The EPA set six common pollutants for quality of ambient air standards, in which particles and ground-level O_3 are the most extensive health danger [13].

1. 1. 2. 1 Ozone (O_3)

Ozone exists in the atmosphere in two regions–at ground level and in the upper one. While the later protects our planet from harmful rays of the sun, the former plays vital component of smog.

The reactions of nitrogen oxides (NOx) with volatile organic compounds (VOC) create ground level ozone. Smog, which is contributed by ozone, frequently occurs in the summer, but can also occur all time in the year.

Active outdoors children, older adults may be particularly sensitive to ozone even relatively low effects on health. Coughing, chest pain, throat irritation, and congestion are common symptoms when breathing ozone. When inhaling, it can cause bronchitis, and asthma. Some health problem related to ground-level ozone such as of lung-function reduction, inflame of lung's linings, or permanently scar lung tissue when repeated exposure to it.

Sensitive ecosystems and vegetation can be harmfully affected by ground level ozone. Exposure to ozone, some sensitive plant species such as cottonwood, black cherry, and pine are subjected to potential risk. Ecosystems have adverse impacts from ozone, including species diversity loss; changes in quality of water and habitat, and cycles of nutrient [14].

Major NOx and VOC, those result in ground level ozone, emits from facilities of industry, motor-driven vehicles, gasoline vapor, electric utilities, and chemical solvents [15].

1. 1. 2. 2 Particulate matter (PM)

Particulate matters are extremely small particles covered by liquid layer those known as particle pollution. They are made up with some components such as nitrates and sulfates, organic compound, soil, dust, or metals particles [16].

Pollution particles are grouped into two categories:

- Inhalable particles, whose diameter in range of 2.5~10 micrometers, those can be easily found near dusty industries or roads.
- Fine particles such as those found in smoke and haze, whose diameter equal to or smaller than 2.5 micrometers. Firing forest, and combustion of fossil fuel in power plant, industries, and automobiles are sources of particle pollution.

Health problems are directly linked to the size of particles. Particles, whose diameters are smaller than 10 micrometers, are especially concerned because they can enter the lung, even get into bloodstream through the nose and throat. Heart and lungs can be affected once inhaled, and some serious health problems can be caused [17]:

- Premature death in people who have disease of heart or lung;
- Heart attacks;
- Heart beat irregularly;
- Asthma become aggravated;
- Decreasing lung function; and

- Increasing respiratory symptoms such as difficult breathing, coughing or irritation of the respiration ways.

Visibility reduction is mainly caused by fine particles. After settling on ground or water, consequence of particles can be made including: acidic lakes and streams; depleting the soil nutrients; changing the nutrient balance in basins of large river and coastal waters; reducing crops and damaging sensitive forests; and affecting the ecosystems diversity [17].

1. 1. 2. 3 Carbon monoxide (CO)

Carbon monoxide, which is an odorless and colorless gas, produced from incomplete combustion. Combustion of fuel in automobile, particularly in urban areas, is major source of emissions CO to ambient air [18]. Chest pain is often accompanied when less oxygen delivered to the heart, brain, and tissues. Death can be caused when exposure to extremely high CO concentrations [19].

1. 1. 2. 4 Nitrogen oxides (NOx)

Nitrogen oxides (NO_X) refer to mixture of nitric oxide (NO) and nitrogen dioxide (NO_2). Globally, major sources of NOx resulted from fossil fuel combustions and biomass burning with amount of around 50% and 20%, respectively. NO_X emissions released from fossil fuels combustion depend not only on the nitrogen amount in the fuel but also on mixing ratio of fuel and air. Rich oxidation conditions with very high combustion temperatures generally favor formation of NO_X. Besides, microbial activity in soils and lightning are

natural sources account for total emissions less than 30%. Microbial source resulted from using fertilizer in agriculture [20].

Some adverse respiratory problems such as inflammation airway for healthy people and increased symptoms with asthmatic people were evidenced for exposure NO_2 in short term. Particles, those formed by moisture, organic compounds, and reaction of NOx with ammonia, can deeply penetrate into the lungs resulting to worse respiratory disease or aggravated heart disease. This leads to an increase in number of patient in hospital and premature death. Additionally, ozone, which affects to health and environment, can be formed by reaction of NOx and VOC under heating and sunlight conditions [21].

1. 1. 2. 5 Sulfur dioxides (SO_2)

Sulfur dioxide (SO_2) can be grouped into highly reactive gases. Burning fossil fuel for electricity at power plants and other industrial facilities are the largest SO_2 emissions sources with 73% and 20%, respectively. Combustion of high sulfur fuels by large ships, locomotives, automobile, and non-road equipment release less SO_2 emissions [22].

Similarly NOx effect, increased asthma symptoms and adverse respiratory also related to the short term exposures to SO_2. Particles those forming from reaction of SOx and other compounds can cause or worsen respiratory and heart diseases leading to increased premature death and hospital patients [23]. In addition, SOx results in acid rain reducing vegetation, damaging property and welfare.

1. 1. 2. 6 Lead

Lead (Pb) can naturally found in the environment as well as in manufactured production. On-road vehicles driven by motor such as trucks and cars along with industrial processing are major sources of lead emissions. Lead in the air significantly decreased as a result of effort to remove lead from gasoline using in vehicles on-road. The highest lead levels are appeared near lead smelters, today. Now, processing of metals and ore, and leaded gasoline using in piston-engine aircraft are major sources of lead emissions [24].

Lead is delivered throughout the body via bloodstream and is cumulated in the bones once carried into the body. Nervous, immune, cardiovascular, reproductive and developmental systems, and kidney and is adversely influenced depending on the exposure level to lead emissions. The most common effects encountered for adults are heart disease and high blood pressure in, and for children are neurological effects. Lowered IQ, learning deficits, and behavioral problems can be encountered for young children and infants who are particularly sensitive to lead emission even at low levels [25].

Accumulation of lead in soils and sediments are resulted from air deposition, mining, direct discharge of waste water, and erosion. Wide effect ranges on the ecosystems including biodiversity loss, decreased reproductive and growth rates, neurological impacts have been revealed in points near lead sources [25].

1. 1. 3 Global production and consumption of fuel

1. 1. 3. 1 Natural gas

Natural gas is one among sources for fuel and energy production. Natural gas can be used for heating, or running dual fuel engine. Otherwise, it can be used for fuel for gas turbine in electric generation plant. The global production and consumption of natural gas [26] are shown in Fig. 1-6 and Fig. 1-7.

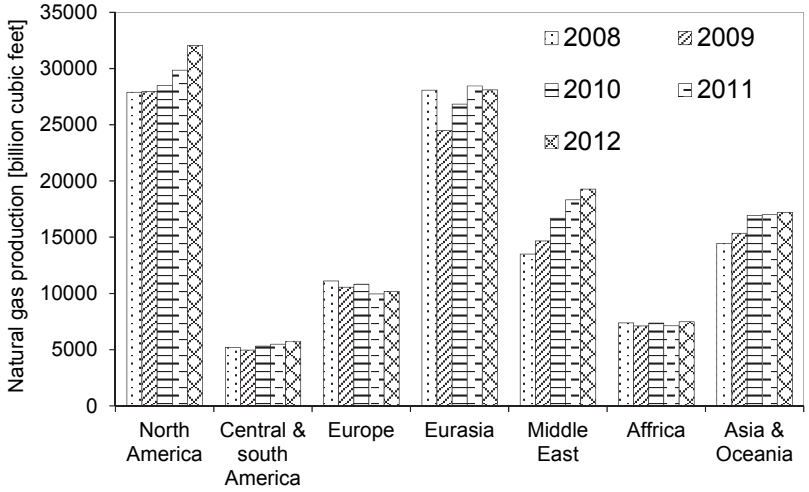

Figure 1-6 Natural gas production by regions from 2008 to 2012 (source: [26])

It can be seen that natural gas was produced mainly from North America, Eurasia, Middle East, and Asia & Oceania. The production of natural gas is increased with time for most regions, especially for Middle East, North America, and Asia & Oceania.

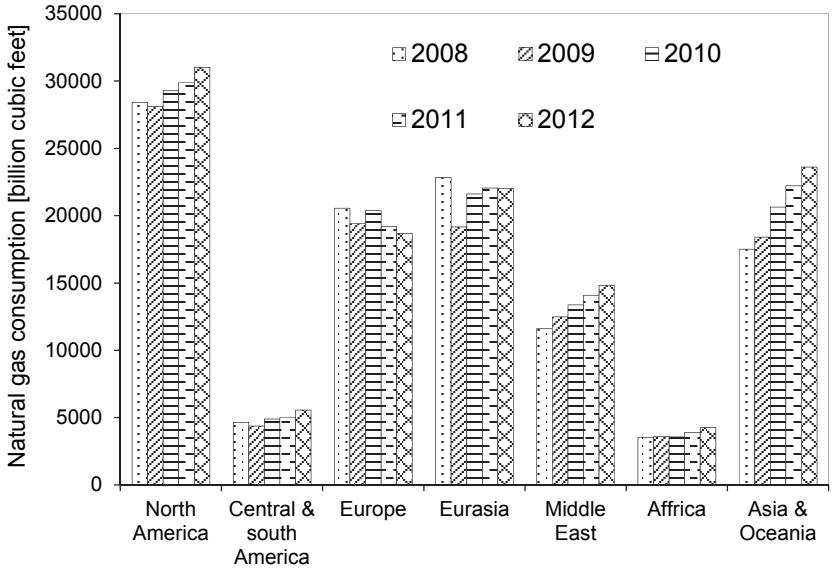

Figure 1-7 Natural gas consumption by regions from 2008 to 2012 (source: [26])

Europe, North America, Middle East, Eurasia, and Asia & Oceania mainly consumed natural gas. The consumption of natural gas in Middle East, North America, and Asia & Oceania increased with time. While, natural gas consumption in Europe and Eurasia slightly decreased. Africa and Central & South America are regions producing and consuming less natural gas. Overall, North America is region producing and consuming much natural gas.

1. 3. 1. 2 Oil and petroleum

Oil and petroleum products are main fuel for automobile, stationary power plant, for construction machines, and ships. In addition, they can be used in industrial sector. Information for oil supply and petroleum consumption is accompanied following.

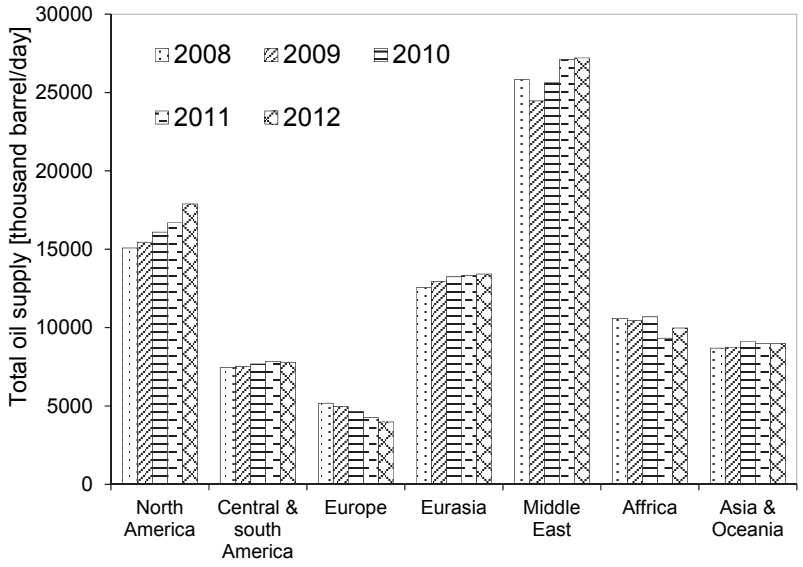

Figure 1-8 Oil production by regions from 2008 to 2012 (source: [26])

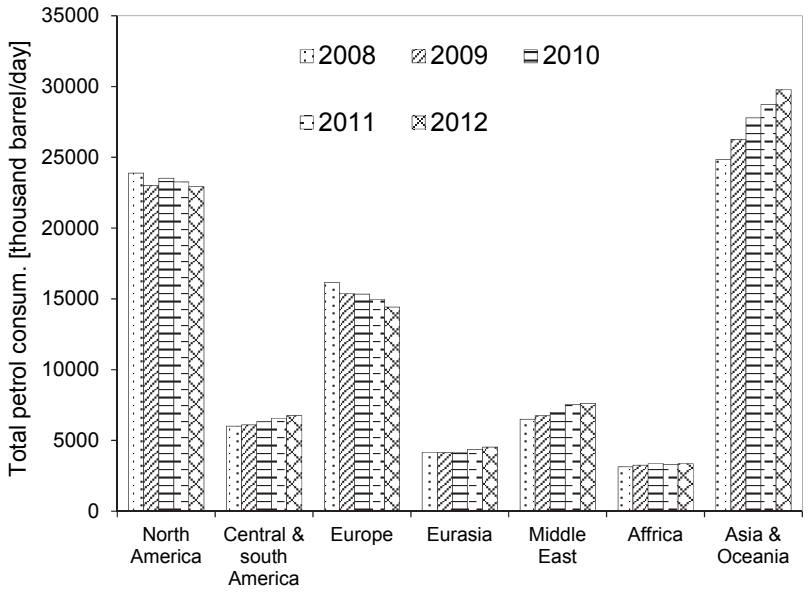

Figure 1-9 Petroleum consumption by regions from 2008 to 2012 (source: [26])

Global oil production is shown in Fig. 1-8 [26]. Most oil is produced in Middle East and in North America. Oil production in these regions increased with time during this period. Eurasia, Africa and Asia & Oceania are regions produced oil moderately. Europe is region producing oil less in the world.

Global petroleum consumption is shown in Fig. 1-9 [26]. Though oil is produced moderately in Asia, but this region consumed most petroleum product, and is followed by North America. China and the U.S. are the biggest markets and probably addressed for high consumption in these regions. Europe is classified as the third region for petroleum consumption despite its low oil production. Eurasia and Africa are regions with a low petroleum consumption of under 5 million barrels per day.

1. 3. 1. 3 Biofuel

Global biofuel production is shown in Fig. 1-10 and global biofuel consumption is shown in Fig. 1-11 [26]. It can be seen that biofuel is mainly produced in America regions followed by Europe. The U.S. and Brazil are leading countries for production of biofuel. In Europe, the nations such as Germany, France, Italy, and Spain are the biggest biofuel producing countries. While China mainly produced biofuel in Asia.

America and Europe are also the regions for the most biofuel consumption. The U.S., North America, and Canada mainly consumed biofuel. Brazil is the biggest biofuel consumed country in South America. In Europe, the United Kingdom together with the other biggest producing biofuel countries are main nations consumed biofuel. China is still the leading country in biofuel consumption in Asia. Recently, India, Thailand, and Korea has been becoming the countries consume more biofuel.

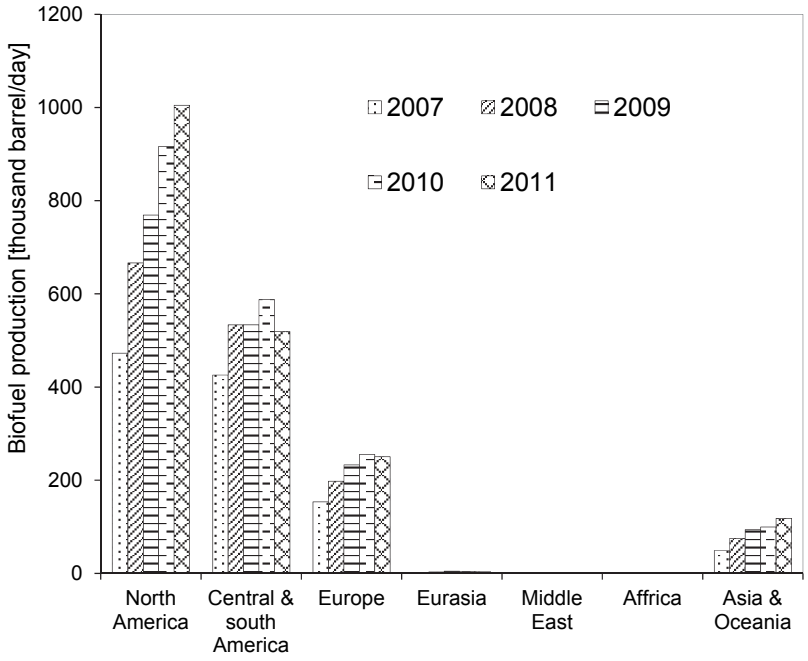

Figure 1-10 Biofuel production by regions from 2008 to 2012 (source: [26])

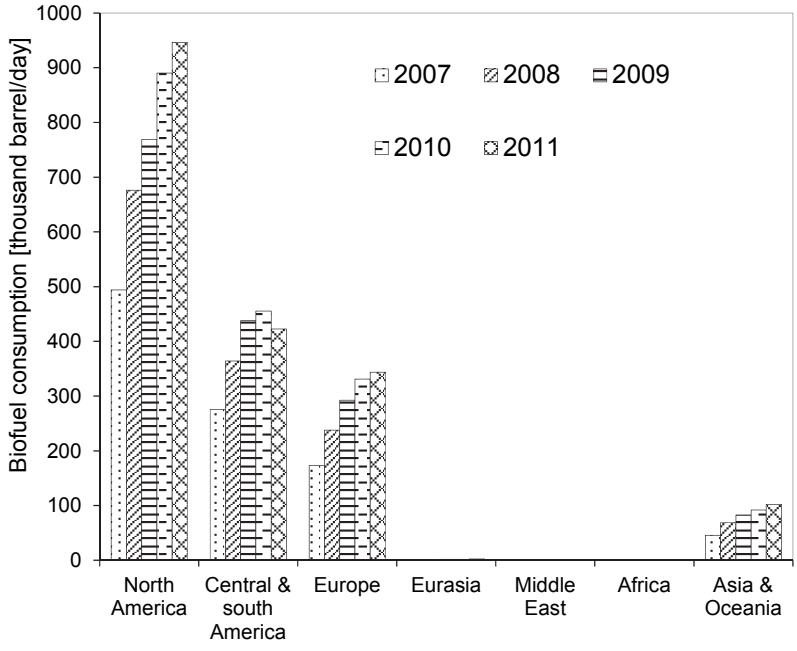

Figure 1-11 Biofuel consumption by regions from 2008 to 2012 (source: [26])

1. 1. 4 Fuel pricing trends

1. 1. 4. 1 Crude oil

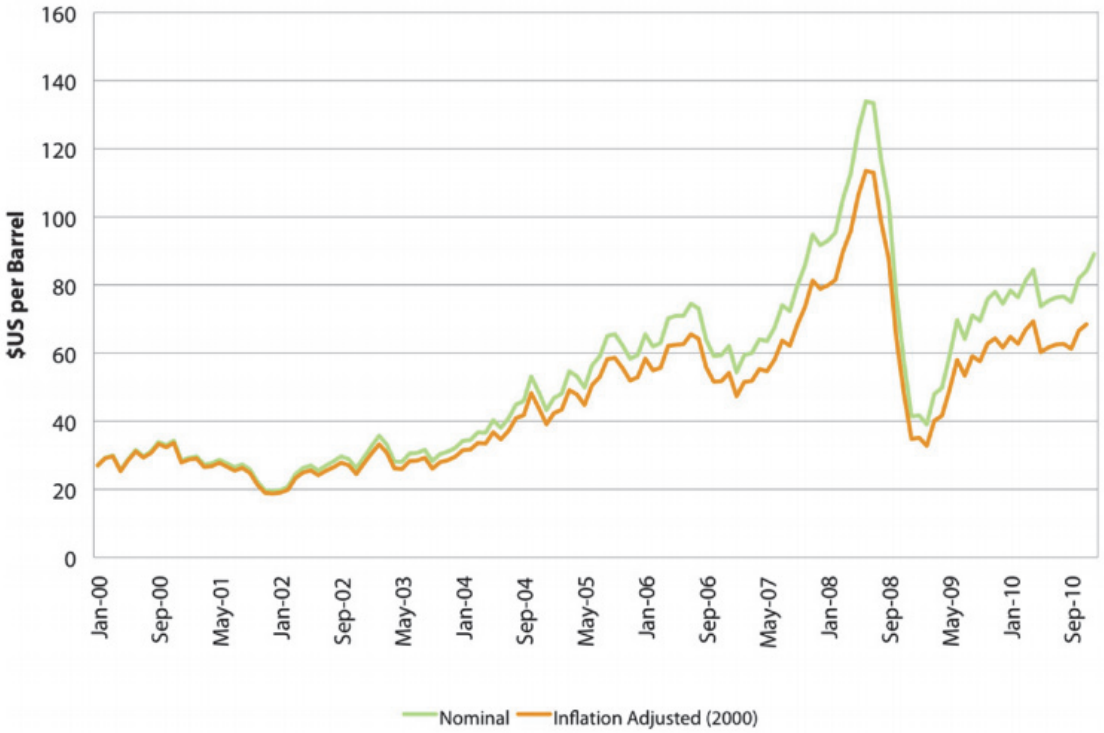

Figure 1-12 Price of crude oil in period between 2000 and 2010 [27]

Buyers and sellers in Canada trade oil mostly based on short-term contracts thus Canada participates the global oil market and this sets the world oil price. Despite the sixth largest world oil producer, about 4% of total daily production produced by Canada, so it has less effect on the world oil price. Consequently, Canada is a price taker. Therefore, the crude oil price trends in Canada shown in Fig. 1-12 can be used to assess world price [27]. The changes in oil price changes are summarized as follows:

- In period of 2000-2003: prices were generally stable at trading rate of around $30/barrel. The OPEC capability of spare producing, weak growth in economy, and oil demand after the event of September 11, 2001 are attributed to this.
- In period of 2004-2006: increasing demand from emerging economies such as China, India, and Brazil forced the prices rising. In 40 months between Sept. 2003 and Dec. 2006, prices increased in 29 months.
- In period of 2007-2008: price extremely volatilized due to significant investment of financial in oil; U.S. dollar falling; emerging economies demand growth; instability in geopolitics; slow growth production in non-OPEC; and finding and development costs rising.
- In period of 2008-2010: housing market collapse in the U.S., stock markets decline, a number of major financial institutions failure featured for global economy decline.

Global price of crude oil is shown in Fig. 1-13[28]. It can be seen that, the trends of crude oil price in Canada are similar to that in global scale. The peak of price was achieved in middle 2008, afterward dropped in early 2009. It then increased gradually until the end of 2010 and kept a stable price between 100 and $120/bbl.

Figure 1-13 Global price of crude oil between 2000 and Mar., 2014 [28]

1. 1. 4. 2 Petroleum products

Crude oil pricing potentially determine petroleum product pricing. Petroleum sector at downstream is high competitive and complex. Factors including supply and demand, pressures of transportation, international and local market factors set regional petroleum product prices. Prices expected being higher once the increased distance from refinery to selling point due to higher transportation costs. In rural areas, where fewer retailers, prices increase due to the less competition compared to larger center. Different tax results in in different in regional prices.

Price of petroleum in Canada is has similar trend with global price. In the second half of the decade, prices of gasoline indicated in Fig. 1-14 were higher and highly volatilized while closely followed prices of crude oil.

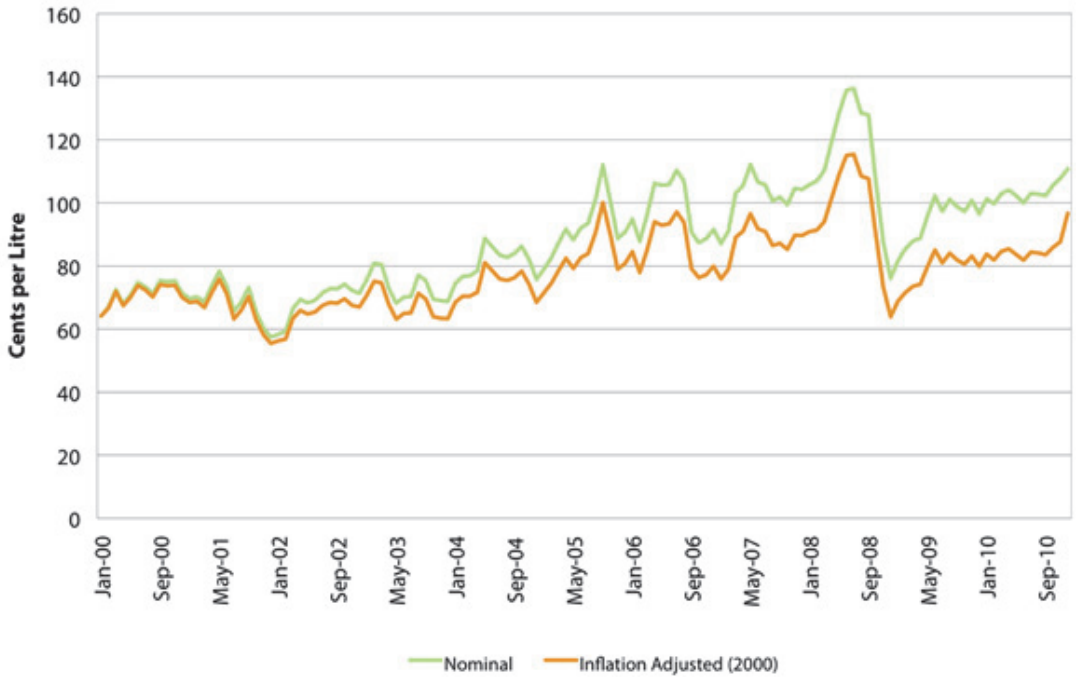

Figure 1-14 Price of regular unleaded gasoline over the period of 2000-2010 [27]

Overall, last decade, higher producing costs and increasing demand especially from emerging economic countries forced the world oil market volatilizing and prices increasing. Petroleum product prices are mainly determined by input costs of crude oil. As a result of higher prices of oil, the prices of gasoline have increased.

1. 2 Fundamentals emissions of Diesel engine

1. 2. 1 Carbon monoxide (CO)

Combustion of rich fuel mixture in an engine emits emissions of carbon monoxide. Some fuel does not burn, others generates CO if there is not enough oxygen to completely convert to carbon dioxides [29].

$$C + 0.5\ O_2 \rightarrow CO$$

Rather than considered as an undesirable emission, emission of CO present combustion energy loss. CO can be further burned to add more heat energy for engine.

$$CO + 0.5\ O_2 \rightarrow CO_2 + \text{heat}$$

When running on rich fuel conditions such as starting or accelerating, CO is significantly generated. Due to the mixing process of fuel and air in the combustion chamber is not perfect, local rich regions occurs even in stoichiometric or lean fuel-air mixture, combustion also results in CO.

1. 2. 2 Carbon dioxides (CO_2)

At moderate concentration, emissions of carbon dioxides are not accounted for air pollutant. However, they are accounted for major GHG resulting in global warming. Burning any hydrocarbon fuel mainly releases CO_2 in the exhaust. The growth of automobile, factories using fossil fuel continuously increase carbon dioxides amount in the atmosphere. A shield of thermal radiation at higher atmosphere elevations is formed as a result of carbon dioxides along with other GHG slightly increasing the global average temperature [29].

1. 2. 3 Unburned hydrocarbon (HC)

In general, emission of hydrocarbon is only about 2% in the exhaust of a diesel engine [29]. As a result of fuel continuously injected during the combustion, the mixture of fuel and air extremely inhomogeneous formed in diesel engines. In the combustion chamber of the engine, there are some points being too rich or

too lean for properly combustion. For under-mixing, particles of fuel in the rich fuel zones never meet oxygen for reaction. While, the combustion is restricted in the lean zones releasing some unburned fuel. For over-mixing, particles of fuel do not totally burn when mixing with burned gases.

Perfect combustion does not occur even when fuel and air entering into an engine with ideal stoichiometric ratio, consequently, in the exhaust, some HC will be emitted. This resulted from incomplete mixing of the air and fuel. In addition, small amount of un-reacted mixture of fuel and air will be escaped as result of the flame quenching due to the walls cooling or the reduction of pressure and temperature in expansion stroke. As a result, the combustion is slowed, and finally the flame is quenched in the later phase of the power stroke. For exhaust gas recycle engines, high exhaust residual levels results in poor combustion and quenching.

Crevice volume: under high pressure conditions of the compression stroke and early combustion stage, the mixtures of fuel and air are compressed into the crevice volume. In the expansion stroke, the fuel- air mixtures get back the combustion chamber when pressures in the cylinder are lower than in the crevice volume. Due to the quenched flame at this time, un-reacted mixtures release as exhaust. Crevice volume around the piston rings is the greatest and can cause HC emissions up to 80%. Moreover, crevice volumes around the valves and valve seats are also sources for HC emissions when the valves open.

Moreover, the absorbed fuel on the deposit on the combustion chamber walls can be desorbed when the cylinder pressures drop, and finally be dispelled in the exhaust stroke.

Similarly, the absorbed fuel air mixture on the cylinder walls oil film the in compression stroke can be desorbed in expansion stroke and blow-down as a source of HC emissions. In the other hand, the high molecular weight hydrocarbon contained lubricating oil, which can be scraped off the cylinder wall and being partly burned during combustion, results in emissions of HC.

1. 2. 4 Nitrogen oxides (NOx)

NOx emissions are usually considered as a group of nitric oxide (NO) and nitrogen dioxide (NO_2), in which, NO is predominantly produced in the cylinder of an engine. In the engine cylinder, NOx is mostly generated by the combustion of nitrogen contained in ambient air. Additionally, fuel nitrogen contributes to a minor NOx in the exhaust gas of the engine. A number of reactions probably occur in combustion process to form NO [29].

$$O + N_2 \rightarrow NO + N \quad (1\text{-}1)$$

$$N + O_2 \rightarrow NO + O \quad (1\text{-}2)$$

$$N + OH \rightarrow NO + H \quad (1\text{-}3)$$

NO_2 can be formed by various further reactions from NO as follows:

$$NO + H_2O \rightarrow NO_2 + H_2 \quad (1\text{-}4)$$

$$NO + O_2 \rightarrow NO_2 + O \quad (1\text{-}5)$$

Diatomic molecules of nitrogen are commonly existed in low temperature conditions of the atmosphere. However, reactive monatomic nitrogen (N) can be generated from atomic nitrogen (N_2) under very high temperatures occurring in the engine cylinder:

$$N \rightarrow N_2 \quad (1\text{-}6)$$

At high temperatures water vapor and oxygen become reactive and also contribute to NOx formation of:

$$O_2 \rightarrow 2\ O \quad (1\text{-}7)$$

$$H_2O \rightarrow OH + 0.5\ H_2 \quad (1\text{-}8)$$

When high temperatures are achieved by combustion, the reactions (1-6) - (1-8) much further shift to the right side dissociating more diatomic nitrogen, N_2, and forming more NOx.

. Therefore, maximum formation of NOx are demonstrated at slightly lean equivalence ratio (Ø = 0.95). Besides, NOx formation is dependent on combustion duration and pressure, and ratio of air to fuel.

1. 2. 5 Particulate matter (PM)

Soot particles of solid carbon commonly generate in the fuel-rich zones of injection spray within the combustion chamber and emit as exhaust of diesel engine. They are clusters of spheres of solid carbon sizing from 10 nm to 80 nm, mostly in 15-30 nm. Trace of HC and other components on the surface of solid carbon forms the spheres [29].

$$CxHy + z\ O_2 \rightarrow a\ CO_2 + b\ H_2O + c\ CO + d\ C\ (s) \quad (1\text{-}9)$$

Most of particles of solid carbon further react with sufficient oxygen to convert to CO_2

$$C\ (s) + O_2 \rightarrow CO_2 \quad (1\text{-}10)$$

Over 90% of original soot particles those formed within the combustion chamber are consumed before exhausting out of the engine.

Lubricating oil components contribute about 25% of the carbon in soot during combustion, while 0.2-0.5% of the amount of fuel contributes to the rest one. High boiling point components in fuel and lubricating oil so-called soluble organic fraction (SOF) will condense on the soot particles as a result of temperature drop in the cylinder during power and expansion stroke. The SOF amount highly depends on temperature inside cylinder. SOF can be 3% of the total mass at higher loads, while, up to 50% of soot mass at low load conditions when temperature drop to 200 ^oC in later phase of expansion and exhaust. Main component of hydrocarbon along with some hydrogen, NOx, SO_2, and trace amounts of others forms SOF.

1. 3 Research background

1. 3. 1 Background of Jatropha

1. 3. 1. 1 Jatropha plant

Firstly described by Carl Linnaeus, Jatropha curcas is one among many species of Jatropha genus. Most Jatropha is native to the new world with 170 species,

although 66 species identified as originating in the old world. Three varieties are identified including Nicaraguan (fewer but larger fruits), Mexican (less or non-toxic seed) and Cape Verde. Throughout Asia and Africa, the Cape Verde is commonly detected [30].

Jatropha can be small tree or perennial shrub with heights over 5 meters depending on nutrient and water conditions. The leaves with length and width of 6 to 15 cm are alternately arranged on the stem. Male and female flowers are separated on the same plant with an averages ratio of 29:1. However, this ratio is highly varied with range 25-93 male to 1-5 female flowers. Fruiting capacity may increase with an increase of age of plant when male-to-female flower ratio reported declining. The fruits of Jatropha are ellipsoidal in shape, fleshy and green when young, and turn yellow and then brown as aging. After flowering around 90 days, fruits become mature and are ready to harvest. Mature and immature fruits are simultaneous due to the continuously lowering and fruiting. Two or three black seeds in size of around 2 cm x 1 cm are contained in each fruit. On average, 35 % of oil is contained in the mass of seed [30]. Fig. 1-15 shows the immature and mature fruits.

Figure 1-15 Fruit and seeds of Jatropha [30]

The plant of Jatropha readily grows from stem or seed reaching one meter and start flowering under good conditions after five months. As usual, the plant becomes maturity after four to five years with a height of 3 to 5 meters under good conditions [30].

In rainy season, vegetative growth occurs and plant will drop leaves during dry season. Rainfall triggers flowering and the plants produces theirs seeds until end of rainy season. In the first or second year of growth, the seeds are produced. Lifespan of Jatropha trees are believed be over 30-50 years [30].

1. 3. 1. 2 Jatropha cultivation and seed yields

Climate

Jatropha plant can be cultivated in tropical and subtropical areas doped into latitudes between 30ºN and 35ºS as shown in Fig. 1-16. It is suitable for growing with altitudes higher sea level and lower 0-500 meters. Jatropha may flower at any period of the year and in-depend on latitude. Annual rainfall of 250 to 300 mm is limit for Jatropha surviving and it need at least 600 mm for flowering and fruiting. The optimum rainfall of between 1000 and 1500 mm corresponding to sub-humid ecologies is for seed production. Temperatures of 20˚C and 28˚C are optimum for Jatropha plant, and the yields can be depressed with very high temperature. It is intolerant of frost, well adapted to high intensity of light, and is unsuited in shade conditions [30].

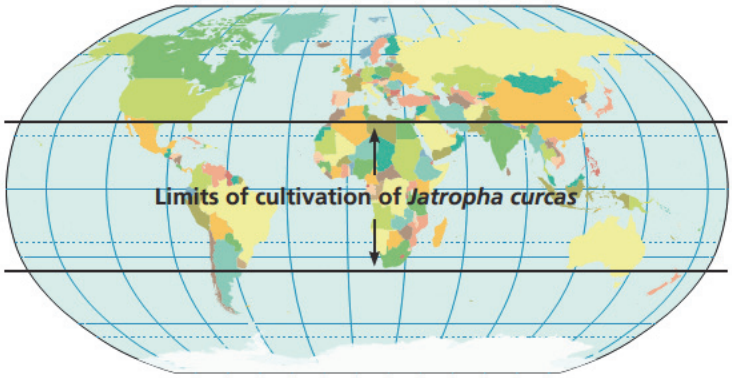

Figure 1-16 Cultivation limits of Jatropha curcas [30]

Soil

Aerated loams and sands with the depth of at least 45 cm are the best soils for Jatropha. Because of being intolerant of waterlogged conditions, cultivation of Jatropha plants should be avoided with heavy clay soils, particularly where drainage is limited. The pH in soil should be within 6.0 to 8.0/8.5 even Jatropha is able to grow in alkaline soils condition. Saline water and poor irrigation conditions are acceptable for Jatropha. Soil health managements such as minimum soil disturbance, legume cover crops, and organic mulch cover are needed for Jatropha production [30].

Seed yields

The seed yields depend on many factor including genetic, age, cultivation method, tree spacing, rainfall, soil type, and fertility. For conditions of semi-arid, common yields are at 1.0 ton/ha. During a 17-year period, averaged yield is less than 1.25 ton/ha. Under optimal conditions such as with good soil, optimal rainfall management, the yields are 5.0–7.0 tons/ha or even up to 7.8 tons/ha [30].

1. 3. 1. 3 Jatropha seed harvest and oil extraction

Harvesting

After flowering around 90 days, when the fruits turning yellow-brown from green, seeds can be harvested. In semi-arid areas, the harvest may be confined to 2 months, while it continuously fruiting throughout the year in more humid conditions. The seeds will be removed after drying the fruits. For cultivation, the seeds are shade dried. For oil production, the seed are dried in the sun to reduce moisture to around 6–10% [30].

Oil extraction

Kernels roasting and pounding, water adding and boiling, then oil separating are required processes for traditional oil extraction. An engine-driven expeller of manual screw press can be used for extracting the oil. Seeds should be heated in the sun or by ten minutes gently roasted to enhance the efficiency of oil extraction by the hand expellers. Whole seeds are commonly fed to the expeller for production in small scale. The husk can be firstly removed and can be used as a fuel in large processing plants. Fig. 1-17 shows oil refining steps [30].

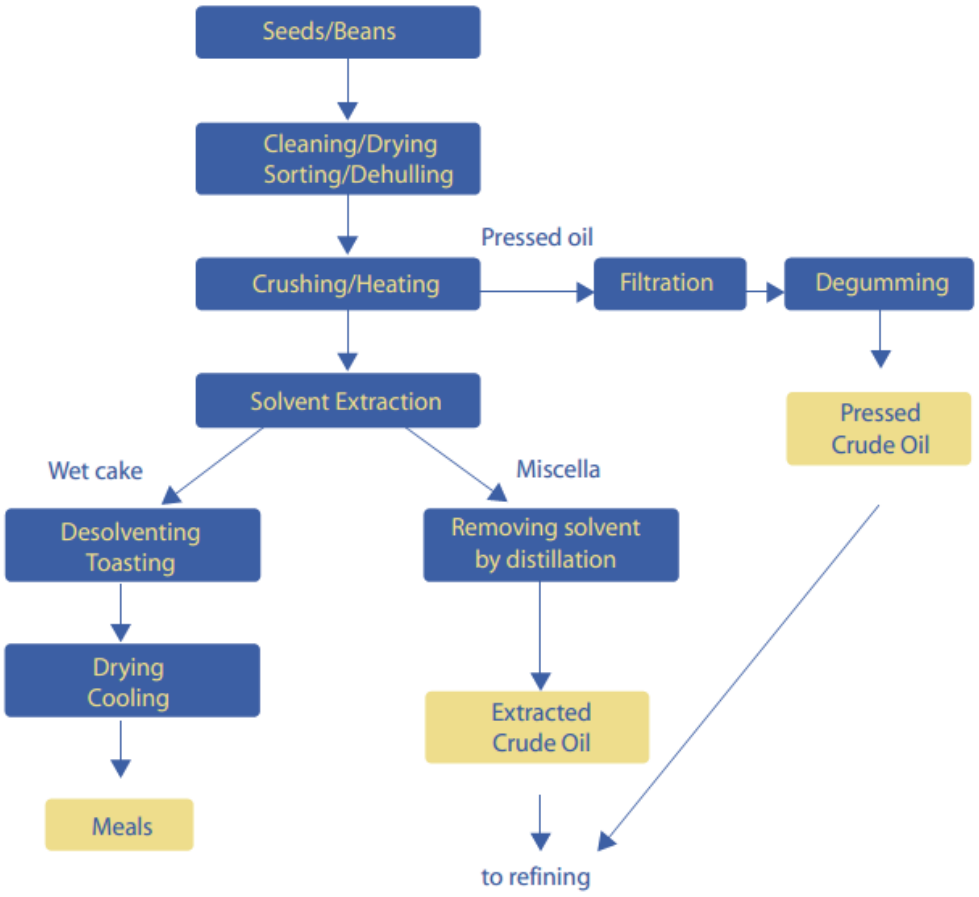

Figure 1-17 Refining crude vegetable oil to purified vegetable oil [30]

By weight, 19–22% of the dry whole seed and 30% of the seed kernel can be extracted as oil by manual expellers. For engine driven screw expeller, 75–80% of available oil can be extracted. The extraction rate can be further improved in large-scale processing by pre-heating, continuous pressings, and solvent addition. Solids containing in the oil after extraction must be eliminated by centrifuging, settling, or filtering to improve storability [30].

1. 3. 1. 4 Physical and chemical properties of Jatropha oil

The physical and chemical properties of Jatropha oil can be extremely influenced by environment and genetic interaction. The fatty acid compositions

of the oil can also be affected by the fruits maturity. Moreover, processing and storage influence the quality of oil [30].

Crude Jatropha oil is more relatively viscous than the rapeseed oil. Low free fatty acids improve the storability, even though it prone to oxidation in storage due to unsaturated oleic and linoleic acids. It remains in fluid phase at lower temperatures as a result of presence of unsaturated fatty acids (high iodine value). Cetane number of Jatropha oil is relatively high. The oil contains low sulfur presenting less sulfur dioxide in exhaust when using oil is as a fuel [30].

1. 3. 2 Literature review

1. 3. 2. 1 Jatropha fueled diesel engine

Jatropha oil was identified as a leading candidate for an alternative fuel for commercialization among various non-edible vegetable oils [31]. Jatropha plant can be grown in arid conditions on almost any kind of ground, and does not suffer excessively from droughts or require concentrated irrigation. Therefore, unlike other common biofuel crops, it is very easy to cultivate, even on poor soil. Jatropha oil has been fueled and tested for combustion, performance and emissions of diesel engines in previous studies. In the studies of K. Pramanik [32], D. Agarwal et al. [33], higher specific fuel consumption, lower thermal efficiency of the engine ran on Jatropha oil was also observed due to poor combustion characteristics as a result of its high viscosity and less volatility, poor atomization and mixing with air. Consequently, this slows the combustion

rate when compared to Jatropha biodiesel. Furthermore, B. S. Chauhan et al. [34] reported a lower the engine brake thermal efficiency when fueling with Jatropha resulting from larger viscosity, inferior heating value, and bulky molecules of Jatropha fuel oil.

Lower peak pressure, less premixed combustion, slower burning rate, longer combustion duration, and higher exhaust gas temperature were proven in the literature [33]. Higher exhaust gas temperature of Jatropha oil fueled diesel engine was also revealed in the work of K. Pramanik [32]. These resulted from physical- and chemical-properties of Jatropha oil.

Lower NOx emissions were shown, while CO, HC emissions, and smoke were reported higher in most studies in the literature [33-35]. The lower NOx emissions were attributed to lower peak combustion temperature due to lower heating value, less premixed combustion. Higher CO, HC, and smoke were resulted from larger viscosity, less volatility contributing to worse atomization and mixing with air.

In summary, it is said that the combustion, performance, and emissions of diesel engine fueled with straight Jatropha oil were worse in comparison with those of diesel oil or biodiesel of Jatropha oil except lower emissions of NOx. This results from properties of neat Jatropha oil. It is necessary to adjust some operational factors and fuel to improve its combustion, and emissions characteristics of diesel engine running on straight Jatropha oil.

1. 3. 2. 2 Multiple/split injections diesel engine

Split or multiple injections can be carried out easily on a common rail diesel engine. It permits changing the injection pattern, consequently, resulting in the change in combustion and engine emissions. Split injection can reduces NOx emissions of diesel engine. The reduction of NOx resulted from the cooling effect of the secondary injection [36]; the reduction of peak combustion pressure and peak of heat release at the premixed combustion [37, 38]; or the lower combustion temperatures and resident time of high temperatures [39]. Split injection reduces concentration of fuel in rich-fuel zones, increases air entrainment, and elevates temperature in the cylinder and later phase thus the second injection can be combusted rapidly and effectively, finally enhances soot oxidation rate and CO. The reduction of soot has been revealed in the literature [36-38, 40, 41] due to the reduction in precursor formation [36]; the reduction in particulate number concentration; the enhanced soot oxidation by second injection [36, 38, 40]; and the leaning-out spray and improved mixing with air [38, 42]. However, research has also reported a reverse trend of higher NOx [40] and higher PM [42] with split injection. However, for HC, and CO emission, it was reported higher in the research of M. Y. Kim et al. [37], while it was lower in the study of S. H. Park et al. [40]. Overall, the influences of the split injections on the engine combustion and emissions may vary from research

to research and may depend upon the operational factors such as used fuel, and operational conditions.

1. 3. 2. 3 Water emulsion fueled diesel engine

The usage of water in diesel engine to reduce peak temperature and finally decline NOx emissions can be in the way of directly injection water in to the combustion chamber or in emulsified fuel. To inject water separately from fuel, the injection system has to modify to carry out this task. While injection of water into the combustion chamber by emulsified fuel do not need modifying the fuel injection. Emulsify fuel is a way mixing insoluble fluid into the fuel by adding some surfactant to increase surface tension and finally to suspend the insoluble fluid particles stably in the fuel.

Emulsifying fuel with water is well known way to decline significantly NOx emissions and soot/PM from diesel engines that has been proven in the literature [43, 44-46]. The reduction in NOx is attributed to the cooling effect due to vaporization of water in emulsion fuel [44-46]. While the reduction of soot is a consequence of better atomization and mixing with air resulting from micro-explosion or the presence of OH radicals releasing during the combustion process [44, 46]; or more air entrainment [47].

1. 3. 2. 4 Hydrogen peroxide blends fueled diesel engine

Hydrogen peroxide (H_2O_2) is effective for soot oxidation due to the presence of the Hydroxyl radical (OH) dissociated during the combustion process as

reported in the articles of B. Franz et al. [48] and C. Born et al. [49]. K. S. Nagaprasad et al. [50] found higher engine brake thermal efficiency with increased concentrations of H_2O_2, and D. S-K. Ting et al. [51] reported a significant reduced ignition delay with H_2O_2 addition. The burning velocity of methane was improved owing to the presence of OH, O, and H radicals thus produced less CO emissions [51, 52]. M. C. Mulenga et al. [53] reported that emissions of NOx were lower as a result of a lower average-cycle temperature. Hence, it can be summarized that the addition of H_2O_2 to the engine combustion chamber may improve the combustion and emissions. However, addition of H_2O_2 to Jatropha oil has not been tested until now.

Chapter 2 Research Aim, Theory, and Infrastructure

2. 1 Research aim

The objective of the research is to improve combustion, performance and emissions of diesel engine fueled with Jatropha oil, and its emulsion fuels. To approach this target, in this study, I modify the fuel injection pattern and fuel input. By changing injection from single into double/split one, the combustion and consequently the emissions of the engine would be enhanced. In addition, according to properties of the Jatropha oil, I found that emulsifying Jatropha oil may also improve the combustion and emissions of the engine using emulsified fuels when compared with the neat Jatropha fueled diesel engine. In this research, the Jatropha oil was emulsified with pure water or with a solution of water and hydrogen peroxide. Moreover, a combination of Jatropha water emulsion with double injections was carried out to test theirs influence to the combustion and emissions characteristics of diesel engine. The combustion parameters of the engine including ignition delay, combustion duration, heat release rate, and timing of 50% total heat release (THR) were assessed. The performance parameters consisting of in-cylinder and exhaust gas temperatures, and thermal efficiency was evaluated. While the emissions of the engine including CO, CO_2, HC, NOx, dust, and smoke were read and assessed.

2. 2 Theoretical considerations

2. 2. 1 Net heat release rate calculation

We consider that combustion chamber as an open system at which occurring heat, mass, and work transfer into and out of the system. Mass transfer is resulted from fuel injection and fuel flow into and out of the crevice. Heat transfers from the burned gases in the cylinder chamber and the chamber walls. The work is piston work under pressure by burned gases [54]. The first law for such a system is

$$\frac{dQ}{dt} - p\frac{dV}{dt} + \sum \dot{m}_i h_i = \frac{dU}{dt} \tag{2.1}$$

Where dQ/dt is the heat transfer rate across the system boundary into the system, $p(dV/dt)$ is the rate of work transfer done by the system due to system boundary displacement, $\dot{m}_i$ is the mass flow rate into the system across the system boundary at location i, h_i is the enthalpy of flux i entering or leaving the system, and U is the energy of the material contained inside the system boundary. When the intake and exhaust valves are closed, the fuel and the crevice flow are only mass flows across the system boundary. When crevice flow is small, it can be omitted from equation 2.1

$$\frac{dQ}{dt} - p\frac{dV}{dt} + \dot{m}_f h_f = \frac{dU}{dt} \tag{2.2}$$

If U and h_f in Eq. (2.2) are taken to be the sensible internal energy of the cylinder contents and the sensible enthalpy of the injected fuel, respectively,

then dQ/dt becomes the difference between the chemical energy or heat released by combustion of the fuel and the heat transfer from the system. Since $h_f \approx 0$, Eq. (2.1) becomes

$$\frac{dQ_n}{dt} = \frac{dQ_{ch}}{dt} - \frac{dQ_{ht}}{dt} = p\frac{dV}{dt} + \frac{dU}{dt} \tag{2.3}$$

The net heat release rate, dQ_n/dt, which is the difference between the gross heat release rate, dQ_{ch}/dt and the heat transfer rate to the walls dQ_{ht}/dt, equals the rate at which work is done on the piston plus the rate of change of sensible internal energy of the cylinder contents.

If we further assume that the contents of the cylinder can be modeled as an ideal gas, then equation (2.3) becomes

$$\frac{dQ_n}{dt} = p\frac{dV}{dt} + mc_v\frac{dU}{dt} \tag{2.4}$$

From the ideal gas law, $pV = mRT$, with R assumed constant, it follows that

$$\frac{dp}{p} + \frac{dV}{V} = \frac{dT}{T} \tag{2.5}$$

Equation (2.5) can be used to eliminate T from equation (2.4) to give

$$\frac{dQ_n}{dt} = \left(1 + \frac{c_v}{R}\right)p\frac{dV}{dt} + \frac{c_v}{R}V\frac{dP}{dt}$$

With γ is ratio of specific heats, $\gamma = c_p/c_v$, then

$$\frac{dQ_n}{dt} = \left(\frac{\gamma}{\gamma - 1}\right)p\frac{dV}{dt} + \frac{1}{\gamma - 1}V\frac{dP}{dt} \tag{2.6}$$

An appropriate range for γ for diesel heat release analysis is 1.3 to 1.35 [54]. However, the value of γ can be calculated according to temperature, T (K), of the gases in the cylinder [55]

$$\gamma = 1.338 - 6.0 * 10^{-5} * T + 1.0 * 10^{-8} * T^2 \quad (2.7)$$

2. 2. 2 Emission unit conversion

During experiment, exhaust gas emissions were read from the exhaust gas analyzers. However, the units indicated on the analyzers are in part per million (ppm). This section shows the steps for conversion the units of exhaust gas emissions from ppm to standard unit of gram per kilowatt hour (g/kWh).

$$GASx = \frac{U \times conc \times G_{exhaust}}{N_e} \quad (2.8)$$

where:

- $GASx$: exhaust gas emission, [g/kWh];
- U: constant factor given in Table 2.1;
- $conc$: concentration of exhaust gas x, [ppm];
- $G_{exhaust}$: flow rate of exhaust gas, [kg/h];
- N_e: power of engine, [KW].

Table 2-1 Constant factor, *U*

Gas	*U*
NO_x	0.001588
HC	0.00048
CO_2	9.67
O_2	15.19
CO	11.04

Flow rate of exhaust gas, $G_{exhaust}$, is calculated by following equation

$$G_{exhaust} = G_a + G_f \quad (2.9)$$

where:

- G_a: intake air flow rate [kg/h];
- G_F: fuel consumption [kg/h].

❖ **Intake air flow rate**

Intake air flow rate is calculated by following equation

$$G_a = 0.001252 \times m \times \alpha \times D_t^2 \times \xi \times \sqrt{\gamma_1 \Delta P} = 9.6 \times \sqrt{\gamma_1 \times \Delta P} \quad (2.10)$$

where:

- α: flow rate coefficient, $\alpha = 0.8$;
- D_t: diameter of pipe on surge air tank, [mm];
- ξ: adjustment coefficient of compressed air;
- $m = \frac{d^2}{D_t^2}$; d: diameter of orifice, [mm];
- ΔP: pressure difference between orifice, [kPa];
- γ_1: density of air before orifice [kg/m^3];

$$\gamma_1 = 1.2931 \times \frac{273}{273 + t_0} \times \frac{P_0 - 0.378 \times \emptyset \times F}{760} \quad (2.11)$$

  - t_0: ambient air temperature, [^{0}C];
  - P_0: atmospheric pressure, [mmHg];
  - F: saturate vapor pressure, [mmHg];
  - $\emptyset$: Relative humidity of atmosphere [%].

In case of NOx emissions, the following equation is used to convert the unit from ppm to g/kWh.

$$GASx = \frac{U \times conc \times G_{exhaust}}{N_e} \times K_{hd} \quad (2.12)$$

$$K_{hd} = \frac{1}{1 - 0.0182 \times (H_a - 10.71) + 0.0045 \times (T_a - 298)} \quad (2.13)$$

where:

- T_a*:* temperature of air in surge air tank, [K];
- H_a*:* absolute humidity of air in surge tank;

$$H_a = \frac{6.22 \times R_a \times P_a}{P_b - P_a \times R_a \times 10^{-2}} \quad (2.14)$$

- R_a: relative humidity of intake air, [%];
- P_b*:* atmospheric pressure, [kPa];
- P_a*:* saturate vapor pressure, [kPa];

$$P_a(\mathrm{t}) = 6.11 \times 10^{\frac{7.5 \times \mathrm{t}}{\mathrm{t} + 237.3}}, [\mathrm{hPa}] \quad (2.15)$$

t: room air temperature, [^{o}C].

❖ **Fuel flow rate**

Flow rate of fuel was measured by micro flow meter during each step of the experiments.

2. 3 Research infrastructure

2. 3. 1 Diesel engine

In my current study, the engines using are four-stroke, high speed, direct injection, horizontal-single cylinder diesel engines to conduct the experiments. They were made by YANMAR diesel Maker with one model of YANMAR NFD 13-MEK, and the others is YANMAR NFD 13-ME. The former uses a mechanical fuel system including some main components such as mechanical fuel pump, and mechanical injector. The later uses a modified common rail fuel injection system from the original mechanical fuel system. To measure in-cylinder pressure, a pressure sensor was fitted into the modified engine body. The piston heads were also modified suitably for experiment setup, currently, they have cup-shape. The specifications of the engine are given in Table 2-2.

Table 2-2 Test engine specifications

Model	YANMAR NFD 13-MEK/ME
Engine Type	4-stroke, high speed, direct injection
Bore × Stroke	92 × 96 [mm]
Displacement	638 [cm^3]
Compression ratio	17.7
Rated output	8.1kW@2400rpm
Injection pump	Mechanical/Common rail type
Nozzle type	4-hole nozzle
Injector opening pressure	19 [MPa]

2. 3. 2 Fuel system

Mechanical fuel system includes a fuel tank, a jerk-type pump, and a fuel injector. These elements are connected together by fuel pipes. The fuel pump, which is driven from the cam shaft of the engine, supplies fuel from fuel tank to the combustion chamber through the injector under high pressure. The mechanical injector operates by balancing the force created by spring and the force creating from fuel pressure that acts on the conical surface of the needle. When the force generated from fuel pressure is larger than the spring force, the needle valve opens the injector and the injection commences.

For the common rail diesel engine, the conventional mechanical fuel system was replaced by a common rail injection system. The system was designed and modified by a Maker (FC Design Co. Ltd., Japan). The fuel pump and rail are Bosh type. The pump, which is driven by an electrical motor, supplies fuel from fuel tank to the common rail at a set pressure under the upper limit (130 MPa). The electronic injector of the common rail fuel system is connected to the mechanical injector of the engine. Under this condition, the fuel injection process not depends on only directly the electronic injector but also indirectly the mechanical injector. The opening timing of the electronic injector can be set through an electronic control unit (ECU). While the opening timing (injection timing) of the mechanical injector depend on the coming fuel pressure. Diagram

of the common rail system is presented in Fig. 2-1. Photos of fuel pump and rail, and injector are shown in Fig. 2-2, Fig. 2-3, respectively.

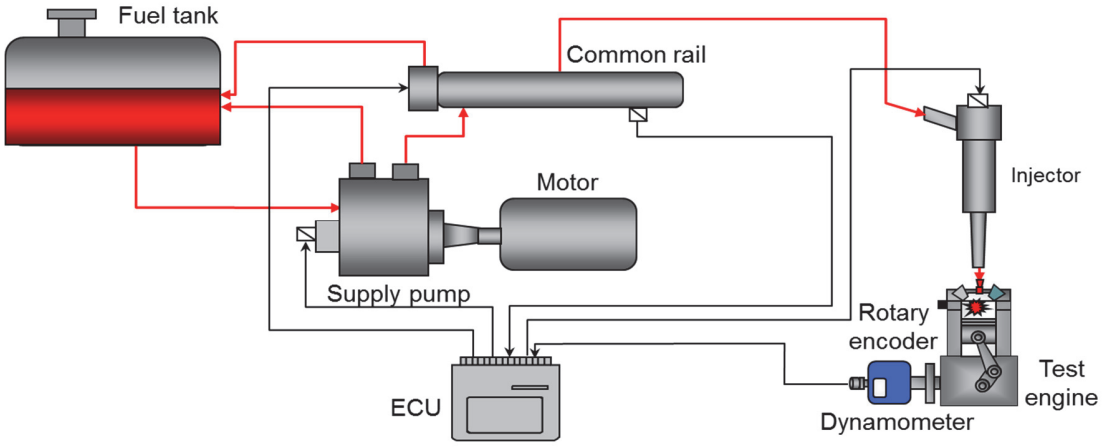

Figure 2-1 Fuel injection system diagram

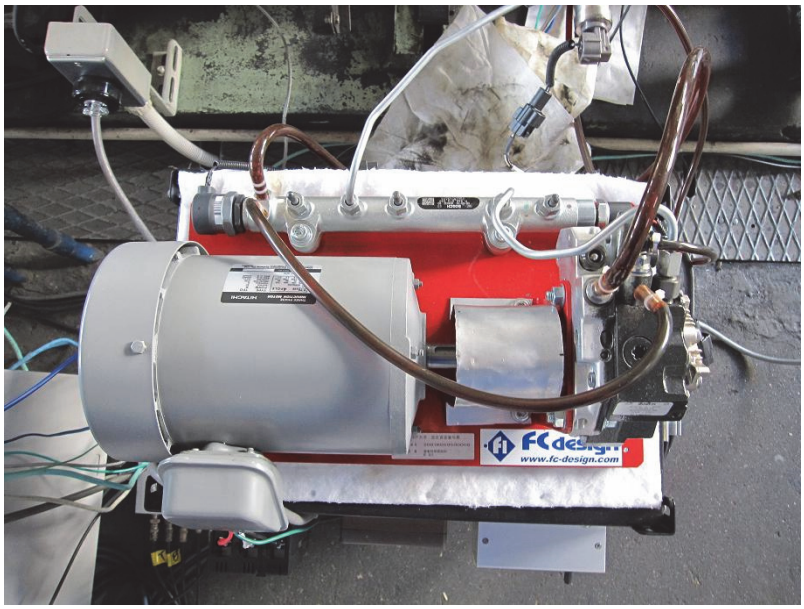

Figure 2-2 Photograph of fuel pump and common rail

The fuel rail pressure can be controlled on the ECU, while injection timing of the electronic injector can be set through the ECU or via the computer. By

changing the discharge rate of supply pump and the return rate from the rail, the rail pressure can be kept in a designed range. The system permits the injection of fuel with multiple injections by setting the number of injection time on the ECU or on the PC. The appearance of the ECU is shown in Fig. 2-4.

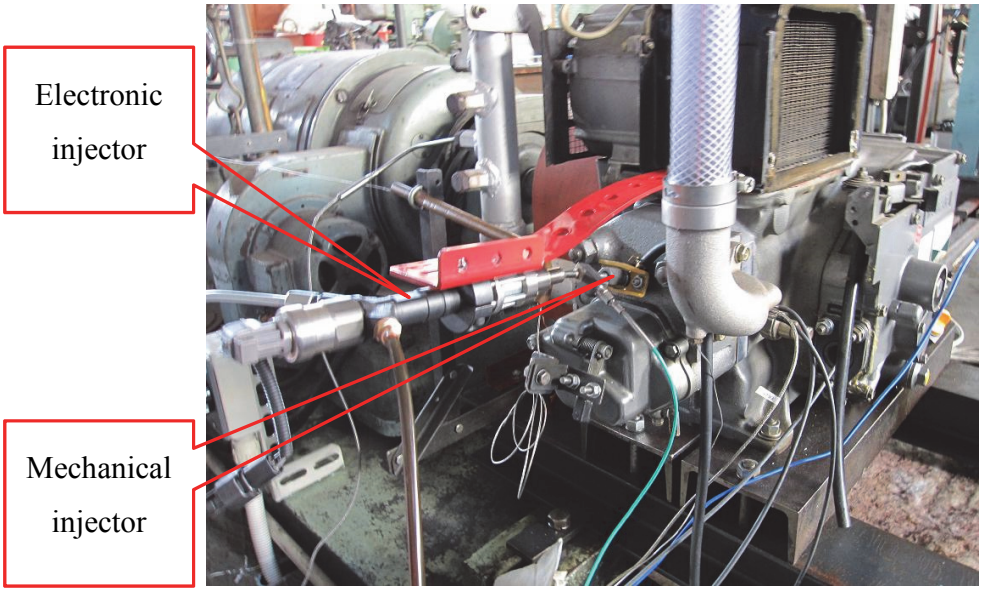

Figure 2-3 Photograph of fuel injectors

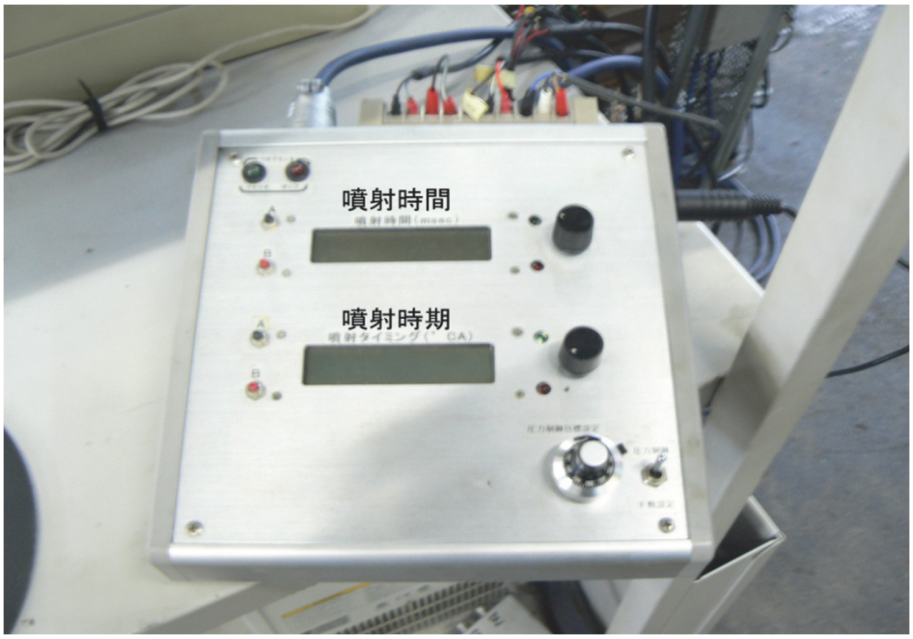

Figure 2-4 Appearance of ECU

2. 3. 3 Measuring system

To start up and to set the load for the common rail engine, an electrical dynamometer was used. This is three-phase electrical MVB361/6 dynamometer manufactured by Toyo Electric Mfg. Co., Ltd. The mechanical fueling engine is started up by an electrical starter powered by a battery, and is loaded by a water-dynamometer.

For in-cylinder pressure measurement, a piezoelectric pressure transducer (KISTLER) with model of 6061B combined with a digital charge amplifier with a model of 5041C was used. To record fuel injection pressure history, a pressure transducer with a model of 4067A (KISTLER) was fitted to the fuel line between electronic-injector and mechanical-injector. The signals of these pressures were magnified by an amplifier type 4618A2, and were transmitted to the combustion analyzer (Yokogawa). This is Yokogawa 4ch100ks combustion analyzer with measurement module of WE7245 was used to receive signal from pressure sensors. The output signals are supplied to the computer for monitoring, and recording pressure during the experiments. ;

To inject fuel at a proper timing, the crank angle monitoring is necessary. This is done by a RS-72 type rotary encoder (Ishikawajima-Harima Heavy Industries Co., Ltd.) coupled to the shaft of the engine. This encoder has an outer diameter of 42 mm, and has 720 pulses per rotation.

Intake air temperature, fuel tank temperature, and exhaust gas temperature were measured by thermal couples and recorded by a digital temperature recorder model 3874 (Yokogawa).

To measure fuel flow rate, a micro stream OF05ZAT-A0 type (Aichitokei denki) was used.

2. 3. 4 Emission analyzer, smoke meter, and PM sampler

Exhaust gas from the engine was conducted to emission analyzers including a series of O_2-CO_2-NOx analyzer, CO-HC analyzer, smoke meter, and particulate sampling unit to measure emissions and particulate dust concentration of the engine. Emissions were measured by HORIBA analyzers, while smoke was collected by BANZAI smoke meter DSM-10 type, and read by Bosch type smoke reader. NOx emissions were measured basing on chemiluminescence method. Emission of CO_2 is measured by non-dispersion equation infrared spectrometry. HC and CO emissions were measured by non-dispersive infrared analysis. A set of gas analyzers VIA-510, CLA-510SS (Horiba) was used to measure the emissions of CO_2, NOx, respectively, and along with MEXA-324J (Horiba) for measurement of CO, HC. A general sampling unit ES-C510SS type (Horiba) was used to servers the working of O_2-CO_2-NOx analyzers. Dust matters were trapped on the ADVANTEC PG-60 paper filters (glass fiber Fluorine coated filter, Toyo Roshi Kaisha, Ltd.) in 10 liters of exhaust gas at each step of the experiments with the help of a D-25UP gas sampler (OCT

science, Ltd.). The gas absorber containing silicagel was used for removal corrosive gas, moisture in the exhaust gas before coming into the gas sampler.

2. 3. 5 Fuel measuring and filtering equipment

Raw Jatropha oil, that had hold in large containers, was withdrawn to small container. However, mud and wax that was formed probably due to storing the fuel period of time. This impurity was eliminated from the fuel oil by filtering equipment that made at our lab. Filtering equipment included a fuel tank, a number of paper filters putted along the hold-drilled-tube positioned in the filtering fuel tank, and a lower container for filtering process. The photo of the filtering equipment is shown in Fig. 2-5.

Figure 2-5 Photo of fuel filtering equipment

I this study, I measured viscosity and specific gravity of tested fuels including Light oil, Jatropha oil, Jatropha water emulsion, and Jatropha hydrogen peroxide emulsions. To measure fuel viscosity, Brookfield DV-E, RV-model viscometer was used. The images of the viscometer and measurement rigs are shown in Fig. 2-6.

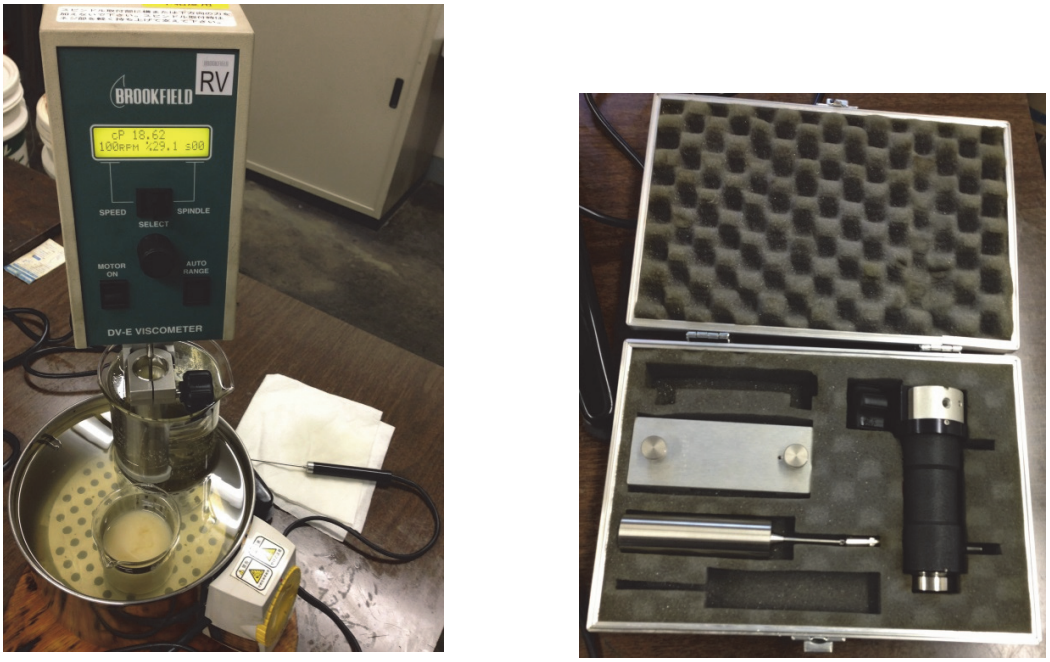

Figure 2-6 Photo of Viscometer and its rigs

Specific gravity of fuel was measured by hydrometer. Depending on fuel and temperature range, the different hydrometer in scale range was used for measurement. Densities of the fuels were calculated from the specific gravities those measured from the experiments.

2. 3. 6 Other device

Dust particle paper filter was use to collect and measure dust particulate concentration emits from the exhaust gas. The paper filters were kept in a dust

collector connecting to the exhaust pipe and the gas sampler. Paper filters were dried in a dryer (One Corporation ONW-450 type) and their mass were measured by a micro balance (Shimadzu, AUW120D model) and stored in the dry-sealed-pot before the experiments. The pictures of the dust collector, and micro balance are shown in Fig. 2-7 and Fig. 2-8, respectively.

Figure 2-7 Photo of dust collector

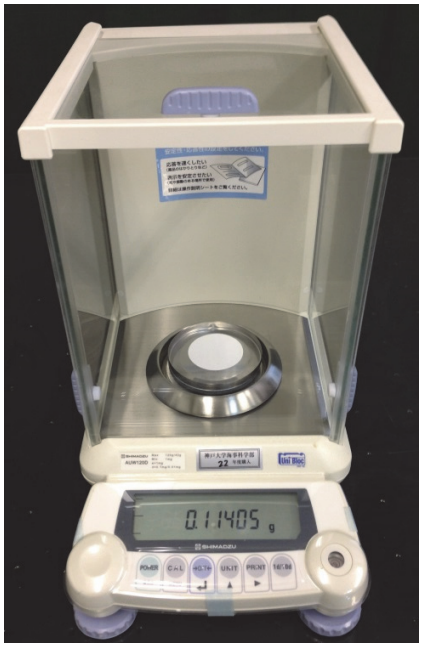

Figure 2-8 Photo of microbalance

Chapter 3 Effect of Injection Pattern to Neat Jatropha Oil Combustion in Direct Injection Diesel Engine

3. 1 Introduction

Recently, the use of diesel engines has been facing problems such as the fossil fuel crisis and air pollution. Harmful pollutants, namely Nitrogen oxides (NOx) and Particulate matter (PM), from diesel engines are very difficult to reduce simultaneously. Additionally, the production of the global warming gas (CO_2) is unavoidable whatever the fuel when using diesel engines. Vegetable oils, that are biodegradable, that have low aromatic and sulfur content, have recently gained attention as a promising alternative fuel for a greener future. Short-term tests have indicated that most vegetable oils are capable of being used directly in existing diesel engines with little or no modification. However, in long-term tests, some issues were reported such as piston ring sticking, injector coking, severe engine deposits, gum formation and oil thickening [56-58]. This is primarily attributed to the high viscosity and poor volatility due to their large molecular weight and bulky molecular structure. These physical properties of vegetable oils lead to poor atomization, inadequate mixing with air during injection and atomization process, consequently contribute to incomplete combustion when using vegetable oil as fuel for diesel engines. This results in an increase in particulate, CO, and HC emissions, but lowers NOx emissions compared to those when using diesel oil [33, 59-62]. Among vegetable oils,

Jatropha curcas has been of interest recently, because it is a non-edible oil, thus there is no issue of the food-fuel conflict [33].

Jatropha oil was identified as a leading candidate for an alternative fuel for commercialization among various non-edible vegetable oils [31]. Jatropha plant can be grown in semi-arid conditions on almost any kind of ground, and does not suffer excessively from droughts or require concentrated irrigation. Therefore, unlike other common biofuel crops, it is very easy to cultivate, even on poor soil. High viscosity, low volatility, and low cetane number of the Jatropha oil have been reported in previous studies [32, 34, 63]. M. S. Kumar et al. [33] observed higher smoke, HC, CO and NOx emissions of the engine operated with Jatropha oil. Lower NOx and break thermal efficiency, and higher CO, HC of Jatropha oil compared to those of diesel were reported by B. S. Chauhan et al. [35] due to the high viscosity and low volatility. Higher smoke, CO, HC emissions of Jatropha oil were also observed in the studies of D. Agarwal et al. [34], J. N. Reddy et al. [64], and A. S. Ramadhas et al. [65]. The drawbacks of Jatropha oil could be overcome by preheating [35] or esterification and blending with diesel [66, 67], increased injection pressure, or perhaps a dual fuel engine.

Advanced injection timing increases the peak pressure resulting in increase of NOx, and reduction of HC, CO, and smoke as reported previously [68, 69]. This is consequence of more available time for oxidation process. Conversely,

retarded injection timing shifts the combustion to the later phase, lowers peak of pressure, and shortens resident time of high temperature, results in reduction of NOx emissions. Multiple injections are reported to be successful in reducing NOx emissions due to the cooling effect of the second injection [36], lower peak pressures, and lower peak of heat release rate [70], or lower combustion temperatures and resident time of high temperatures [39]. L.D.K. Nguyen [36] reported that reduction of soot was due to reduced precursor formation and increased soot oxidation in split injection.

From this one might surmise that multiple injections may reduce NOx and particulate of a diesel engine fueled with Jatropha oil. However, this test has not been tried to the best of our knowledge. Our experimental research was conducted to remedy this. In this chapter I studied experimentally the influence of double injection timings in term of main- and after-injection, and amount of after-injection on the combustion, performance, and emissions of a high speed, 4-troke, direct injection diesel engine fueled with neat Jatropha oil. Combustion, performance parameters such as in-cylinder pressure, rate of heat release, ignition delay, and thermal efficiency; and emissions of CO, CO_2, HC, NOx, and dust were analyzed according to double injections with various injection timings, and amount of after-injection.

3. 2 Experimental setup and procedures

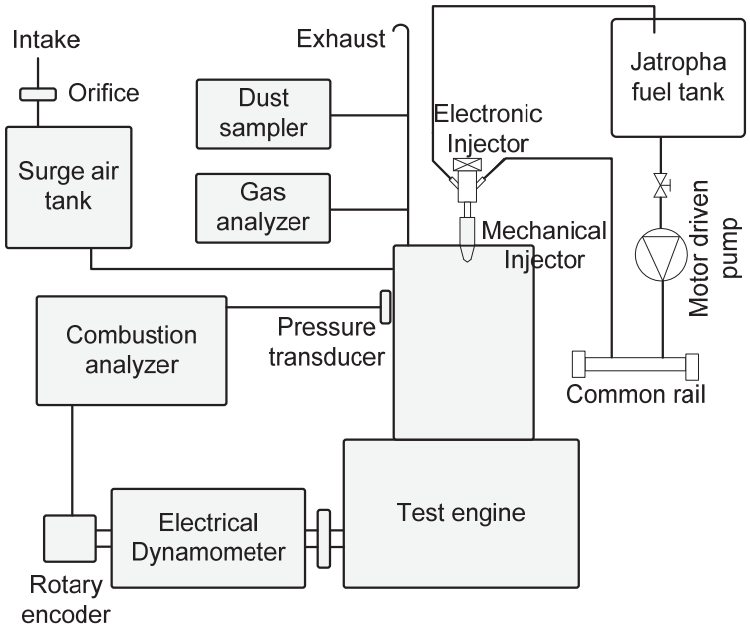

Fig. 3-1 Schematic diagram of experimental setup

Table 3-1 Specification of test engine

Model	YANMAR NFD 13-ME
Engine type	Horizontal, single cylinder, four stroke engine
Combustion type	Direct injection
Bore × Stroke	92 × 96 mm
Displacement	0.638 liter
Compression ratio	17.7
Rated output	8.1 kW @ 2400 rpm
Injection nozzle	4-hole nozzle
Nozzle opening pressure	19MPa

Experiments were conducted on a single cylinder, four-stroke, high speed, direct injection diesel engine (Yanmar Co., Ltd., Japan). A schematic diagram of the experimental setup is illustrated in Fig. 3-1, and the main specifications of the test engine are given in Table 3-1. The mechanical fuel injection system

of the engine was replaced by a common rail injection system, however, mechanical injector was remained. Main components of the common rail system include a motor-driven-pump (radial piston pump), a common rail (high pressure tube), an electronic injector, and an electronic control unit. The ECU was connected to a computer via a combustion analyzer (Yokogawa) to record the data. Injection parameters such as injection timing, injection duration, injection mode, along with rail pressure can be displayed on the ECU screen. Rail pressure can also be adjusted via the ECU, while, injection timing, and injection duration can be set through the ECU or the computer. The electronic injector of the common rail system is connected to the engine's mechanical injector used to inject the fuel into the combustion chamber. The in-cylinder pressures were measured using a piezoelectric pressure transducer (Kistler) fitted into the cylinder of the engine and connected to a charge amplifier. The signals from the pressure transducer and the shaft encoder were acquired and transmitted to the computer via the combustion analyzer for recording the in-cylinder pressure and crank angle. Load of the engine was set through an electrical-dynamometer (Toyo Electric Co., Ltd.) coupled to the shaft of the engine. A set of gas analyzers VIA-510, CLA-510SS (Horiba) was used to measure the emissions of CO_2, NOx, respectively, and along with MEXA-324J (Horiba) for measurement of CO, HC. Dust matters were trapped on the ADVANTEC PG-60 paper filters (glass fiber Fluorine coated filter, Toyo Roshi

Kaisha, Ltd.) in 10 liters of exhaust gas at each step of the experiments with the help of a D-25UP gas sampler (OCT science, Ltd.). The paper filters were kept in a dust collector connecting to the exhaust pipe and the gas sampler. In each experiment step, I collected the dust on 4 paper filter sheets. The trapped paper filters were then dried at 50 ^{o}C in one hour to eliminate water content in the filters. They were averaged from the differences of the mass of the trapped filters and the mass original paper filters. These were dust. Afterward, soluble organic fraction in the dust trapped filters was dissolved by dichloromethane and was calculated by balancing the mass of the filters before and after extraction (average value). In-soluble organic fraction was calculated by subtraction of the paper filter mass after SOF dissolving and the original filter.

Table 3-2 Properties of test fuels [33]

Properties	Diesel	Jatropha
Density (kg/m^3)	840	918.6
Viscosity (cSt)	4.59	49.93
Cetane number	45-55	40-45
Flash point (^{o}C)	50	240

The engine was fed with neat Jatropha oil at room temperature and the data was recorded at each setting power of 3.0 kW, 4.5 kW, and 6.0 kW with a speed of 2000 rpm. Properties of Jatropha oil compared with diesel are given in Table 3-2. In this study, I tested double injections with various timings of main- and

after-injection those given in Table 3-3; and various after-injection quantities those given in Table 3-4. Gas emissions were read from the analyzers. While, dust was captured on paper filters from 10 liters of exhaust gas, and was analyzed into soluble organic fraction (SOF) and in-soluble organic fraction (ISF). It is emphasized that interval between injections was kept constant at lower loads (3.0 and 4.5 kW). Perhaps, at 6.0 kW, affected by main-injection, thus after-injections occurred later.

Table 3-3 Set of injection timings

Power [kW]	Injection timings *				
3.0	m-15,a-2.5	m-13,a-0.5	m-11,a+1.5	m-9,a+3.5	m-7,a+5.5
4.5	m-15,a-2.5	m-13,a-0.5	m-11,a+1.5	m-9,a+3.5	m-7,a+5.5
6.0	m-15,a+0.5	m-13,a+3.0	m-11,a+6.0	m-9,a+7.5	m-7,a+11

* m, and a indicated for main- and after-injection, respectively

3. 3 Results and discussions

3. 3. 1 Effect of Injection timing

3. 3. 1. 1 Combustion and performance characteristics

The pressure data was collected in 4 times at each step, and we checked their consistency during experiments. After finding their consistency, we selected one among the recorded data for analyzing.

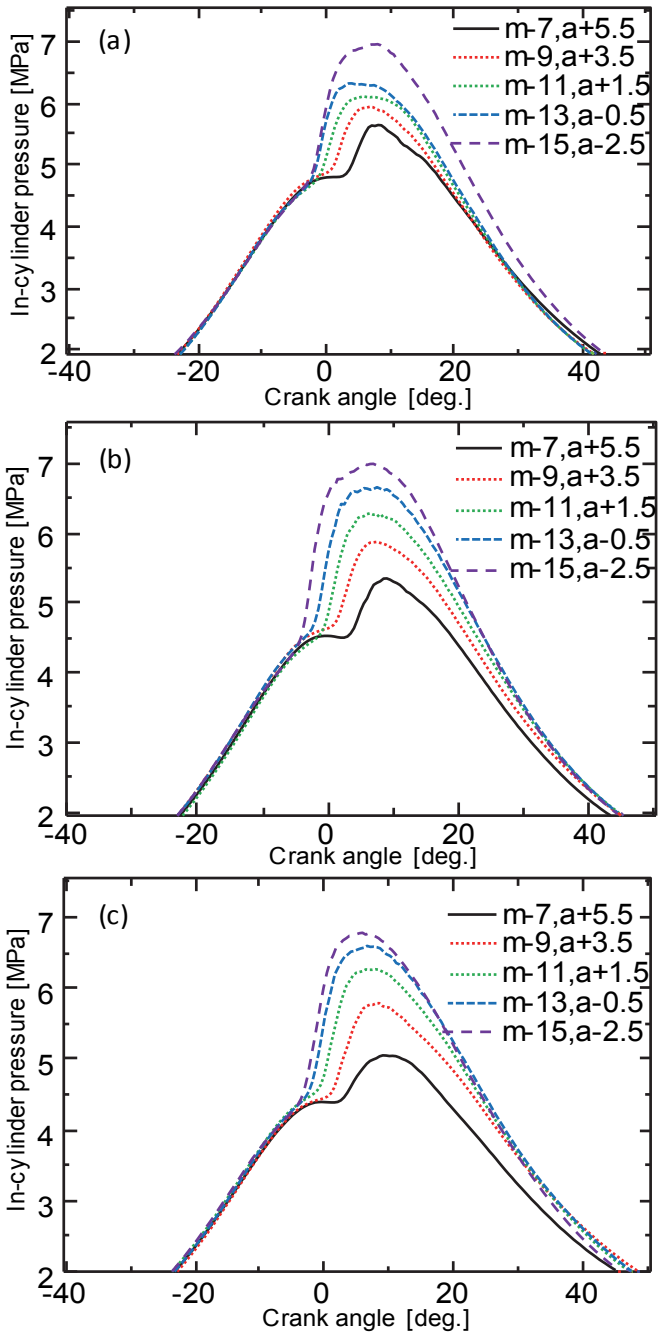

Figure 3-2 In-cylinder pressure with different double injection timings at (a) 3.0 kW, (b) 4.5 kW, (c) 6.0 kW @ 2000 rpm

In-cylinder pressure is indicated in Fig. 3-2. It can be seen that fast development of the pressures with advanced injection timings as a result of the accumulated fuel combusting near the top dead center (TDC). For late injections, the peak

pressures substantially reduced due to the combustion occurred after the TDC. At 6.0 kW, the peak pressures were lower than those of lower loads due to the fact that second injection could be affected by first one. This increases residual gases as a role of internal exhaust gases reducing the peak pressures.

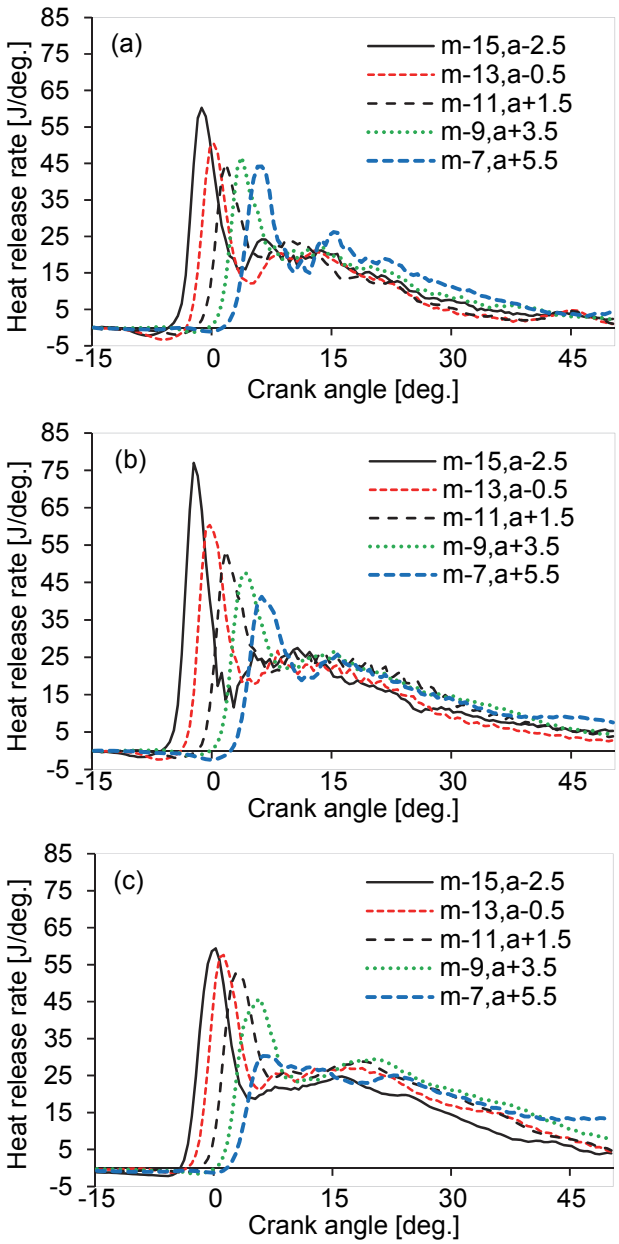

Figure 3-3 Heat release rate with different double injection timings at (a) 3.0 kW, (b) 4.5 kW, (c) 6.0 kW @ 2000 rpm

Heat release rate (HRR) is shown in Fig. 3-3. At 3.0, 4.5, and 6.0 kW, the peaks of HRR reduced significantly when double timings were retarded. It reduced from 60.2, 77 and 59.4 J/deg. of m-15,a-2.5 to 44.2, 41.2, and 30.3 J/deg. of m-7,a+5.5 with a relative reduction of 26.6, 46, and 48.9%, respectively. This can be attributed to less accumulated fuel during the ignition delay period as a result of the better combustion conditions with later injection timings. Moreover, the cooling effect of second injection could also reduce the peak of HRR. In the other hand, later double injection timings increased HRR at the later combustion stages. When compared with lower loads, the peaks of HRR at 6.0 kW were lower as a result of much more internal exhaust gases.

Ignition delay (ID) is indicated in Fig. 3-4a. ID increased slightly when double timings were advanced as a result of worse combustion conditions with early injection timing when compared with timing near the TDC. Slight reduction can be observed at 4.5 kW when compared with those at 3.0 kW. This may resulted from the better conditions for combustion at higher engine load. ID slightly increased again at 6.0 kW. This can be attributed to the rich fuel sprays at high load, and the imperfect gas exchange process.

Brake thermal efficiency (BTE) is depicted in Fig. 3-4b. It was higher for higher engine loads since the better combustion conditions. At 3.0 and 4.5 kW, for timings between m-9,a+3.5 and m-13,a-0.5, BTE were comparable at

around of 21.3 and 26.4%, , respectively, while they were 20.2, and 24.3% for m-7,a+5.5. At 6.0 kW, BTE reached to 26.5% for m-11,a+1.5, while for m-7,a+5.5 and m-15, a-2.5, they were 23.5 and 25%, respectively. Late injection increases heat lost due to the late combustion phase, while early injection develops negative work before the TDC. Overall, the optimum timings were between m-11,a+1.5 and m-13,a-0.5.

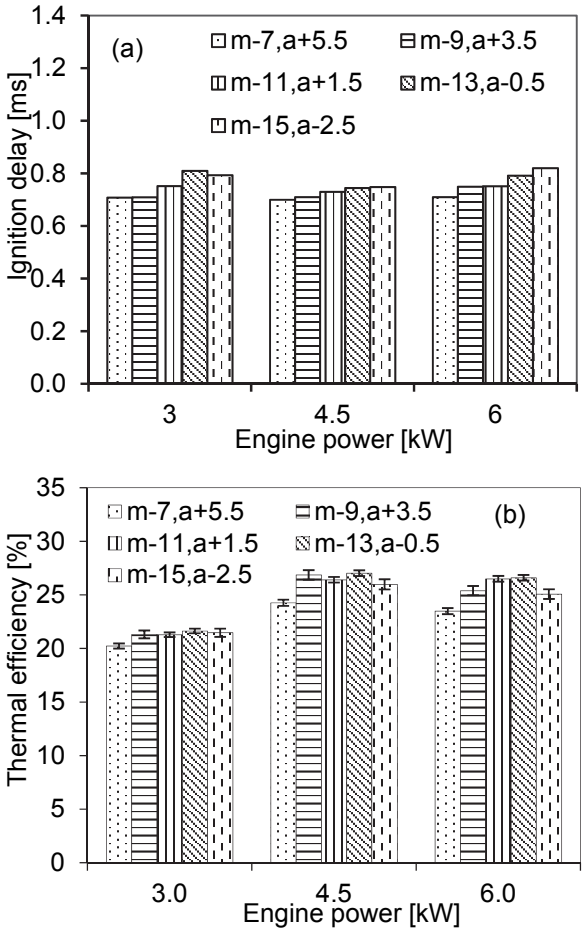

Figure 3-4 (a) Ignition delay, and (b) break thermal efficiency with different double injection timings @ 2000 rpm

3. 3. 1. 2 Emission characteristics

The emissions of the engine including CO_2, CO, HC, NOx, smoke, dust, SOF, and ISF concentration are indicated in Fig. 3-5.

Fig. 3-5a shows the reduction of CO_2 with an increase in the power as a result of better combustion conditions at higher loads. In comparison with m-7,a+5.5, it was observed a reduction of CO_2 of 6.0 and 11.5% for m-11,a-1.5, while it was 6.9, 11.6% for m-13,a-0.5 at 4.5 kW and 6.0 kW, respectively. At 3.0 kW, m-13,a-0.5 had a reduction of 4.8%. This may result from the better thermal efficiency at these timings. Early or late injection lowers BTE resulting in an increase in fuel injection, and increase in emission of CO_2.

CO emissions are shown in Fig. 3-5b. At 3.0 kW, there are small differences between emissions of CO with different timings due to less injected fuel at low load. At 4.5 and 6.0 kW, there is a sudden reduction of 66.4, 24.8% for m-11,a+1.5, and 72.1, 18.4% for m-13,a-0.5 when compared with m-7,a+5.5. At 6.0 kW, early or late injection induced high emissions of CO due to the inferior combustion conditions, and the shorten time for oxidation, respectively.

In comparison with 3.0 kW, except two early injection patterns, CO emissions reduced at 4.5 kW due to not only better combustion conditions but also not rich enough fuel injection. 6.0 kW produced the local rich fuel zone leading to high increment of CO emissions.

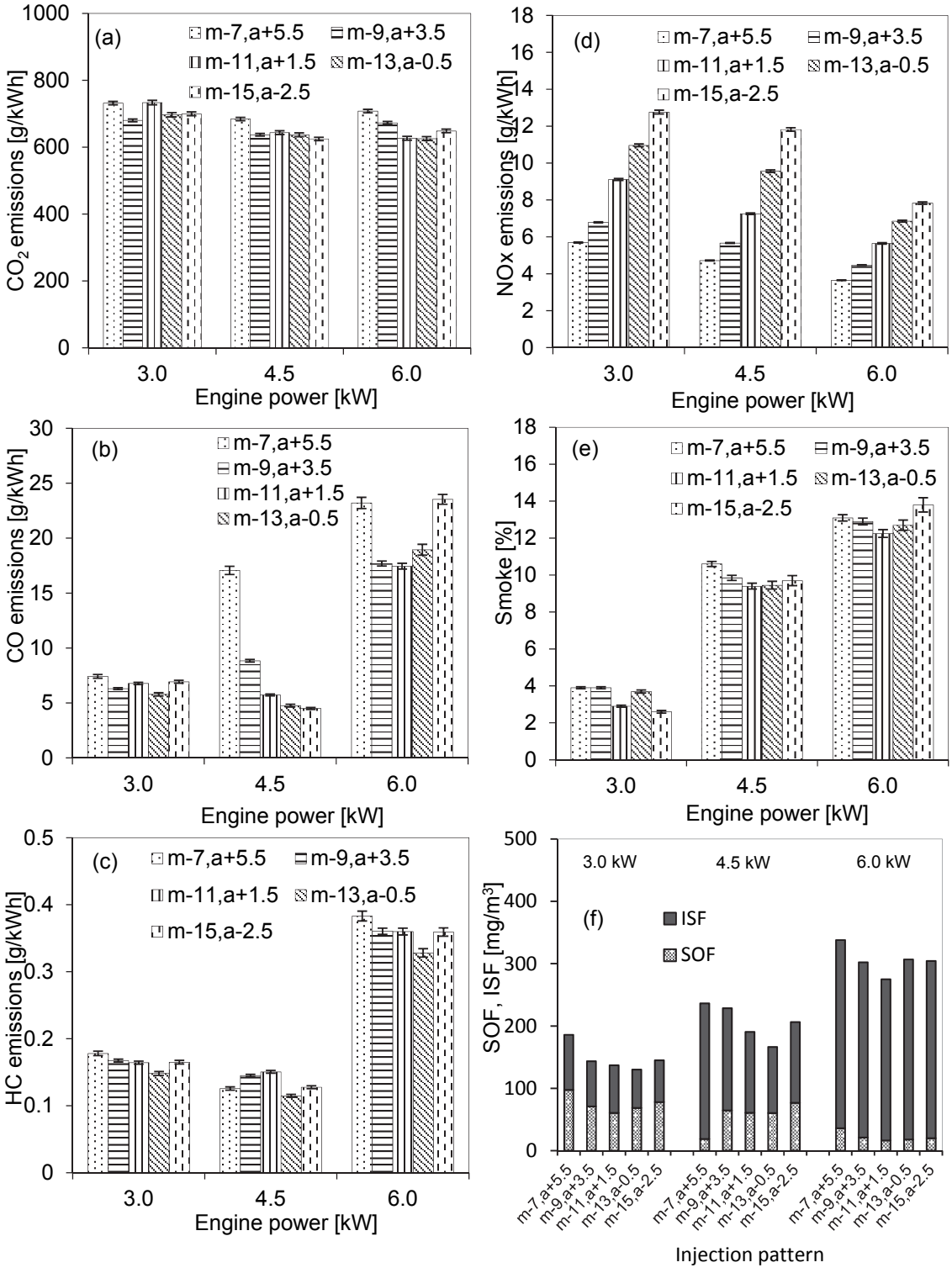

Figure 3-5 Exhaust emissions with different timings of main-injection and after-injection

Fig. 3-5c indicates HC emissions. When compared with 3.0 kW, HC decreased at the engine power of 4.5 kW and increased significantly at 6.0 kW. The former is due to the better combustion conditions, the latter is consequence of local rich fuel injections. The optimum timings were at m-13,a-0.5 at which it had a reduction of 16.8, 8.6, and 14.3% in comparison with m-7,a+5.5 at 3.0, 4.5, and 6.0 kW, respectively. Other double timings had a comparative or slight difference in emissions of HC.

NOx emissions are depicted in Fig. 3-5d. The emissions of NOx decreased with an increase in the engine power and with retarded double timings. Timings of m-7,a+5.5 considerably reduced NOx of 37.5, 35, and 35.3% when compared with m-11,a+1.5, while the reduction was 48, 50.7, and 46.7% when compared with m-13,a-0.5. The reduction of the NOx emissions with retarded double injections can be attributed to the reduction of peaks pressure and peaks HRR as result of less accumulated fuel in delay period, and the cooling effect of second injection.

Smoke is shown in Fig. 3-5e. Smoke increased substantially with an increase in the engine power as result of rich combustion conditions at higher loads. At higher loads, m-11,a+1.5 had a slight reduction of 4.6, and 5% when compared with early or late injections. This is due to early and late injections needed much more fuel to offset the negative work, and heat loss, respectively.

Dust concentration is indicated in Fig. 3-5f. Dust concentration increased with an increase of the engine load. The main component of dust is ISF especially for higher loads. These resulted from richer injection and higher combustion temperatures which enhanced ISF growth. The optimum timing for dust concentration was at m-11,a+1.5 or m-13,a-0.5 with a reduction of 30, and 18%.

3. 3. 2 Effect of amount of after-injection

Timings of m-11,a+1.5 were tested with small and large amount of after-injection so-called m-11,a+1.5-S and m-11,a+1.5-L those given in Table 3-4.

Table 3-4 Quantity of fuel in different injection patterns

Power [kW]	Injection patterns	main-injection [mg/cycle]	after-injection [mg/cycle]
3.0	m-11,a+1.5-S	8.48	2.69
	m-11,a+1.5-L	7.15	4.86
4.5	m-11,a+1.5-S	10.9	4.35
	m-11,a+1.5-L	9.6	5.05
6.0	m-11,a+6.0-S	17.8	3.15
	m-11,a+6.0-L	16.5	4.35

3. 3. 2. 1 Combustion and performance characteristics

In-cylinder pressure is illustrated in Fig. 3-6. The peak pressures were 6.1 and 6.3 MPa for m-11,a+1.5-S at 3.0 and 4.5 kW, while it dropped to 5.6 and 5.5 MPa for m-11,a+1.5-L with a relative reduction of 8.2 and 12.7%. At 6.0 kW they were comparable at around 6.3 MPa. At lower loads, the peak pressures

significantly reduced for m-11,a+1.5L since they were determined mainly by main-injections.

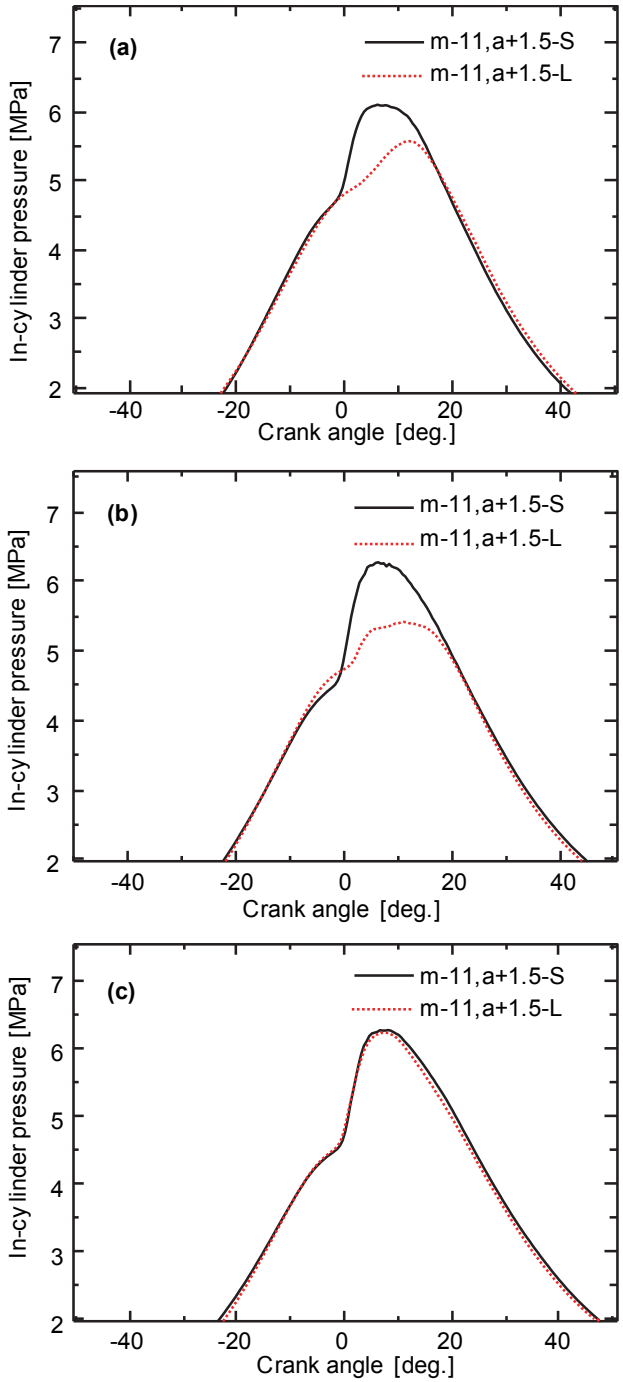

Figure 3-6 In-cylinder pressure with different amounts of after-injection at (a) 4.5 kW, (b) 4.5 kW, (c) 6.0 kW @ 2000 rpm

Perhaps, at lower loads, the differences in main-injections amounts could lead to this difference, but at 6.0 kW it could not make difference due to the upper threshold of pressures at these timings.

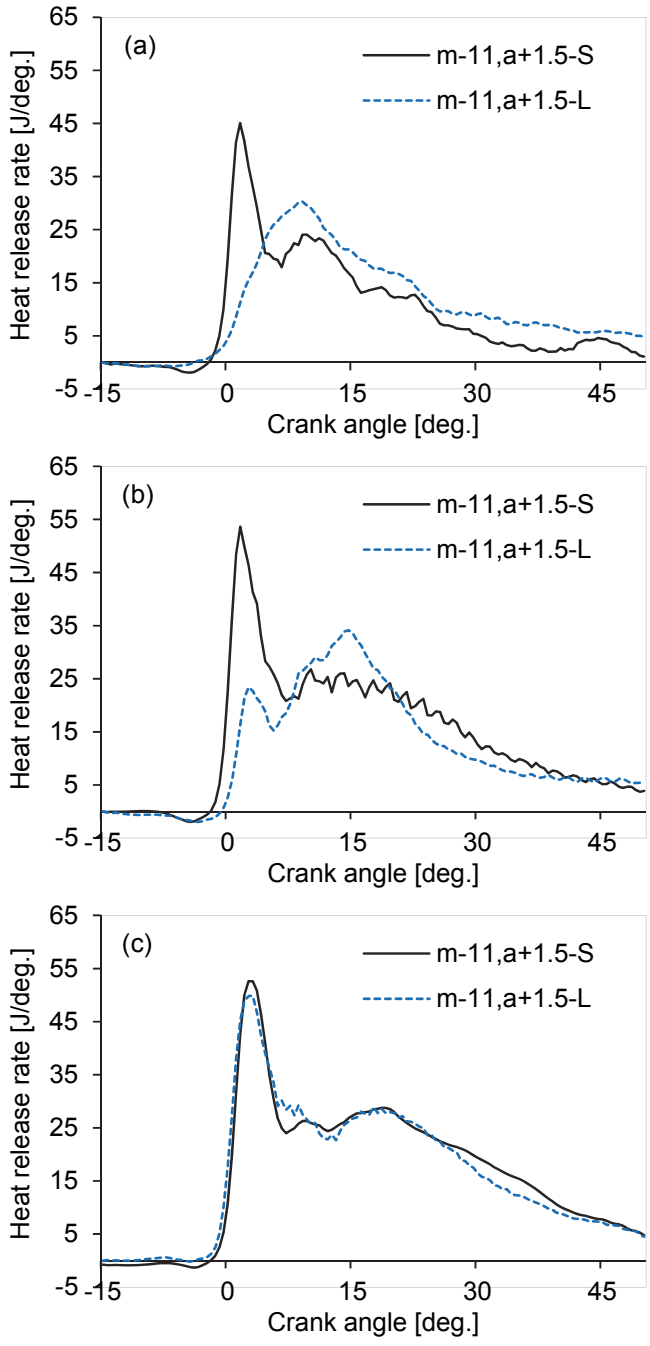

Figure 3-7 Heat release rate with different amounts of after-injection at (a) 4.5 kW, (b) 4.5 kW, (c) 6.0 kW @ 2000 rpm

HRR is shown in Fig. 3-7. Peaks of HRR had a reduction of 32.8, 36.3, and 5.2% when dropped from 45, 53.6, and 52.6 J/deg of m-11,a+1.5-L to 30.3, 34.2, and 49.4 J/deg. of m-11,a+1.5-S at 3.0, 4.5, and 6.0 kW, respectively. These reductions resulted from the reduction of peak pressures as illustrated in Fig. 7. Moreover, the peak HRR of m-11,a+1.5-S was near the TDC, while it was far from the TDC for m-11,a+1.5-L at lower loads. At 4.5 kW large enough amounts of after-injections created second peak. At 6.0 kW, comparable pressures resulted in comparable HRR.

Break thermal efficiency is indicated in Fig. 3-8. It is evident that m-11,a+1.5-L reduced BTE. This resulted from the lower HRR and late combustion, thus much more heat lost when the piston moved toward the BDC. Conversely, less heat loss for m-11,a+1.5-S increased the BTE.

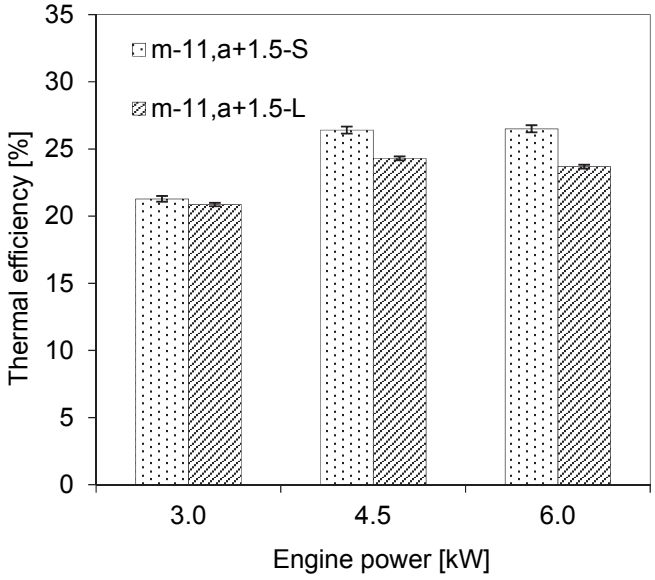

Figure 3-8 Thermal efficiency with different amounts of after-injection @ 2000 rpm

3. 3. 2. 2 Emission characteristics

Fig. 3-9a shows that CO_2 emissions reduced particularly at higher loads when using m-11,a+1.5-S with a relative reduction of 2.6, 7.0, and 11.1% for 3.0, 4.5, and 6.0 kW. Lower specific fuel consumption as consequence of better BTE of m-11,a+1.5-S resulted in lower CO_2. Conversely, more heat lost for m-11,a+1.5-L increased specific fuel consumption, consequently increased CO_2.

Fig. 3-9b indicates emissions of CO. There was a significant reduction of CO of 50, 78, and 49% for m-11,a+1.5-S at 3.0, 4.5, and 6.0 kW. Moreover, for m-11,a+1.5-S, emissions of CO decreased slightly at 4.5 kW before increasing at 6.0 kW as result of better combustion conditions and not so rich enough of fuel injection. At 6.0 kW, late combustion phase as a result of delayed after-injection along with the local rich fuel injection resulted in higher CO emissions. The phenomenon is more conspicuous for m-11,a+1.5-L.

Fig. 3-9c shows higher HC emissions for m-11,a+1.5-S when compared with m-11,a+1.5-L. The relative increment was 77.8% at 4.5 kW, while it increased 7.5-fold at 6.0 kW. HC increased with an increase of the engine power for m-11,a+1.5-S, while it reduced with m-11,a+1.5-L. Perhaps, more fuel in main-injection for m-11,a+1.5-S along with main-injection near the TDC, the injection jets could impinge the piston head, consequently resulted in higher HC. Conversely, the m-11,a+1.5-L reduced fuel impingement when after-injection combusted very fast after injection, consequently, reduced HC.

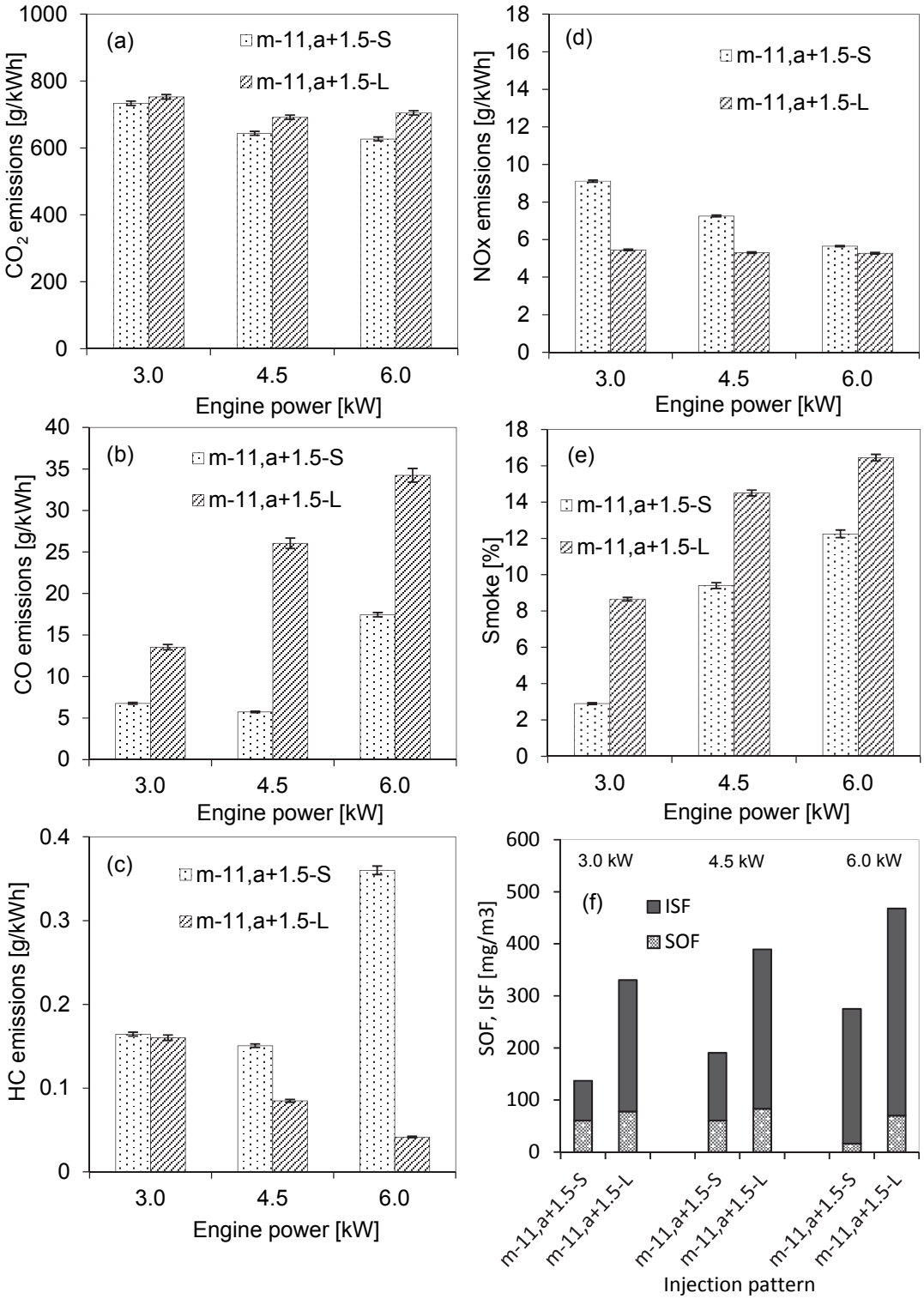

Figure 3-9 Exhaust emissions with different amounts of after-injection @ 2000 rpm

Emissions of NOx decreased with an increase of the engine power as illustrated in Fig. 3-9d. For m-11,a+1.5-L, the reductions of NOx were observed of 40.2, 26.9, and 6.7% at 3.0, 4.5, and 6.0 kW. At lower loads, larger reduction in emissions of NOx were observed for m-11,a+1.5-L as a result of considerably suppressed of premixed combustion as indicated obviously in the HRR graph.

Smoke is depicted in Fig. 3-9e. It increased with an increase in the engine power and with m-11,a+1.5-L. For m-11,a+1.5-L, smoke had a relative increment of 198.3, 54.3, and 34.3% when compared to those of m-11,a+1.5-S at 3.0, 4.5, and 6.0 kW. This resulted from the local rich injection at higher loads, and the late combustion phase of m-11,a+1.5-L as a result of increased residual gas for m-11,a+1.5-L.

Fig. 3-9f shows dust concentration. It can be seen that dust and ISF concentration increased with an increase of the engine load, especially, for m-11,a+1.5-L. This resulted from the higher fuel consumption, the shorten time for soot oxidation due to the late combustion phase. When compared with m-11,a+1.5-S, we observed a relative increment of 141, 104, and 70% for m-11,a+1.5-L at 3.0, 4.5, 6.0 kW, respectively. Concentration of SOF slightly decreased with load of the engine as consequence of better combustion condition.

3. 4 Summary

I studied the effects of double injection with various timings of main-injection and after-injection, and amounts of after-injection on the combustion, engine performance, and emissions characteristics of a diesel engine fuelled with Jatropha oil. In summary, the main features are as follows.

1. Effect of double injection timings

i. Retarded double timings significantly reduced the peaks of combustion pressure, peaks of HRR, and shifted the combustion to the later phase. Late double timings increased HRR at the later combustion stage.

ii. There was slight reduction of ID for retarded double timings at low load; ID increased slightly at 6.0 kW due to imperfect gas exchange. Optimum double injection timings for BTE were between m-11,a+1.5 and m-13,a-0.5.

iii. Emissions of CO_2, CO, HC, Smoke and dust were lower at timings between m-11,a+1.5 and m-13,a-0.5. Late double timings significantly reduced emissions of NOx.

Overall, the optimum injection timings for combustion, performance, and emissions were between m-11,a+1.5 and m-13,a-0.5.

2. Effect of amount of after-injection

Timing of m-11,a+1.5 was tested with small and large amounts of after-injection. We found a considerably influence to the combustion, performance and emissions.

i. Peaks of cylinder pressure and HRR were remarkably reduced with m-11,a+1.5-L at 3.0 and 4.5 kW. Otherwise, they were comparable at 6.0 kW with a minor reduction of peak HRR with m-11,a+1.5-L.

ii. When compared with m-11,a+1.5-S, the injection pattern of m-11,a+1.5-L reduced BTE especially at higher engine loads.

iii. For m-11,a+1.5-S, reduction of emissions of CO_2, CO, smoke and dust concentration was observed, while it increased emissions of NOx, and HC.

Chapter 4 Effect of Double Injection on Combustion, Performance, and Emissions of Jatropha Water Emulsion Fueled Direct Injection Diesel Engine

4. 1 Introduction

Advanced injection strategies are reported to be successful in reducing NOx emissions. The reduction of NOx is attributed to the cooling effect of the secondary injection [36]; the reduction of peak combustion pressure and peak heat release at the premixed combustion phase [37, 38]; or the lower combustion temperatures and resident time of high temperatures [39]. The reduction of soot has been revealed in the literature [36-38, 40, 41] due to the reduction in precursor formation; the reduction in particulate number concentration; the enhanced soot oxidation by second injection [36, 39, 40]; and the leaning-out spray and improved mixing with air [38, 41]. However, research has also reported a reverse trend of higher NOx [40] and higher particulate [42] with split injection.

The usage of water emulsion fuel is a well-known way to significantly reduce NOx emissions, and soot/PM from diesel engines as proven in the literature [43, 44-46]. The reduction of NOx is attributed to the cooling effect of the vaporization of water in the emulsion fuel [44-47]. While the reduction of soot is seen as a consequence of the better atomization and mixing with air resulting

from micro-explosion [44, 46]; or the presence of OH radicals releasing during the combustion process [44, 46]; or more air entrainment [47]. From this one might surmise that a combination of an advanced injection strategy with Jatropha water emulsion may reduce both NOx emissions and soot in diesel engine. However, as yet this combination has not been tried to the best of my knowledge.

My experimental study was conducted to remedy this situation. I investigated the effect of double injections pattern and Jatropha water emulsion on the combustion, performance, and emissions characteristics of a diesel engine. The double injections with various injection timings, and injection quantities of second injections were investigated in this study, while the first injections were fixed at the same timing.

4. 2 Material, experimental setup and procedures

This experimental study was conducted on the same engine whose parameter was given in chapter 3. The scheme of experimental setup is shown in Fig. 4-1. I also used the same combustion and emissions apparatus for measurements of the experiments. Procedures and method to conduct experiments were the same with those presented in Chapter 3. However, the fuel was changed. Measurements were carried out using Light oil, Jatropha oil, and JWE with a mixing rate of 10%. To make the emulsion fuel, a mixing system with a tank for JO; a tank for water; a circulating pump; and a static mixer was used. To keep

the emulsion fuel homogeneous and stable, three kinds of surfactants (Rheodol SP-L 10, Rheodol 440V, and Emulgen 103, Kao Chemicals Corp., Japan) were used. Specifications of the surfactants are given in Table 4-1. A schematic diagram of the mixing system is shown in Fig. 4-2. The engine was fed with LO, and JO with single injection at the injection timing set by the engine Maker of -17 deg. CA. ATDC for baseline data.

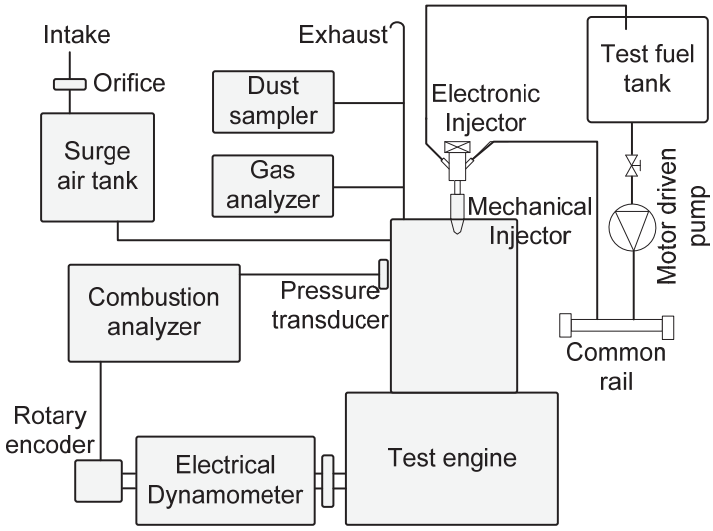

Figure 4-1 Schematic diagram of experimental setup

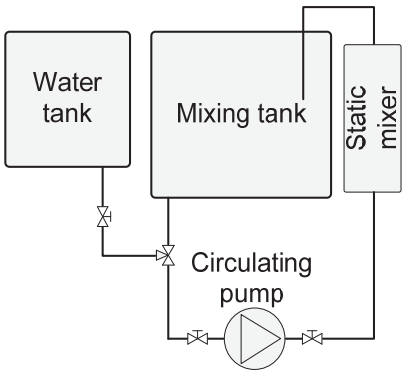

Figure 4-2 Schematic diagram of mixing system

Table 4-1 Specifications of surfactants [chemical.kao.com]

	RHEODOL SP-L10	RHEODOL 440V	EMULGEN 103
Chemical name	Sorbitan monolaurate	Polyoxyethylene sorbitol tetraoleate	Polyoxyethylene lauryl ether
Appearance	Liquid	Liquid	Liquid
Freezing point (°C)	13-14	-	-
Acid value	4-7	10>	-
Saponification value	158-170	72-92	-
HLB	8.6	11.8	8.1

Table 4-2 Injection duration of each experiment [msec.] (* first injection/second injection)

Power	Speed			**JWE10%**							
[kW]	[rpm]	**LO**	**JO**	JWE-23/0*		JWE-23/+3-large*		JWE-23/+3-small*		JWE-23/+6*	
3.0	2000	0.925	0.989	0.681	0.811	0.699	0.895	0.864	0.600	0.904	0.558
4.5	2000	1.017	0.1087	0.709	0.902	0.725	1.045	0.932	0.650	0.929	0.676
6.0	2000	1.149	1.196	0.710	1.122	0.726	1.140	0.964	0.657	0.989	0.695

To investigate the effect of injection pattern and the JWE, the first injection was kept at -23 deg. ATDC and the second injection was set at 0, +3, +6 deg. ATDC for double injection mode. After a preliminary investigation for the lowest smoke opacity, the optimum timing of second injection was chosen to conduct experiments for measurement of dust, soluble and in-soluble organic fraction with different injection quantities in the second injection (hereafter called small and large). The experimental conditions (injection durations) are provided in Table 4-2.

The mass of Jatropha and water was weighed to create emulsion fuel prior to the experiments with a 10% mixing ratio of water. While, the Jatropha oil was circulating from the tank through the pump, the water was supplied from the

water tank through a needle valve which was used to control mixing rate for a homogeneous mixture of emulsion fuel. Table 4-3 provides the properties of the test fuels. All experimental steps were conducted at room temperature and the results were recorded at steady operational conditions of the engine. During the experiments, the engine load was set at different values of 3.0 kW, 4.5 kW, and 6.0 kW with a speed of 2000 rpm, while the rail pressure was kept at 100 MPa. The gas emissions including CO, CO_2, HC, smoke, and NOx were read during each step of the experiments. While, dust was captured on paper filters from 10 liters of exhaust gas for analysis after each experiment when using the small and large second injection amount. The soluble organic fractions (SOF) were extracted from the dust-captured on the filters by dichloromethane. By balancing the mass of the filters before and after the experiments, and after chemical treatment, the concentration of dust, in-soluble organic fraction (ISF), and SOF were determined.

Table 4-3 Properties of test fuels

Parameter		Light oil	JO	JWE10%
Density (kg/m^3) at 30 deg. C	[*]	821.45	895.4	913
Lower heating value (kJ/kg)		42490	39774	-
Viscosity (cSt) at 30 deg. C	[*]	19.1	44.7	48
Cetane number	[**]	45-55	40-45	-
Flash point (^{o}C)	[**]	50	240	-

[*]: measured values, [**] from [33]

4. 3 Results and discussions

4. 3. 1 Combustion characteristics

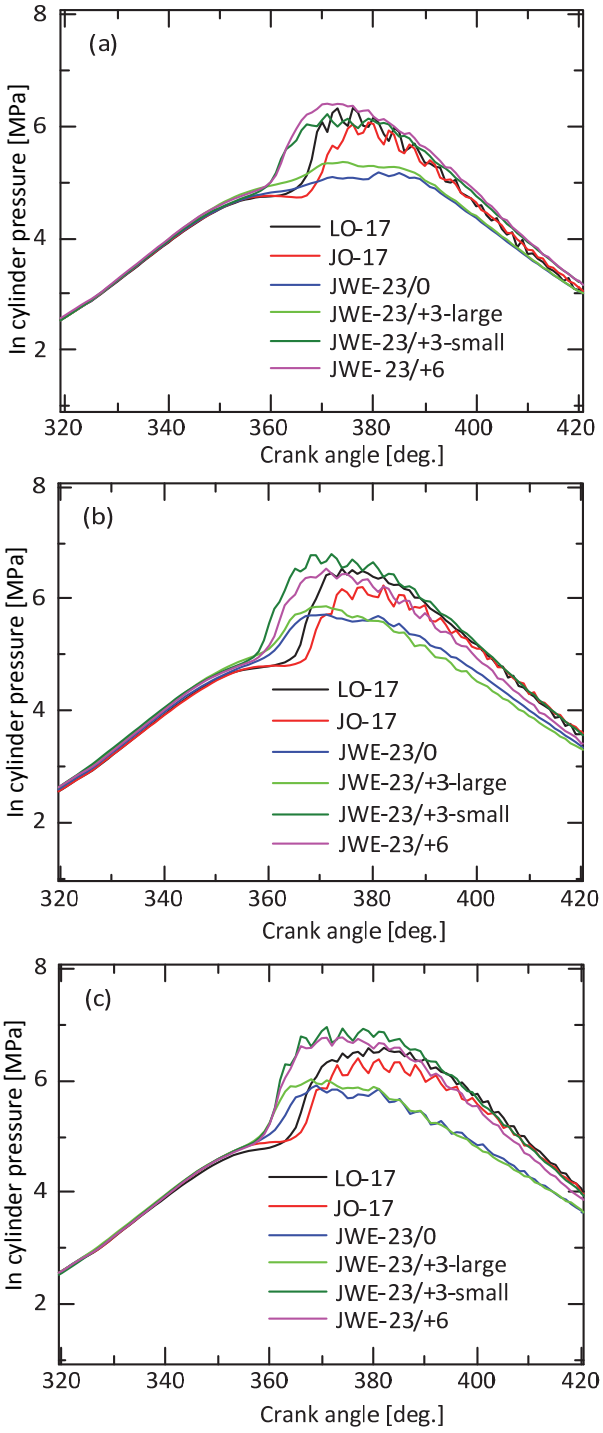

Figure 4-3 In-cylinder pressures at engine power of (a) 3.0 kW, (b) 4.5 kW, and (c) 6.0 kW

The combustion process of a diesel engine depends on the fuel-air mixing process and is related to fuel properties, such as viscosity, volatility, and the fuel injection system itself. With a common rail diesel engine, the operational parameters in terms of injection mode including the number of injections, injection timing, and quantity of injections strongly affect the combustion process. In this section, the combustion characteristics are demonstrated by a number of factors, namely combustion pressure, heat release rate, ignition delay, combustion duration, and center of combustion.

In-cylinder pressure of the engine is indicated in Fig. 4-3. It is clear that the peak pressures of the engine depend on the injection pattern as well as the fuel. The peaks of pressures were lower for the JO fueled engine in comparison with those of the LO. This is because of the lower heating value of the JO fuel, its lower volatility, and the higher viscosity of the JO. For the injection patterns of JWE-23/0 and JWE-23/+3-large, the peak pressures were lower than those of the LO and JO. This resulted from less fuel in first injection of these double injection patterns when compared with JO. Moreover, the cooling effect of the water in the emulsion fuel could reduce the combustion rate and pressure development. While, the peak pressures of JWE-23/+3-small and JWE-23/+6 were higher than those of LO. In these injection patterns, the larger amount of fuel in the first injection, and the timing of the second injection was far away the TDC, respectively, thus the second injection combusted immediately after

fuel injection. Consequently, the in-cylinder pressure's intensity was the highest. The combustion of double injection patterns started earlier than for single injections of LO, and JO as a result of earlier injection timing of the first injection when compared to the injection timing of the single injection mode.

Heat release rate (HRR) in the cylinder of the engine is presented in Fig. 4-4. The sharpest and highest increments of HRR seen are for the LO. The peaks of the HRR were 63, 58, and 53 J/deg. for 3.0, 4.5, and 6.0 kW, respectively. The fast combustion of the LO results from the physical properties of fossil fuel, such as low viscosity, and high volatility, thus it is easier to atomize and mix with air. The maximum of the HRR was lower for the JO and emulsion fuel in most injection patterns. The peaks of the HRR were around 49 J/deg. for the JO. This is equivalent to relative reductions of 22, 15.8, and 7.2 % when compared with those of the LO. This is due to the lower heating value and lower combustion rate of vegetable oil as a result of its physical properties. The injection patterns of JWE-23/+3-small and JWE-23/+6 significantly reduced HRR; while, the HRR dropped suddenly with the injection patterns of JWE-23/+3-large and JWE-23/0. The former generated relative reductions of 48, 25% and 34, 27% when the peaks of HRR reduced to 43 J/deg. or 33 J/deg. for 3.0, and 4.5 kW, respectively; the later showed maximum relative reduction of 75, 56, 46% and 71, 63, 44% when peaks of HRR dropped to 16, 25, 28 J/deg., and 18, 21, 30 J/deg. for 3.0, 4.5, and 6.0 kW, respectively.

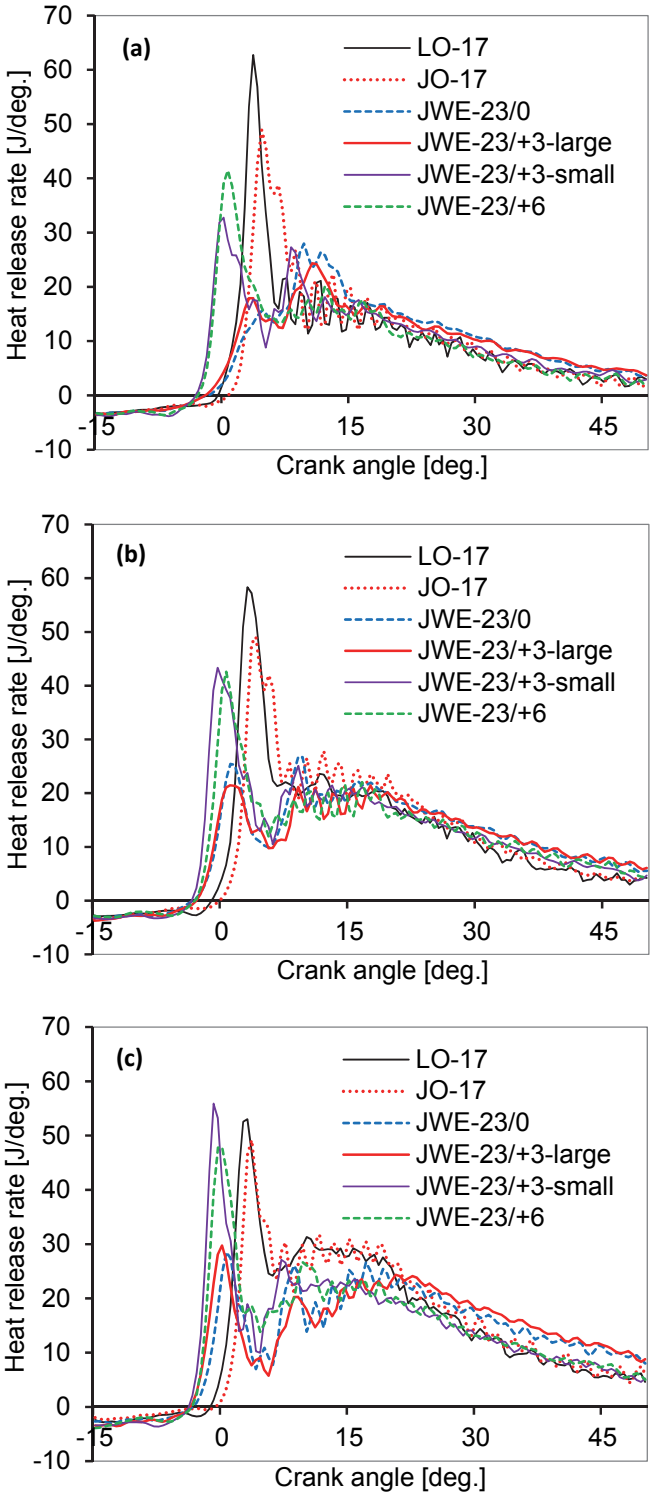

Figure 4-4 Heat release rate at engine power of (a) 3.0 kW, (b) 4.5 kW, and (c) 6.0 kW

This resulted from the reduction in the concentration of fuel spray as a result of split injection. Moreover, the cooling effect of the water content in the emulsion fuel was also a reason for reduction of the HRR. The earlier HRR for JWE fuel was a consequence of the earlier injection timing of the first injection when compared to those of the LO and JO.

The center of combustion, at which 50% of total heat release occurs, is indicated in Fig. 4-5a. It can be seen that the center of combustion shifted to the later stage when the JWE and double injection were utilized. For the LO, the combustion center was at 14.8 to 17.8 deg. ATDC. For the JO, a relative increment of timing of combustion center was 7.3% to 10% for 3.0 to 6.0 kW. While, for JWE-23/0 and JWE-23/+3-large the centers of combustion were at 21.5 to 29 deg. ATDC with relative increments of 46% to 63% when compared with those of the LO. For the JWE-23/+3-small and JWE-23/+6, the combustion center was at 16 to 20 deg. ATDC, with a relative increment of 11% to 20% in comparison with those of the LO. The later combustion center of biofuel is due to the lower rate of combustion, and later timing of second injection with double injection pattern.

Ignition delay is shown in Fig. 4-5b. The ignition delay is the duration from the start of injection to the start of combustion. The start of combustion is determined by the timing at which the HRR changes from a negative to a positive value.

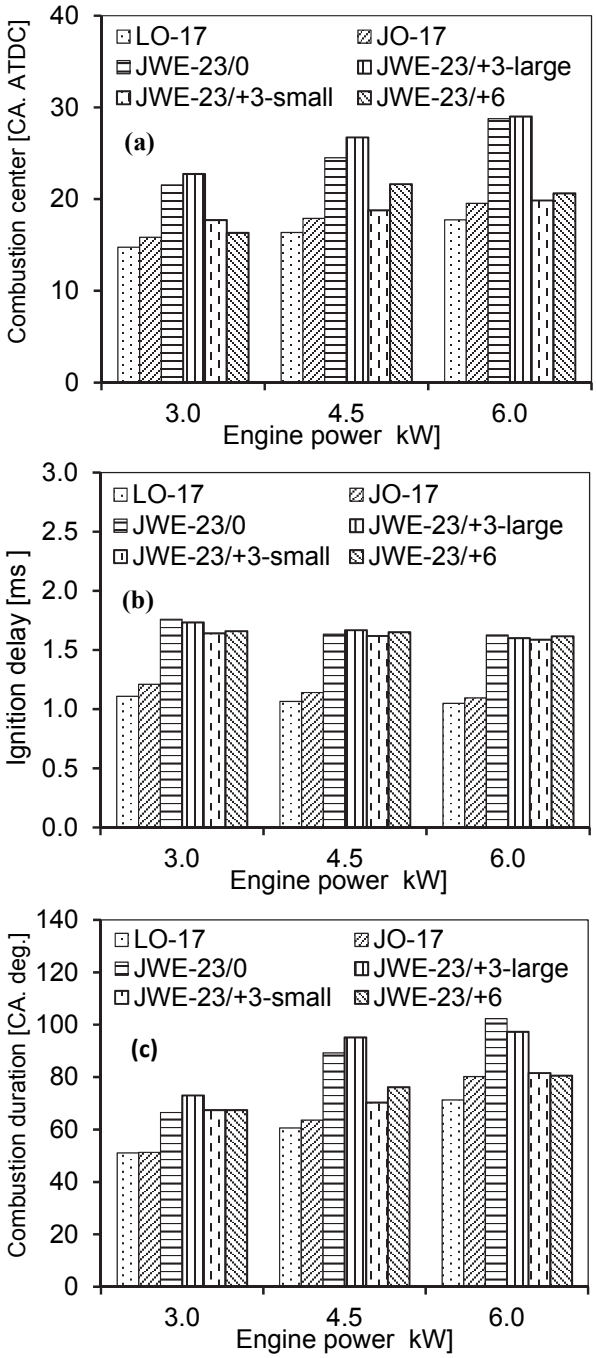

Figure 4-5 (a) Combustion center, (b) ignition delay, and (c) combustion duration

The ignition delay was shorter with an increase in the power of the engine as a consequence of the better combustion conditions such as temperature and pressure inside the combustion chamber. The ignition delays of the engine

using the JWE fuel in double injection patterns were longer than those of the LO with relative increments of 48% to 59% when IDs were around 1.76 msec. to 1.60 msec. Longer ignition delay of JWE resulted from the cooling effect and the dilution of the water content in the JWE fuel. Moreover, for double injection patterns, at the start of injection, the pressures and temperatures inside the combustion chamber were lower than those of the LO and JO increasing the ID. Slight reductions in the ID with different patterns were due to difference in the first injection quantities.

Combustion duration is indicated in Fig. 4-5c. Combustion duration is calculated from the start of combustion to the end of combustion (EOC). The EOC is determined by the timing of 95% total heat release. It can be seen that the CDs of the JWE with double injection were longer than those of the LO, and JO with single injection. The EOCs were at 50, 60, and 70 deg. ATDC for the LO fuel. While, for JWE-23/+3-small and JWE-23/+6, they were at 64 to 77 deg. ATDC. But, they were at 65 to 99 deg. ATDC and at 71 to 94 deg. ATDC for the injection patterns of JWE-23/0, and JWE-23/+3-large. This resulted from the larger amount of fuel in the second injection. Less fuel in the second injection and more fuel in the first injection for the JWE-23/+3-small and JWE-23/+6 resulted in shorter CDs when compared with those of the other injection patterns.

4. 3. 2 Performance characteristics

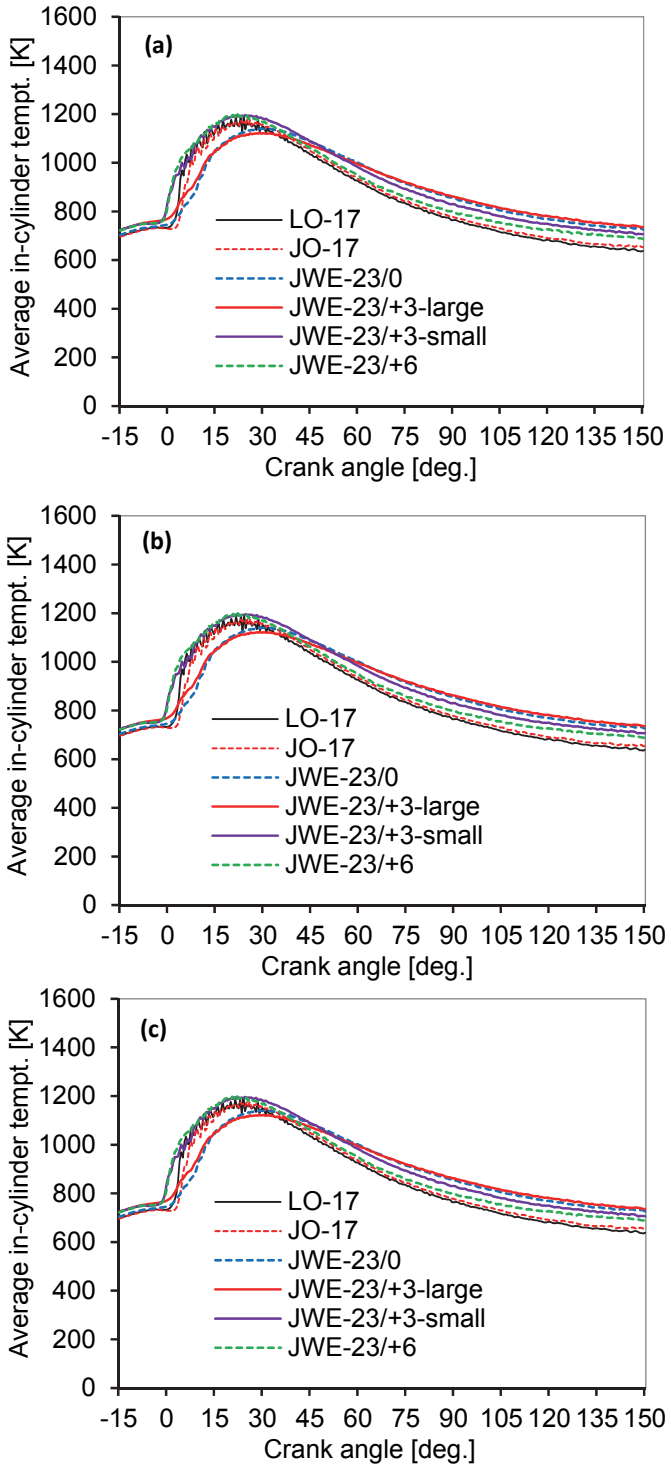

Figure 4-6 In-cylinder temperatures at engine power of (a) 3.0, (b) 4.5, and (c) 6.0 kW

The performance parameters of the engine, such as in-cylinder and exhaust gas temperatures, and brake thermal efficiency will be introduced in this section. In-cylinder temperature was calculated from the in-cylinder pressure history. Exhaust gas temperature was measured by a thermocouple and recorded during the experiments. Brake thermal efficiency was calculated as the ratio of the brake power to the energy supplied by the fuel consumption.

Average in-cylinder temperature is presented in Fig. 4-6. It can be seen that, most double injection patterns showed lower peaks in in-cylinder temperatures when compared with those of LO. The reduction in in-cylinder temperatures are attributed to the cooling effect of the water content in the emulsion fuel, the reduction of fuel injected in the first injection when compared with single injection mode for the LO and JO. At 3.0 kW, the in-cylinder temperature increased from 1192 K with LO to 1199 K with the injection pattern of JWE-23/+6 with only a minor relative increment of 0.6%. Earlier and faster development of in-cylinder temperatures with large amount of fuel in the first injection for patterns of JWE-23/+3-small and JWE-23/+6 were shown. But, in-cylinder temperatures developed later and the peaks of the in-cylinder temperatures were lower for the JWE-23/+3-large and JWE-23/0. In these injection patterns, at 3.0, 4.5, 6.0 kW, the peaks of the in-cylinder temperatures reduced from 1192, 1350, and 1518 K for the LO to 1140, 1265, and 1387 K for the JWE-23/0; and to 1123, 1245, and 1422 K for the JWE-23/+3-large,

respectively. One can also see that the double injection increased temperature at a later stage, particularly, for JWE-23/+3-large and JWE-23/0. The value and timing of the peak in-cylinder temperatures have a great influence on NOx emissions.

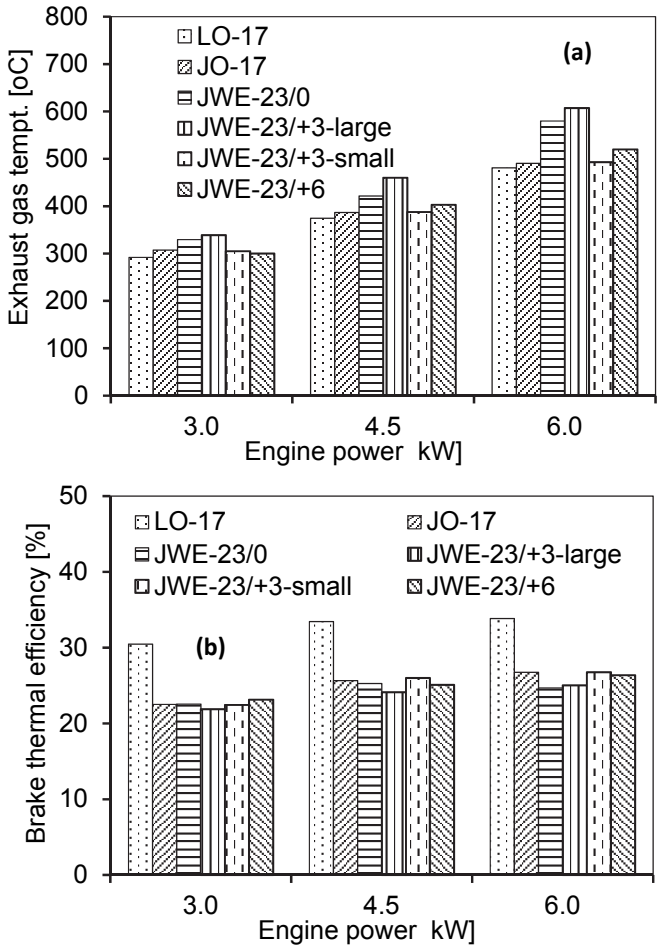

Figure 4-7 (a) Exhaust gas temperatures, and (b) brake thermal efficiency at different powers and 2000 rpm

Exhaust gas temperature is shown in Fig. 4-7a. Exhaust gas temperatures increased with increases in the engine power. This is due to the increased fuel injected and combustion which generates more engine power. When compared with the LO, the exhaust gas temperatures of the double injection increased

much more with the injection patterns of JWE-23/0 and JWE-23/+3-large. However, for the JWE-23/+3-small and JWE-23/+6, only slight increments in the exhaust gas temperatures were found in comparison with those of LO. The exhaust gas temperatures increased from 292, 375, 481 ^{o}C for the LO to 389, 460, 607 ^{o}C for the JWE-23/+3-large; and to 305, 388, 493 ^{o}C for the JWE-23/+3-small, at 3.0, 4.5, and 6.0 kW, respectively. These are equivalent to relative increments of 16, 23, and 26%; and 4.5, 3.6, and 2.5%, respectively. Different in injection patterns have different first injection mass which may explain these results. For the JWE-23/0 and JWE-23/+3-large, large amount of injected fuel in the second injection shifted the combustion to a later stage, and as a result, it increased the exhaust gas temperatures. This is consistent with the results of in-cylinder temperatures as shown previously. The minor increments in the exhaust gas temperatures for the JWE-23/+3-small and JWE-23/+6 when compared with those of the LO are attributed to the double injection pattern with less injected fuel in the second injection. The in-cylinder temperature, and exhaust gas temperature are strongly related to the break thermal efficiency of the engine.

Brake thermal efficiency (BTE) of the engine is indicated in Fig. 4-7b. It is clear that the highest BTE was achieved by using LO. The single injection with JO, and double injection with JWE had lower BTE. This resulted from the combustion characteristics of the biofuel as explained above due to the physical

properties of the biofuel itself. Increased ignition delay, later combustion center, and longer combustion duration are reasons for reduction of the BTE, particularly, for the JWE-23/0 and JWE-23/+3-large. At 3.0, 4.5, and 6.0 kW, BTE were 30.5, 33.4, and 33.9% for the LO; and were 22.5, 25.7, and 26.7% for the JO. While, they were 21.9, 24.1, and 25% for the JWE-23/+3-large; and were 22.5, 26.0, 26.8 % for the JWE-23/+3-small. It is clear that the BTE increased with an increase in first injection quantity seen in the injection patterns of JWE-23/+3-small or JWE-23/+6. Moreover, for the JWE-23/+3-small, the BTE were comparable to those of the JO.

4. 3. 3 Emissions characteristics

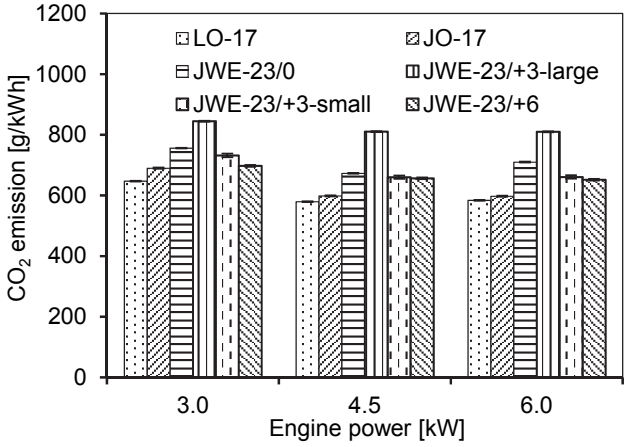

Figure 4-8 Emissions of CO_2 with different injection patterns

The gas emissions of the engine such as CO_2, CO, HC, and NOx are indicated in Fig. 4-8 to Fig. 4-11. The smoke opacity, dust, soluble organic fraction, and in-soluble organic fraction are shown in Fig. 4-12 to Fig. 4-15.

Emission of CO_2 is presented in Fig. 4-8. It is clear that the emissions of CO_2 were higher for biofuel including JO and JWE when compared with LO. Combustion of biofuel lasted to later phase due to slow combustion characteristics and double injections, therefore, the engine consumed more fuel to generate the same power thus increased emission of CO_2. It is also clear that different injection patterns made differences in the emissions of CO_2. The JWE-23/0 and JWE-23/+3-large induced the highest increments of CO_2. While, the JWE-23/+3-small and JWE-23/+6 gave less increments of CO_2. For the JWE-23/0, relative increments of CO_2 were 16 to 21.5%, while, they were 30.5 to 40% for the JWE-23/+3-large when compared with those of the LO. However, the JWE-23/+3-small and JWE-23/+6 had relative increments of 7.8% to 14% when compared with CO_2 emissions with the LO. This resulted from more injected fuel in the second injection in the injection patterns of JWE-23/0 and JWE-23/+3-large; and vice versa in the injection patterns of JWE-23/+3-small and JWE-23/+6. This is also relevant to the combustion characteristics as explained previously.

Emission of CO is shown in Fig. 4-9. This figure shows clearly that the emissions of CO of biofuel were much higher than those of the LO, especially, for the JWE fuel. At 3.0, 4.5, 6.0 kW, the emissions of CO of the JWE-23/+3-large had 2.4 and 17.3 times higher than those of the LO; while, for the JWE-23/+6, they were 1.1, 19.8 and 3.5 times higher than the LO. But, for the JWE-

23/+3-small, the emissions of CO were 1.7, 7.4, 3.6 times higher than those of the LO at 3.0, 4.5, and 6.0 kW.

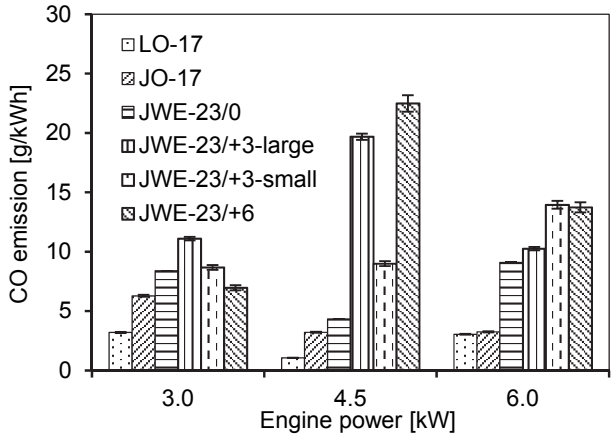

Figure 4-9 Emissions of CO with different injection patterns

Very high increments of the CO when using the JWE-23/+3-large and JWE-23/+6 at 4.5 kW are probably attributed to the cooling effect of the water content in the JWE and the late timing of the second injection. At 6.0 kW, in these injection patterns, the emissions of CO were reduced when compared with those at 4.5 kW. This is probably due to the dominant effect of higher in-cylinder temperatures, so there was less effect of cooling seen. The higher the combustion temperature, the better the second atomization as a result of micro-explosion of water droplets in the emulsion fuel is, and the more CO converted to CO_2. Finally, it reduced emissions of CO in comparison with those at 4.5 kW. For the JWE-23/+3-small, emission of CO was kept almost constant at 3.0 and 4.5 kW, it comparably increased to that of the JWE-23/+6 at 6.0 kW. To

achieve higher engine power, a rich injection occurred where much more fuel was injected into the combustion chamber and this increased the amount of CO.

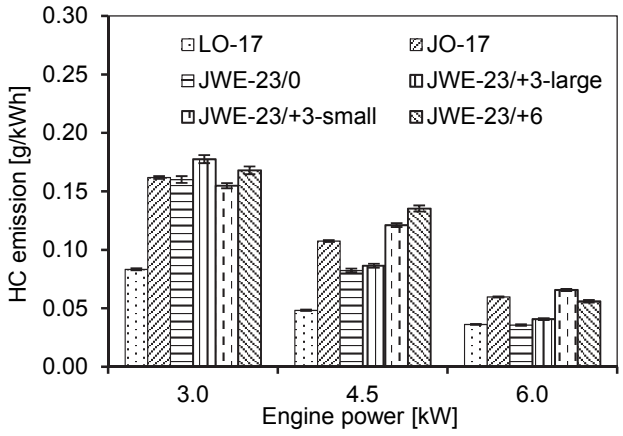

Figure 4-10 Emissions of HC with different injection patterns

HC emission is indicated in Fig. 4-10. The emission of HC depends on the power of the engine, the injection pattern, and the fuel. The emissions of HC decreased with an increase in the engine power. This is due to the higher combustion temperatures at higher engine powers. The biofuels produced much higher HC emissions especially at low loads. At 3.0 kW, the maximum increment of HC was 113% for the JWE-23/+3-large, while it was a minimum of 86% for the JWE-23/+3-small when compared with those of LO. At low engine power, with low combustion temperatures, the cooling effect of a large amount of fuel injected in the second injection for the JWE-23/+3-large increased the emissions of HC much more than for the 23/+3-small. At higher engine powers, the emissions of HC of the JWE were higher than those of the LO, but they were lower than those of JO when the JWE-23/0 and JWE-23/+3-

large were used. In these injection patterns, less fuel injected in the first injection, along with probably micro-explosions at higher combustion temperatures, the dilution and better mixing of the fuel and air in the combustion chamber thus reduced emissions of HC when compared with those of JO. In the injection patterns of the JWE-23/+3-small and JWE-23/+6, the first injection quantity was large, thus an over rich mixture was generated, and the cooling effect dominated over the effect of micro-explosion, and thus the amount of HC was higher than that of the JO.

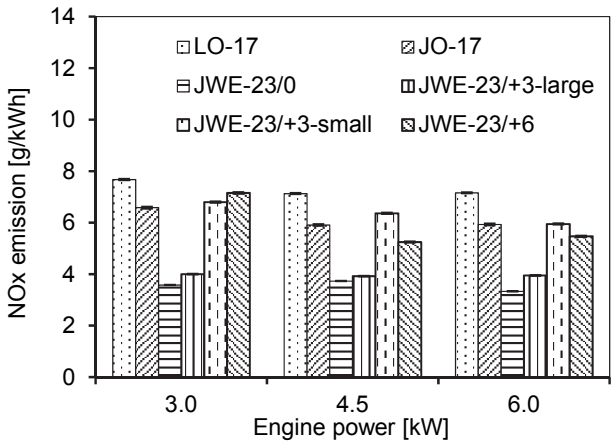

Figure 4-11 Emissions of NOx with different injection patterns

Fig. 4-11 displays NOx emissions of the engine. The emissions of NOx had a strong correlation to the fuel and injection patterns. It is clear that combustion of the LO released more NOx than the biofuels. This is due to its higher heating value and higher combustion rate than the biofuels. We found a slight reduction of the NOx when using the injection patterns of JWE-23/+3-small and JWE-23/+6 for the JWE fuel, while, a significant reduction of NOx emissions was

found for injection patterns of the JWE-23/0 and JWE-23/+3-large. Maximum reductions of NOx in these injection patterns were 45 to 54% when compared with those of the LO. This is a consequence of the combustion characteristics as explained previously. The HRR in these injection patterns dropped suddenly because less fuel was injected reducing the maximum temperatures in the combustion spots of the fuel spray, dramatically reducing the emissions of NOx. The marginal reduction of NOx emissions for the JWE-23/+3-small and JWE-23/+6 is attributed to the increased first injection quantity leading to less reduction in the HRR.

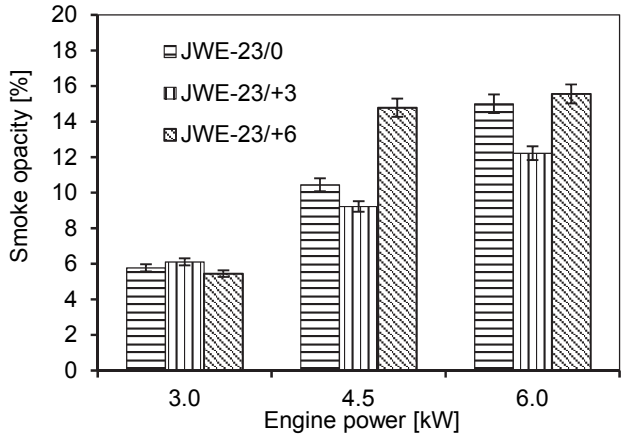

Figure 4-12 Smoke opacity with different second-injection timings

Smoke opacity is indicated in Fig. 4-12. The smoke emission was measured to find the optimum injection timing of the second injection before measuring dust, ISF, and SOF. I measured smoke when running the engine on JWE, and double injection pattern with a fixed first injection timing, and various second injection timings of 0, +3, +6 deg. ATDC. Fig. 4-12 shows that smoke opacity was

comparable at 3.0 kW; it increased with an increase in engine power. This is because more fuel was injected into the combustion chamber for the higher loads. Moreover, the different injection timings of the second injection indicated different smoke opacities. Higher smoke opacities were found with early or late timing of the second injection. This resulted from the cooling effect of the large amount of fuel in the second injection at the TDC; the rich mixture in the first injection and reduced-combustion temperatures when the second injection started for the late second injection. The optimum injection pattern was JWE-23/+3 for lower smoke emissions.

Concentration of dust, ISF, and SOF are displayed in Fig. 4-13 to Fig. 4-15. This shows that the dust emissions were higher for biofuels at lower loads of the engine in comparison with those of the LO.

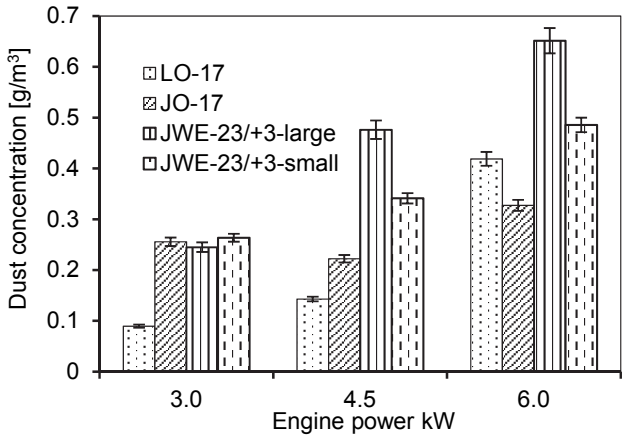

Figure 4-13 Dust concentration with different injection patterns

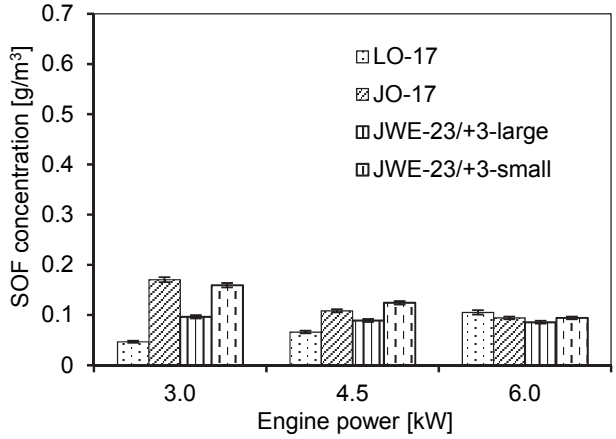

Figure 4-14 SOF concentration with different injection patterns

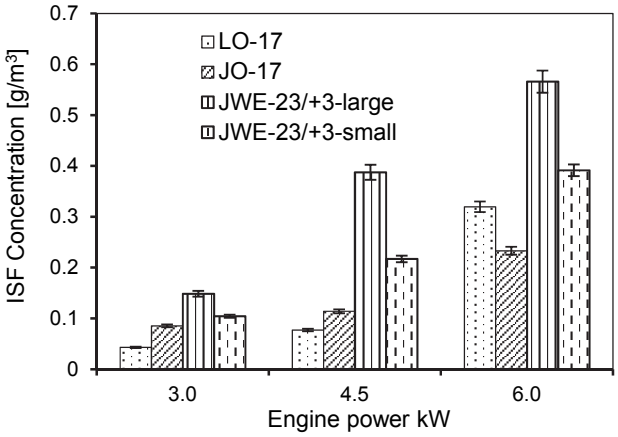

Figure 4-15 ISF concentration with different injection patterns

At 3.0 kW, the concentrations of dust was comparable at around of 0.26 g/m^3, while it was 0.09 g/m^3 for the LO. The higher viscosity of the biofuels and the cooling effect of the emulsion fuels increased the ISF and SOF, and thus consequently increased the dust concentrations. At higher engine powers, the fastest developments of dust concentrations were for the JEW-23/+3-large with relative increments of 2.3 and 0.6 times when compared with those of the LO. Large amount of the second fuel injection under high burning gas temperatures

enhanced the conversion of fuel into the ISF, while reduced the SOF. For the JWE-23/+3-small, with more first injection quantity and longer time for the oxidation process to reduce the ISF, we found less increment of the dust concentration in this injection pattern. At 6.0kW, the lower dust concentration of the JO in comparison with those of the LO is attributed to the higher oxygen content in the vegetable oil that probably reduced the ISF as shown in this figure.

4. 4 Summary

A direct injection diesel engine operated with Jatropha water emulsion was used to investigate the effects of double injection patterns and JWE fuel on the combustion, performance, and emissions of the engine. In summary, the main features are as follows.

1- Large amount of fuel in the second injection in injection patterns such as JWE-23/0 and JWE-23/+3-large dramatically reduced the peaks of in-cylinder pressure; suddenly reduced the peak of HRR; and increased significantly the ignition delay, combustion duration, and shifted the combustion center toward the later stage. For small amount of fuel in the second injection such as JWE-23/+3-small and JWE-23/+6, the peaks of the in-cylinder pressures were higher, while, other parameters had the same tendency with lower intensity when compared with those of the LO.

2- Large amount of fuel in the second injection dramatically reduced the in-cylinder temperatures, increased the exhaust gas temperatures, and lowered the BTE in comparison with those of the JO. The opposite occurred when small second injection amount was used as in JWE-23/+3-small and JWE-23/+6. I also found that when using the JWE-23/+3-small the BTE was higher than that of the JO.

3- The emulsion fuel and double injection increased CO_2, CO, and HC emissions when compared with those of the LO. However, in comparison with those of the JO, the large second injection quantity such as the JWE-23/+3-large reduced the HC emissions. NOx emissions were related to the combustion characteristics of the engine with different injection patterns. The emulsion fuel, and double injection patterns reduced NOx emissions when compared with those of the LO. Large second injection amount such as the JWE-23/0 and JWE-23/+3-large significantly reduced the NOx emissions.

4- In three timing tests, the JWE-26/+3 reduced smoke opacity when using JWE and double injection. The ISF was the main element, while the SOF was a minor element of the dust. Large second injection amount increased the ISF and dust concentration much more than a small second injection amount.

Chapter 5 Combustion, Performance, and Emissions of Direct Injection Diesel Engine Fueled by Jatropha Hydrogen Peroxide Emulsion

5. 1 Introduction

Previous chapters presented the combustion, performance, and emissions of the engine fueled with water emulsion fuel oil and double injections with the aid of common rail system. The drawbacks of Jatropha oil when using in diesel engines could be overcome by preheating [35] or esterification and blending with diesel [66, 67], increased injection pressure, or perhaps a dual fuel engine. The benefits of the water emulsified fuels to the combustion and emissions of compression ignition engines have been tested, and proven in the literature [43, 44, 46, 47, 71-73]. But, operation of diesel engine fueled with Jatropha hydrogen peroxide emulsion has not been reported as yet.

Hydrogen peroxide (H_2O_2) is effective for soot oxidation due to the presence of the Hydroxyl radical (OH) dissociated during the combustion process as reported in the literatures [48-49]. Higher engine brake thermal efficiency with increased concentrations of H_2O_2 was found in study of K. S. Nagaprasad et al. [50], and ignition delay was reported a significant reduction with addition of H_2O_2 in research of D. S-K. Ting et al. [51]. The burning rate of methane fuel was enhanced owing to the presence of OH, O, and H radicals thus produced less CO emissions [51, 52]. NOx emissions were lower as a result of a lower

average cycle temperature as reported in investigation of M. C. Mulenga et al. [33]. Hence, the addition of H_2O_2 to the engine combustion chamber may improve the combustion and emissions of the diesel engine. However, addition of H_2O_2 to Jatropha oil has not been tested as yet.

Therefore, this experimental research was designed and conducted to gather information on the engine performance, combustion, emissions, and to identify the optimum mixing ratio of hydrogen peroxide solution to Jatropha oil. This chapter presents the experimental work conducted on a direct injection diesel engine fueled with Jatropha hydrogen peroxide emulsion by a mechanical fuel injection system.

5. 2 Material, experimental setup and procedures

In this study, test fuels include the neat Jatropha oil (JO), Jatropha hydrogen peroxide emulsions (JHE) with light oil (LO) as the baseline fuel. The properties of the test fuels are given in Table 5-1. Hydrogen peroxide in a solution of water at a concentration of 30% was used for making the emulsions in this research.

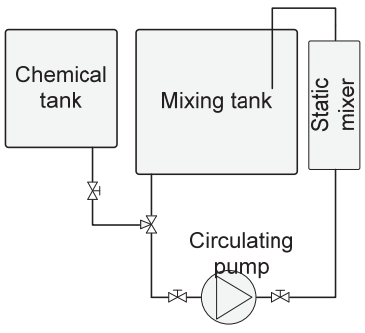

Figure 5-1 Schematic diagram of mixing system

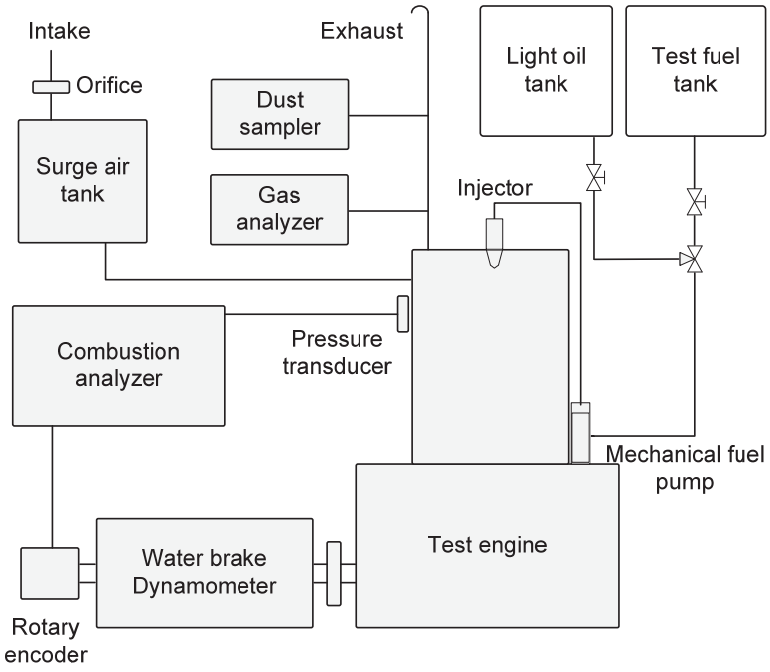

Figure 5-2 Schematic diagram of experimental set-up

To make the emulsion fuel, a mixing system was used that included tanks for Jatropha oil and chemical (H_2O_2 solution), a circulating pump, and a static mixer. Diagram of the mixing system is given in Fig. 5-1. The Jatropha oil mass was measured during each step of the experiments. Mixtures of Jatropha oil with solutions of hydrogen peroxide were created according to the Jatropha oil mass with mixing ratios of 5%, 10% and 15% (hereafter so-called JHE5%, JHE10%, and JHE15%). To keep emulsified fuels homogeneous and stable, three kinds of surfactants (Rheodol SP-L 10, Rheodol 440V, and Emulgen 103, Kao Chemicals Corp., Japan) were used. While the Jatropha oil was circulating through the mixing pump, the chemical was added through the chemical tank

and the flow rate of the chemical was controlled by a needle valve for homogeneous mixed fuels.

The experiments were conducted on a single cylinder, four-stroke, high speed, direct injection diesel engine (Yanmar Co., Ltd., Japan). To inject the fuel into the combustion chamber, a set of mechanical fuel injection system including a fuel pump and a mechanical injector was utilized. The engine was equipped with a piezoelectric pressure sensor and a rotary encoder for measurement of the in-cylinder pressure and crank angle. The pressure and crank angle signals are transmitted to a computer via a charge amplifier. These signals were used for monitoring cylinder pressure history and for calculation of heat release after the experiments. Load of the engine was set through a water-dynamometer coupled to the shaft of the engine. Exhaust gas emissions and dust particulate were measured and collect with the same apparatus and method those described in previous chapters.

Firstly, the engine was fed with the light oil and the results were recorded at each load of the engine. After this, we switched to the test fuels including neat Jatropha oil, and Jatropha hydrogen peroxide emulsions. During the experiments, the engine load was set at different values of 1.55, 3.02, 4.67, and 6.20 kW with a speed of 2000 rpm. At each load, reading the emissions of CO, CO_2, HC, and NOx was made through the exhaust gas analyzers, while, the dust

particulate were collected on the filter papers. A schematic diagram of the experimental set-up is illustrated in Fig. 5-2.

5. 3 Results and discussions

5. 3. 1 Combustion characteristics

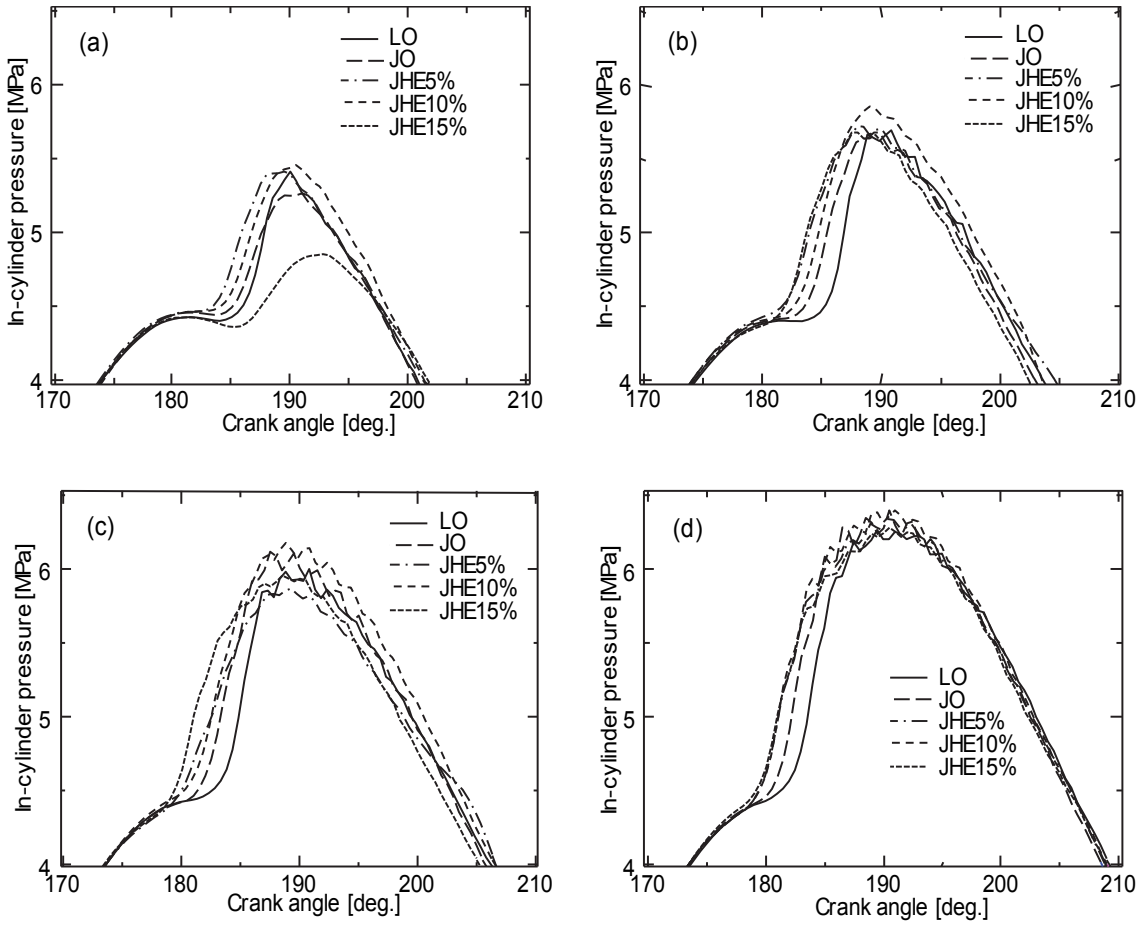

Figure 5-3 In-cylinder pressure at engine power of (a) 1.55 kW, (b) 3.02 kW, (c) 4.67, and (d) 6.20 kW @ 2000 rpm

The combustion process of a diesel engine depends on the fuel-air mixing process and is related to fuel properties, such as viscosity, volatility, and the fuel injection system itself. With existing engines, the combustion is determined

mainly by the properties of the fuel and operational parameters. In this chapter, the combustion characteristics are demonstrated mainly by a number of factors, namely combustion pressure, ignition delay, combustion duration, heat release rate, net cumulative heat release and center of combustion.

In-cylinder pressure of the engine is indicated in Fig. 5-3. It is clear that the peak pressures of the JHE fueled engine were higher than those of Jatropha oil or light oil in most cases. Moreover, the pressure of the JHE fuel was more advanced in comparison to those of the light oil and neat Jatropha oil except the case of JHE15% at engine load of 1.55 kW. This resulted from the physical characteristics of the JHE fuel such as high compressibility and the effect of H_2O_2 in the combustion process. At lower load, the combustion was far from the top dead center (TDC), and the combustion phase was closer to the TDC when the engine load increased. This is due to the fact that the fuel was injected earlier at higher engine loads.

The start of combustion of the engine is shown in Fig. 5-4 and the ignition delay is indicated in Fig. 5-5. At low load, the low combustion temperature resulted in longer ignition delay and combustion initiated later for the JHE15% fuel. The ignition delay was shorter and combustion started earlier for the JHE5%. At higher loads of the engine, for the JHE5% and JHE15% fuels, the ignition delays were shortened and the start of combustion was earlier in comparison to those of the neat Jatropha oil or light oil. This resulted from the

advanced injection of the emulsion fuels and perhaps the presence of the hydrogen peroxide that enhanced the combustion of the emulsion fuel.

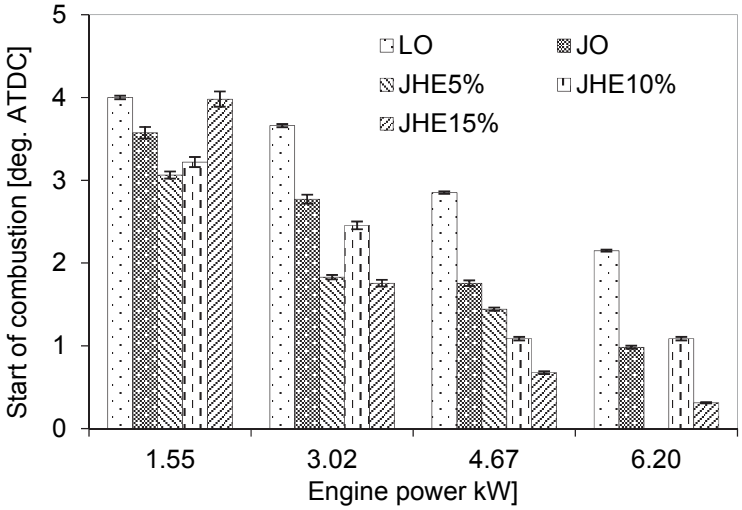

Figure 5-4 Start of combustion of the engine with different powers and fuels

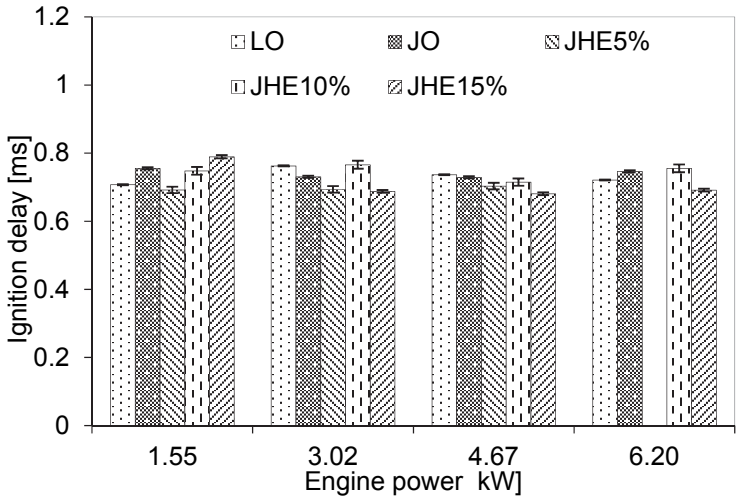

Figure 5-5 Ignition delay of the engine with different powers and fuels

The center of combustion, at which 50% of heat release occurs, is indicated in Fig. 5-6 and the combustion duration is presented in Fig. 5-7. Even though the start of combustion was earlier, it is clear that the combustion center for emulsion fuels tended to be toward the later stages of combustion, especially for

the JHE5% and JHE15% fuels. This is evidence of much more heat release and longer combustion duration as shown in Fig. 5.5. This may result from the oxidation of the soot by the OH radicals in the later combustion phase releasing more heat, so it prolongs the combustion.

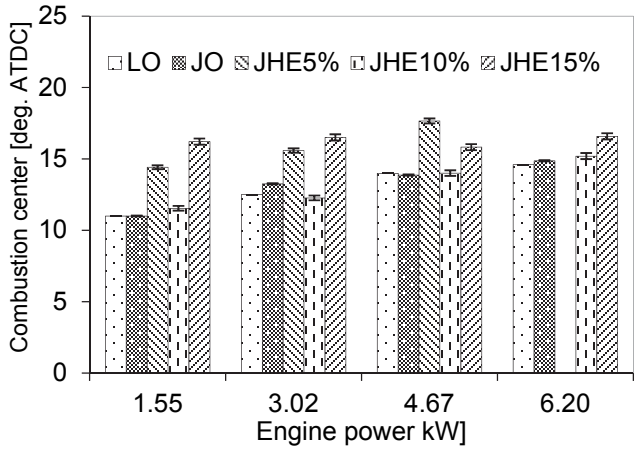

Figure 5-6 Combustion center of the engine with different powers and fuels

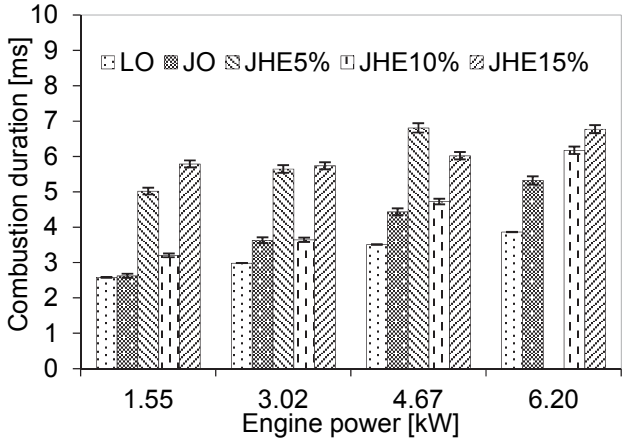

Figure 5-7 Combustion center of the engine with different powers and fuels

Heat release rate (HRR) in the cylinder of the engine is presented in Fig. 5-8 to Fig 5-11. The sharp and highest increment of the heat release rate is for the light oil. The fast combustion of the light oil results from the physical properties of fossil fuel, such as low viscosity, and high volatility, thus it is easier for

atomizing and mixing with air. It is clear that, the combustion of the emulsion fuels initiated earlier, but the maximum values were lower in comparison to those of the light oil or the neat Jatropha oil. At 1.55 kW, 3.02 kW, 4.67 kW and 6.20 kW, the peaks of the HRR were 62.4, 66.2, 71.2, and 69 for the LO, respectively, while the JHE15% caused a relative reduction of 28.4%, 25.2%, 39.3%, and 33% when compared to the LO. For the other emulsion fuels, the peaks of the HRR were between 44.1 and 56.3 depending on the fuel and load conditions. This may result from the cooling effect of the water content in the emulsion fuels and their lower heating value. In the diffusion combustion phase, there is a large magnitude of oscillation in the heat release rate and the release of heat lasted into the late combustion phase with the JHE5% and JHE15% fuels. This can be attributed to the heat radiated from oxidation of soot by the OH radicals in the late combustion phase.

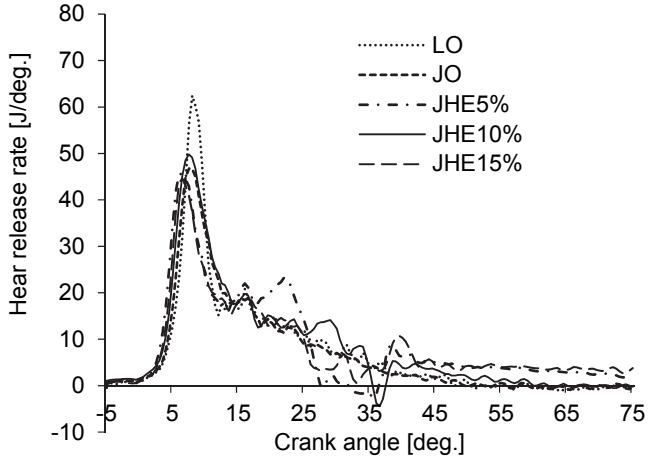

Figure 5-8 Heat release rate of the engine with different fuels at 1.55 kW

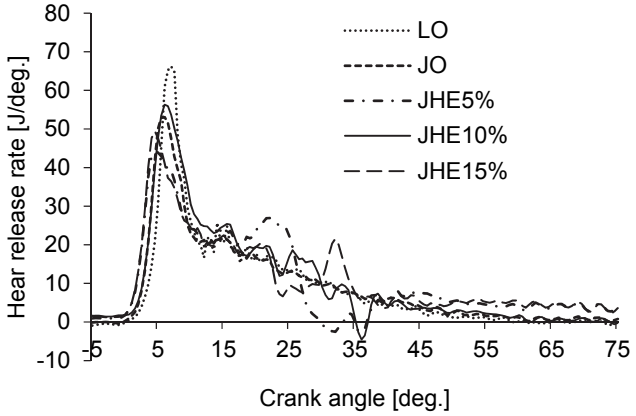

Figure 5-9 Heat release rate of the engine with different fuels at 3.02 kW

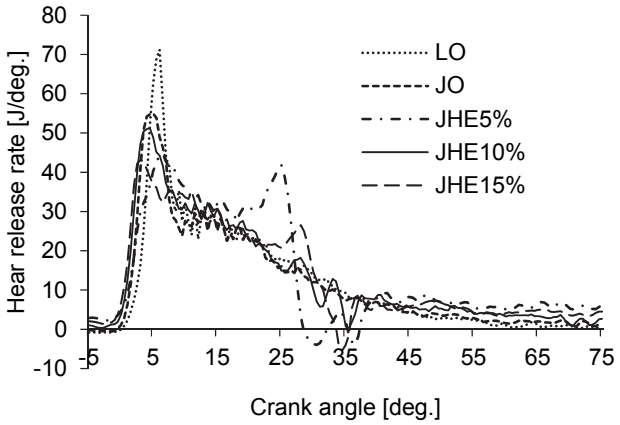

Figure 5-10 Heat release rate of the engine with different fuels at 4.67 kW

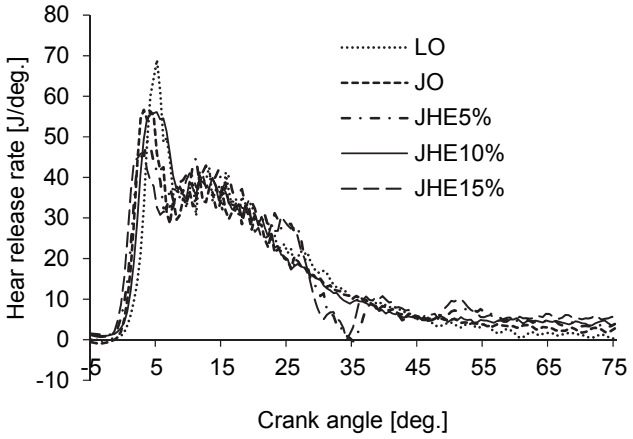

Figure 5-11 Heat release rate of the engine with different fuels at 6.20 kW

Net cumulative heat release (HR) is shown in Fig. 5-12 to Fig. 5-15. It is evident that the heat release was higher for the emulsion fuel, but the complete combustion of the emulsion fuel wasn't until the later stage.

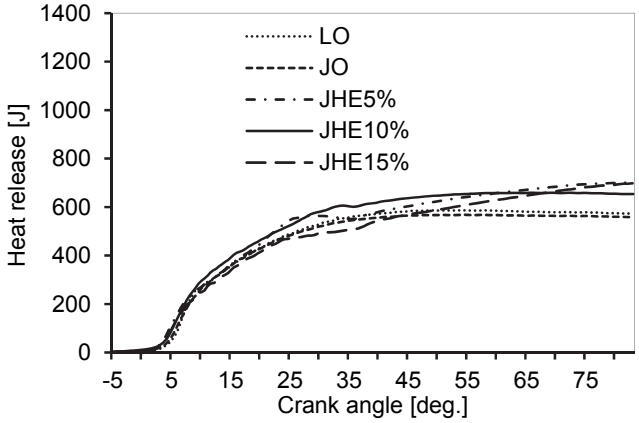

Figure 5-12 Net heat release of the engine with different fuels at 1.55 kW

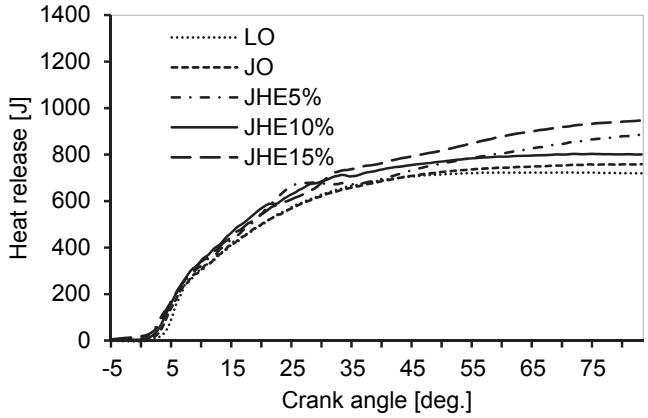

Figure 5-13 Net heat release of the engine with different fuels at 3.02 kW

At 1.55 kW, the peaks of the HR were 586.9, and 568.4 for the LO and JO while the JHE5%, JHE10%, JHE15% increased 23.4%, 15.9%, and 22.9% when compared relatively to the JO. At 6.20 kW, it was 1174 for the JO, and climbed up to 1274.5, 1288.9, and 1322.5 with a relative increment of 8.6%, 9.8% and 12.6% for the JHE5%, JHE10%, JHE15%, respectively, when compared to the JO. The longer combustion of the emulsion fuel was explained previously as a result of oxidation of soot particles by the OH radicals in the later stage. The longer heat release rate due to soot oxidation contributed to

higher and later heat release of emulsified fuel. It was especially true for the JHE5% and JHE15%.

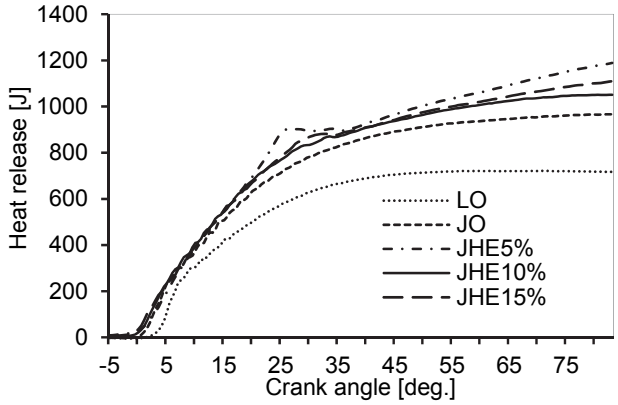

Figure 5-14 Net heat release of the engine with different fuels at 4.67 kW

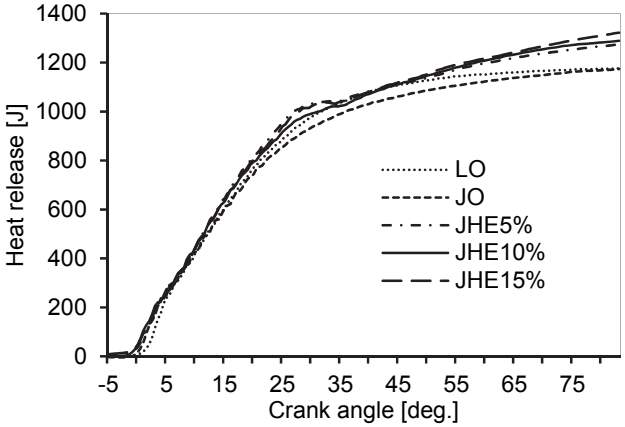

Figure 5-15 Net heat release of the engine with different fuels at 6.20 kW

5. 3. 2 Performance characteristics

In this section, the performance parameters of the engine such as in-cylinder and exhaust gas temperatures, and brake thermal efficiency will be introduced. Combustion temperature was calculated from the in-cylinder pressure history. Exhaust gas temperature was recorded by computer during the experiments. Brake thermal efficiency was calculated as the ratio of the brake power to the energy supplied by the fuel consumption.

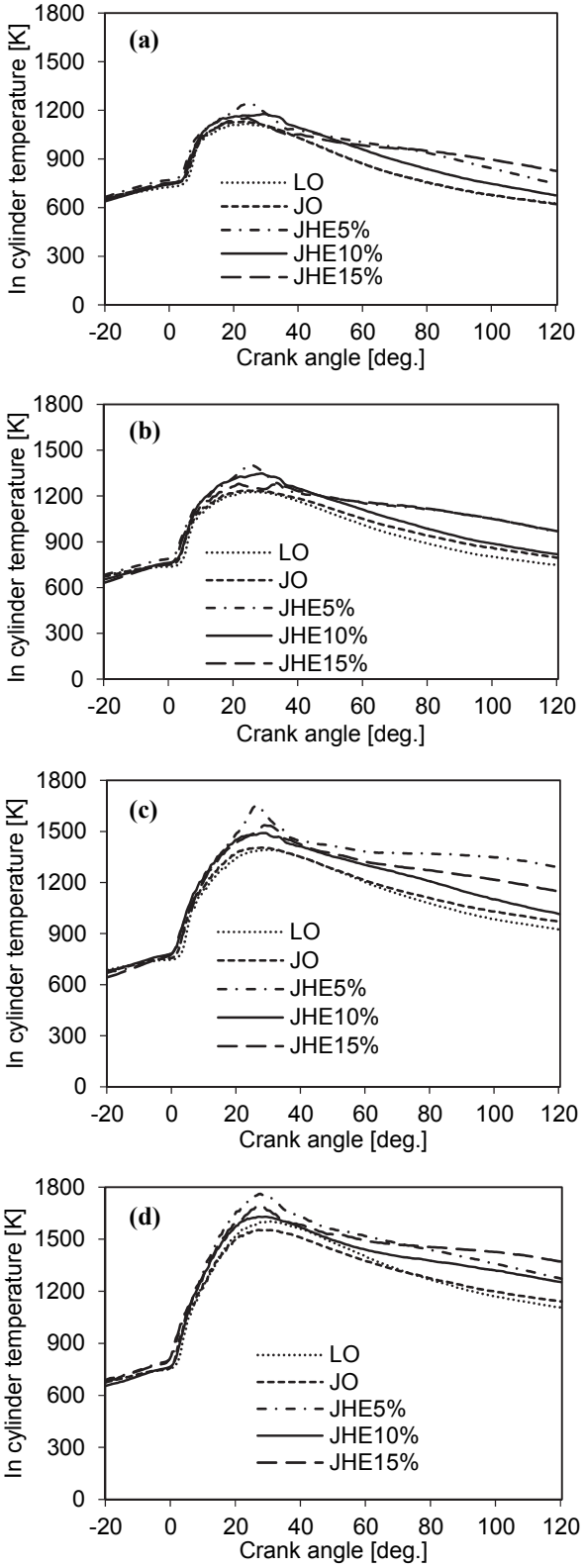

Figure 5-16 In-cylinder temperature of the engine at (a) 1.55, (b) 3.02, (c) 4.67, and (d) 6.20 kW

In-cylinder temperature is presented in Fig. 5-16. It can be seen that in-cylinder temperatures of the engine when fueled with the neat Jatropha oil and light oil were very close. However, there were relatively large differences for emulsion fuels especially in the late combustion stages. The JHE5% and JHE15% showed higher in-cylinder temperatures in most cases. In comparison with the JO, the JHE5% had an increment in in-cylinder temperatures of 112.2, 166.4, 247.9, and 204.8 ^{o}C, while the JHE15% induced 22.5, 43.9, 131.8, and 136.5 ^{o}C higher than those of the JO at 1.55, 3.02, 4.67, and 6.20 kW, respectively. This was a consequence of the heat release rate and the heat release histories. Higher heat releases of emulsion fuels in the later combustion stage caused higher in-cylinder temperatures.

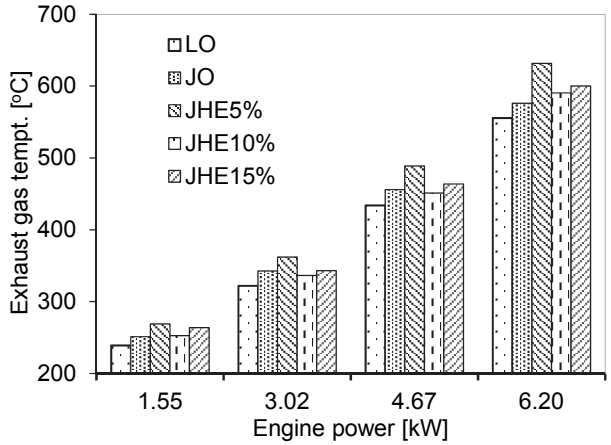

Figure 5-17 Exhaust gas temperature of the engine at different powers and fuels

Exhaust gas temperature is depicted in Fig. 5-17. Lower temperatures were at lower loads and increased with an increase of engine load. This is because more fuel is needed to burn to produce higher power. Exhaust gas temperatures of the

engine fueled with emulsified fuels were higher than those of the light oil or neat Jatropha oil, especially for the JHE5% and JHE15% at higher loads. At 1.55 kW, exhaust gas temperatures were 239.2, 251.4 ^{o}C for the LO, JO, while they climbed up to 269.2, 252.8, and 264 ^{o}C for the JHE5%, JHE10%, JHE15%, respectively. At 6.20 kW, it was 576.2 ^{o}C for the JO, and the JHE5%, JHE10%, JHE15% increased 9.6%, 2.5%, 4.2% rising to 631.6, 590.5, 600.2 ^{o}C, respectively. Higher heat release, and a longer-extended-combustion stage resulted in increasing the exhaust gas temperatures. Earlier completed combustion of the JHE10%, and high heat release in the premixed combustion phase lowered exhaust gas temperatures as compared to the JHE5% or JHE15%.

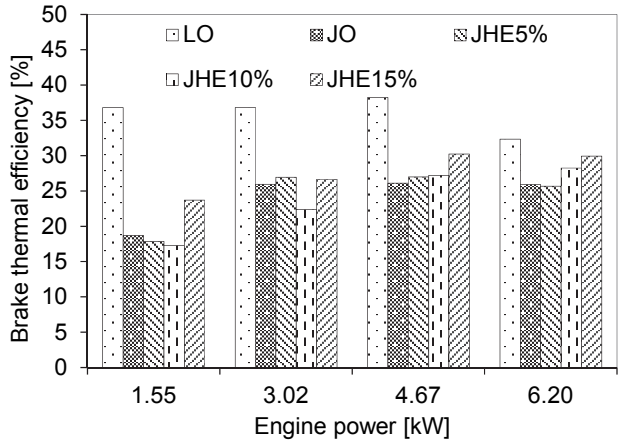

Figure 5-18 Brake thermal efficiency of the engine at different powers and fuels

Fig. 5-18 shows the brake thermal efficiency (BTE) of the engine. The BTE was the highest for light oil fuel due to its better combustion characteristics. For the JO, starting at 18.7% at a power of 1.55 kW, then BTE climbed up to around 26% at medium and higher powers. At powers of 1.55 kW, and 3.02 kW,

when compared relatively to the JO, the BTE of the JHE10% were reduced 7.7% and 13.7%, while they increased 26.7% and 2.7% for the JHE15%. At higher powers, both emulsion fuels increased BTE, particularly for the JHE15% with an increment of 15.7% compared relatively to the JO. For the JHE10%, the reduction in BTE at lower powers may be attributed to the cooling effect, and not enough hydrogen peroxide to improve combustion. To produce higher power, more fuel quantity must be injected into the combustion chamber, thus 15% of a solution of hydrogen peroxide was enough to enhance combustion and increase thermal efficiency as compared to the neat Jatropha oil and other emulsion fuels.

5. 3. 3 Emission characteristics

The emissions of the engine including CO_2, CO, HC, NOx, particulate matter and soot are indicated in Fig. 5-19 to Fig. 5-25.

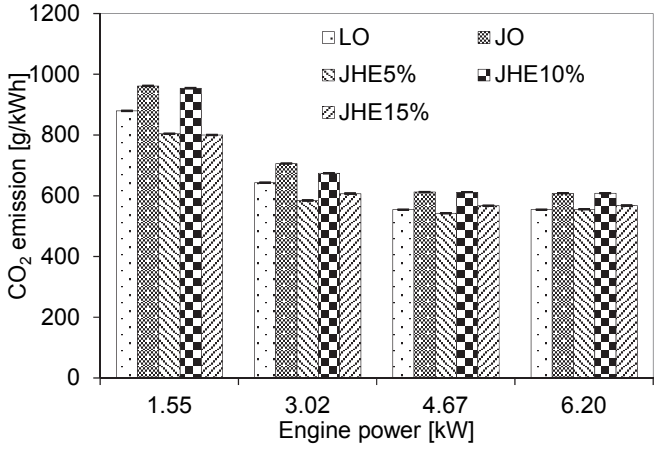

Figure 5-19 CO_2 emission of the engine at different powers and fuels

Fig. 5-19 shows clearly that the emissions of CO_2 decreased with an increase in the engine power. This results from the better combustion condition at higher loads. Moreover, JHE5% and JHE15% reduced emissions of CO_2 when compared to the JO. The JHE5% had a reduction rate of 16.4%, 17.2%, 11.5%, and 8.7% corresponding to the engine power from 3.02 kW to 6.20 kW, respectively, when compared to the JO. For the JHE15%, the reduction rate was 16%, 14%, 7.4%, 6.6%. This can be attributed to enhanced heat release from oxidation of soot in the later combustion stage, thus higher thermal efficiency, and less fuel consumed while lowering CO_2 emissions.

CO emissions, resulting from incomplete combustion, versus engine power are illustrated in Fig. 5-20. When compared to the JO, at low load, due to the inferior combustion condition and the cooling effect, for the JHE10%, the emissions of CO increased 14.5%, while the JHE5%, JHE15% gave a comparable result. At medium loads, temperatures in the cylinder were elevated, so the emulsion fuels were more completely combusted. At 3.02 kW and 4.67 kW, the reduction rate was up to 23.9% and 20.5% for the JHE5%, while the JHE15% reduced 14.9% and 35.6%, respectively. At 6.20 kW, much more fuel had to be injected into the combustion chamber, therefore, the local rich fuel combustion and the cooling effect of the JHE5% caused an increment of 37%. While the JHE10% diluted the fuel to avoid local rich fuel injection resulting in a reduction of CO of 4.6%.

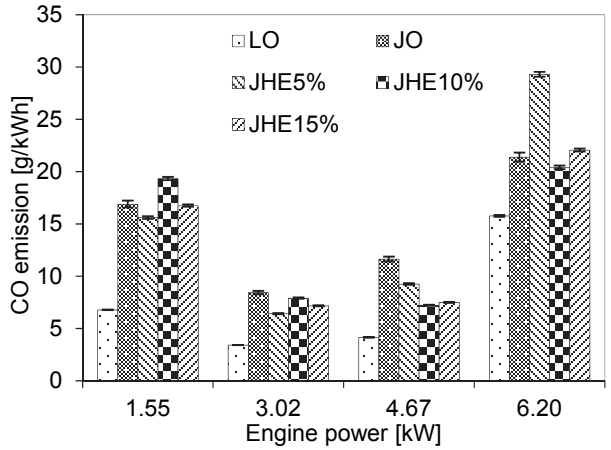

Figure 5-20 CO emission of the engine at different powers and fuels

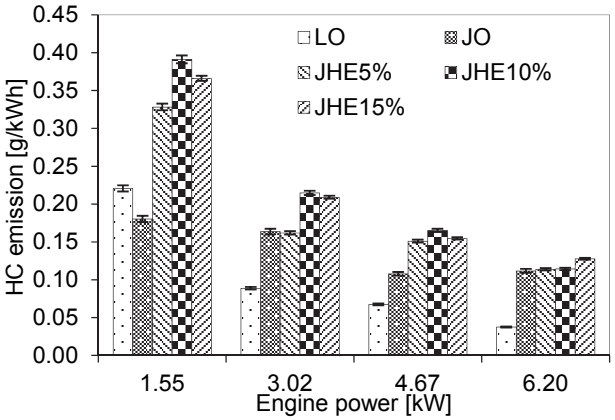

Figure 5-21 HC emission of the engine at different powers and fuels

Fig. 5-21 indicates HC emissions of the engine. The emissions of HC decreased with an increase in the engine power. This is due to the higher combustion temperatures at higher engine loads. The emulsified fuels produced much more HC emissions especially at low loads. At 1.55 kW, HC increased 82%, 116.8%, and 102.9% for the JHE5%, JHE10%, and JHE15%, respectively, when compared relatively to the JO. This may result from the higher density of the emulsified fuels that caused to deep entrancement of the sprays. Moreover, at low loads the cooling effect of the emulsion fuel was dominant due to the low

combustion temperatures. At higher loads, the differences in emissions of HC between the Jatropha oil and the emulsified fuels became smaller due to the better combustion. At 6.20 kW, it is observed that the HC emissions of the JHE5%, JHE10%, and JHE15% had an increment of 1.8%, 2.2%, and 14.3%, respectively, when compared relatively to the JO.

NOx emissions are depicted in Fig. 5-22. NOx emissions of the JHE10% were higher than the Jatropha oil in most cases due to the higher peak heat release rate. When compared relatively to the JO, the JHE10% increased 7%, 4.3% and 7.2% at 1.55 kW, 4.67 kW, and 6.20 kW, respectively. NOx emissions form at high temperatures where the heat release rate may be at the maximum. For the JHE5% and JHE15%, the lower peaks of the heat release rates, and the cooling effect resulted in lower NOx emissions in most cases when compared to the Jatropha oil. The JHE15% had a reduction rate of 3.7%, 16.5%, 0.8% at 1.55 kW, 3.02 kW, and 4.67 kW, respectively, while it had an increase of 4.8% at 6.20 kW. The JHE5% seems to be the best for reduction NOx emissions.

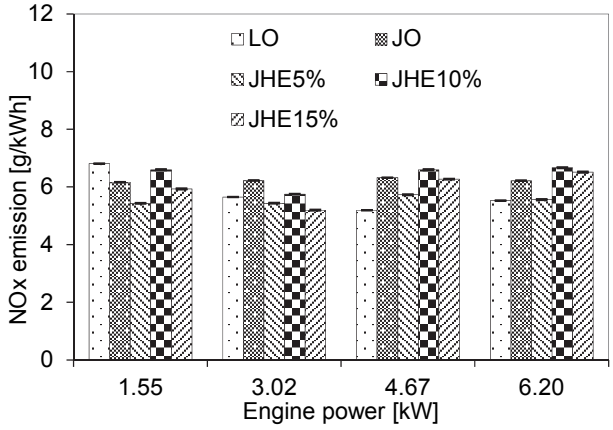

Figure 5-22 NOx emissions of the engine at different powers and fuels

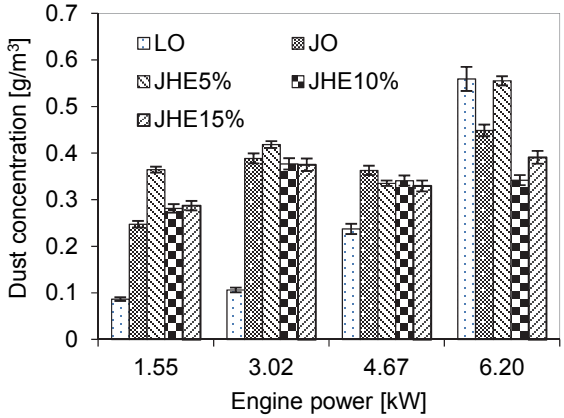

Figure 5-23 Dust concentration of the engine at different powers and fuels

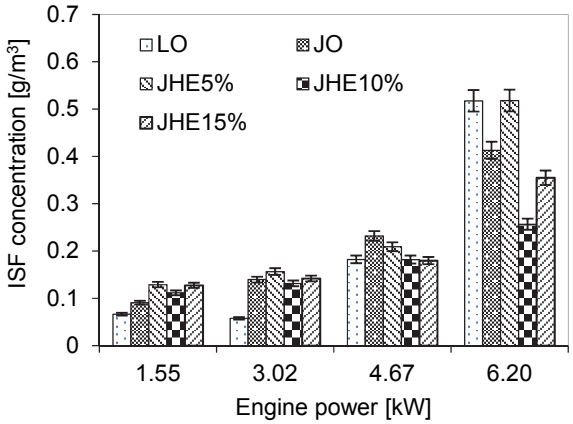

Figure 5-24 ISF concentration of the engine at different powers and fuels

Dust particulate and soot are shown in Fig. 5-23 and Fig. 5-24, respectively. When compared with LO, it is clear that dust increased with an increase of the engine power for most biofuels till medium power of the engine. At the power of 6.20 kW, the reduction of dust concentration was indicated evidently for biofuel, especially for the JHE10%. This results from the cooling effect of the emulsion fuels and the poor combustion characteristics of the biofuel at lower powers. This also increased ISF concentration with an increase of the engine power. Perhaps, at high enough temperature of combustion such as at 6.20 kW,

micro-explosion could happen and aid improving the atomization of fuel, consequently, reduce ISF and dust concentration especially for the JHE10%. Moreover, when combustion temperatures elevated, the combustion of the JHE fuel could result in OH radicals those oxidized soot, thus reduced concentration of ISF and dust. For the JHE5%, dust increased when compared with those of JO due to increase of viscosity, cooling effect, and not enough hydrogen peroxide to enhance oxidation. When compare with JO, it increased dust 47.4, 7.6, and 23.8% at 1.55, 3.02, and 6.20 kW, respectively. While at 1.55 kW, the JHE10% and JHE15% increased 13.7 and 16.2%. When power of the engine increased, higher mixing rate of hydrogen peroxide especially the JHE10% had significantly reduction of dust and ISF. For the JHE10%, the reduction of dust was 3.0, 6.1, and 23.8%, while the reduction ISF was 5.7, 21.6, and 37.8% at 3.02, 4.67, and 6.20 kW. At these range of power, for dust concentration, the JHE15% had a slight reduction of 3.5, 9.2, and 12.9%. While for ISF, it had a reduction of 22.6 and 14% at 4.67, and 6.20 kW.

5. 4 Summary

A direct injection diesel engine operated with neat Jatropha oil, and a Jatropha hydrogen peroxide emulsion with mixing ratios of 5%, 10% and 15% were studied to investigate the effects of the JHE fuel on the combustion, performance, and emissions of the engine. In summary, the main features are as follows.

1- The engine has operated experimentally on the Jatropha hydrogen peroxide emulsion up to the 15% mixing ratio. The combustion of the emulsified fuels shifted to the earlier stage and extended to the later stage. The peak of the heat release rate was reduced with emulsified fuels and there was a large magnitude of oscillation in the heat release rate in the diffusion combustion phase. The heat release rate in the late combustion stage for the emulsified fuels was higher than those of the Jatropha oil and light oil, and the cumulative heat release for the emulsified fuel was also higher.

2- In-cylinder and exhaust gas temperatures were higher especially for the JHE5% and JHE15% as compared to those of the Jatropha and light oil. The JHE15% improved brake thermal efficiency of the engine in most cases as compared to other emulsion fuels and Jatropha oil.

3- The JHE5% and JHE15% reduced CO_2 and NOx emissions, while, they also reduced CO emissions at low and medium loads. The emulsion fuels increased HC emissions. At medium and high power conditions, dust and ISF concentration were significantly reduced by the emulsion fuel, especially for the JHE10% and JHE15%. Overall, this study found that the optimum mixing ratio of hydrogen peroxide to improve combustion, performance and emissions in diesel engine was 15%.

Chapter 6 Conclusions

Jatropha oil was identified as a leading candidate for an alternative fuel for commercialization among various non-edible vegetable oil. However, it was reported that the combustion of Jatropha oil in diesel engine produced higher particulate, CO, and HC. Moreover, some operational problems such as injector coking, severe engine deposits, gum formation, and oil thickening were reported in long term test. This is attributed to its high viscosity, poor volatility, large molecular weight and bulky molecular structure. Therefore, the combustion of Jatropha should be studied to improve the combustion and emissions of Jatropha based fueled diesel engine.

In this study, I made research work on the diesel engines fueled with Jatropha with double injection, Jatropha water emulsion with double injection, and Jatropha hydrogen peroxide emulsion. The experiments were conducted on high-speed, four-stroke, direct injection diesel engines. The two first series of experiments were conducted on a common rail fuel system diesel engine modified from a mechanical one. The later experiments used a mechanical fuel system diesel engine. The modified common rail diesel engine, however, remains mechanical injector that injects fuel into the combustion chamber. In the common rail system diesel engine, injection parameters such as injection timing, injection duration, therefore, were controlled indirectly through the electronic control unit of the system.

- **Chapter 1 and 2**, I outlined the information for research background such as literature reviews, research infrastructures, and theoretical considerations.
- **In chapter 3**, I presented the combustion, performance and emissions characteristics of diesel engine fueled with neat Jatropha oil with double injections. The results are summarized as follow.

1- Effect of double injection timings

Retarded double timings significantly reduced the peaks of combustion pressure, peaks of HRR, and shifted the combustion to the later phase. Late double timings increased HRR at the later combustion stage.

There was slight reduction of ID for retarded double timings at low load; ID increased slightly at 6.0 kW due to imperfect gas exchange. Optimum double injection timings for BTE were between m-11,a+1.5 and m-13,a-0.5.

Emissions of CO_2, CO, HC, Smoke and dust were lower at timings between m-11,a+1.5 and m-13,a-0.5. Late double timings significantly reduced emissions of NOx.

Overall, the optimum injection timings for combustion, performance, and emissions were between m-11,a+1.5 and m-13,a-0.5.

2- Effect of amount of after-injection

Timing of m-11,a+1.5 was tested with small and large amounts of after-injection. We found a considerably influence to the combustion, performance and emissions.

Peaks of cylinder pressure and HRR were remarkably reduced with m-11,a+1.5-L at 3.0 and 4.5 kW. Otherwise, they were comparable at 6.0 kW with a minor reduction of peak HRR with m-11,a+1.5-L.

When compared with m-11,a+1.5-S, the injection pattern of m-11,a+1.5-L reduced BTE especially at higher engine loads.

For m-11,a+1.5-S, reduction of emissions of CO_2, CO, smoke and dust concentration was observed, while it increased emissions of NOx, and HC.

- **In chapter 4**, I used the Jatropha water emulsion fuel and double injections to investigate the combustion, performance, and emissions characteristics of diesel engine. Jatropha water emulsion was created by mixing 10% of water with Jatropha. The engine was fed with LO, and JO with single injection at the injection timing set by the engine Maker of -17 deg. CA. ATDC for baseline data. To investigate the effect of injection pattern and the JWE, the first injection was kept at -23 deg. CA ATDC and the second injection was set at 0, +3, +6 deg. ATDC for double injection mode. The main results of chapter 4 are summarized as follows:

1- Large amount of fuel in the second injection in injection patterns such as JWE-23/0 and JWE-23/+3-large dramatically reduced the peaks of in-cylinder pressure; suddenly reduced the peak of HRR; and increased significantly the ignition delay, combustion duration, and shifted the combustion center toward the later stage. For small amount of fuel in the second injection such as JWE-

23/+3-small and JWE-23/+6, the peaks of the in-cylinder pressures were higher, while, other parameters had the same tendency with lower intensity when compared with those of the LO.

2- Large amount of fuel in the second injection dramatically reduced the in-cylinder temperatures, increased the exhaust gas temperatures, and lowered the BTE in comparison with those of the JO. The opposite occurred when small second injection amount was used as in JWE-23/+3-small and JWE-23/+6. I also found that when using the JWE-23/+3-small the BTE was higher than that of the JO.

3- The emulsion fuel and double injection increased CO_2, CO, and HC emissions when compared with those of the LO. However, in comparison with those of the JO, the large second injection quantity such as the JWE-23/+3-large reduced the HC emissions. NOx emissions were related to the combustion characteristics of the engine with different injection patterns. The emulsion fuel, and double injection patterns reduced NOx emissions when compared with those of the LO. Large second injection amount such as the JWE-23/0 and JWE-23/+3-large significantly reduced the NOx emissions.

4- In three timing tests, the JWE-26/+3 reduced smoke opacity when using JWE and double injection. The ISF was the main element, while the SOF was a minor element of the dust. Large second injection amount increased the ISF and dust concentration much more than a small second injection amount.

- **In chapter 5**, combustion, performance, and emisions of a direct injection diesel engine fueled with Jatropha hydrogen peroxide emulsion was investigated. Hydrogen peroxide in a solution of water at a concentration of 30% was used for making the emulsions. Mixtures of Jatropha oil with solutions of hydrogen peroxide were created according to the Jatropha oil mass with mixing ratios of 5%, 10% and 15% (hereafter so-called JHE5%, JHE10%, and JHE15%). The experimental results are featured following:

1- The engine has operated experimentally on the Jatropha hydrogen peroxide emulsion up to the 15% mixing ratio. The combustion of the emulsified fuels shifted to the earlier stage and extended to the later stage. The peak of the heat release rate was reduced with emulsified fuels and there was a large magnitude of oscillation in the heat release rate in the diffusion combustion phase. The heat release rate in the late combustion stage for the emulsified fuels was higher than those of the Jatropha oil and light oil, and the cumulative heat release for the emulsified fuel was also higher.

2- In-cylinder and exhaust gas temperatures were higher especially for the JHE5% and JHE15% as compared to those of the Jatropha and light oil. The JHE15% improved brake thermal efficiency of the engine in most cases as compared to other emulsion fuels and Jatropha oil.

3- The JHE5% and JHE15% reduced CO_2 and NOx emissions, while, they also reduced CO emissions at low and medium loads. The emulsion fuels

increased HC emissions. At medium and high power conditions, dust and ISF concentration were significantly reduced by the emulsion fuel, especially for the JHE10% and JHE15%. Overall, this study found that the optimum mixing ratio of hydrogen peroxide to improve combustion, performance and emissions in diesel engine was 15%.

Recommendation

Double injection and emulsion of Jatropha with water can be employed to reduce the emission of NOx significantly. Unfortunately, too late double injection timings or so much after-injection or second injection increase the emissions of CO, HC, smoke and dust. To reduce negative effects of water emulsion fuel and double injections, the timing and second injection amount should be carefully selected. Moreover, opening injection pressure (for mechanical injector) and rail pressure (common rail injection system) should be elevated to reduce emissions of HC, CO, smoke and dust concentration.

Hydrogen peroxide can improve brake thermal efficiency, reduce NOx emission, and reduce dust and insoluble organic fraction especially at higher engine power, but it increase HC emission. JHE15% was found to be optimum for better combustion, performance, and emissions of diesel engine. Due to the oxidation of hydrogen peroxide, the fuel system elements should be made of stainless steel, and the emulsion should be made short time before using.

List of publications

[Journal Papers (peer reviewed)]

1. Kim-Bao Nguyen, Tomohisa Dan, Ichiro Asano
"Effect of Injection Pattern on Neat Jatropha Oil Combustion in Direct Injection Diesel Engine"
JIME, Journal of the Japan Institute of Marine Engineering, (2015),
(accepted for publication)

2. Kim-Bao Nguyen, Tomohisa Dan, Ichiro Asano
"Effect of Double Injection on Combustion, Performance and Emissions of Jatropha Water Emulsion Fueled Direct-injection Diesel Engine"
Elsevier, Energy, Vol.80, pp.746-755, DOI 10.1016/j.energy.2014.12.033,
(2015-2)

3. Kim-Bao Nguyen, Tomohisa Dan, Ichiro Asano
"Combustion, Performance and Emission Characteristics of Direct Injection Diesel Engine Fueled by Jatropha Hydrogen Peroxide Emulsion"
Elsevier, Energy, Vol.74, pp.301-308, DOI 10.1016/j.energy.2014.03.120,
(2014-9)

[Proceedings Papers]

1. Nguyen Kim-Bao, Shota Tanaka, Tomohisa Dan, Ichiro Asano, Masataka Hashimoto
"Investigation of Jatropha Oil Fueled Diesel Engine with Split Injection"
PAAMES, 5th Pan Asian Association of Maritime Engineering Societies,
Advanced Maritime Engineering Conference 2012 (Taipei), GT_05, pp.1-5,
(2012-12)

2. Masataka Oue, Kim-Bao Nguyen, Tomohisa Dan, Ichiro Asano, Masataka Hashimoto

"Combustion Analysis of Jatropha Emulsified Fuel in Diese Engine –Case of Single Injection in Direct Injection Engine"
JIME, 82th Marine Engineering Conference Proceedings, pp.57-58, (2012-9), (in Japanese)

References

[1] United Nations Statistics Division,

http://unstats.un.org/unsd/environment/air_greenhouse_emissions.htm, (cited on Jan. 9, 2015).

[2] United States Environmental Protection Agency,

http://www.epa.gov/climatechange/ghgemissions/global.html, (cited on Jan. 9, 2015).

[3] United States Environmental Protection Agency,

http://www.epa.gov/climatechange/science/causes.html, (cited on Jan. 9, 2015).

[4] United States Environmental Protection Agency,

http://www.epa.gov/climatechange/ghgemissions/gases/co2.html, (cited on Jan. 9, 2015).

[5] United States Environmental Protection Agency,

http://www.epa.gov/climatechange/ghgemissions/gases/ch4.html, (cited on Jan. 9, 2015).

[6] United States Environmental Protection Agency,

http://www.epa.gov/climatechange/ghgemissions/gases/n2o.html, (cited on Jan. 9, 2015).

[7] Natural Resources Defense Council,

http://www.nrdc.org/globalwarming/fcons/fcons1.asp, (cited on Jan. 9, 2015).

[8] Natural Resources Defense Council,

http://www.nrdc.org/globalwarming/fcons/fcons2.asp, (cited on Jan. 9, 2015).

[9] Natural Resources Defense Council,

http://www.nrdc.org/globalwarming/fcons/fcons3.asp, (cited on Jan. 9, 2015).

[10] Natural Resources Defense Council,

http://www.nrdc.org/globalwarming/fcons/fcons4.asp, (cited on Jan. 9, 2015).

[11] United States Environmental Protection Agency,

http://www.epa.gov/climatechange/basics/, (cited on Jan. 9, 2015).

[12] NASA, http://climate.nasa.gov/effects/, (cited on Jan. 9, 2015).

[13] United States Environmental Protection Agency,

http://www.epa.gov/airquality/urbanair/, (cited on Jan. 9, 2015).

[14] United States Environmental Protection Agency,

http://www.epa.gov/airquality/ozonepollution/health.html, (cited on Jan. 9, 2015).

[15] United States Environmental Protection Agency,

http://www.epa.gov/airquality/ozonepollution/basic.html, (cited on Jan. 9, 2015).

[16] United States Environmental Protection Agency,

http://www.epa.gov/airquality/particlepollution/index.html, (cited on Jan. 9, 2015).

[17] United States Environmental Protection Agency,

http://www.epa.gov/airquality/particlepollution/health.html, (cited on Jan. 9, 2015).

[18] United States Environmental Protection Agency,

http://www.epa.gov/airquality/carbonmonoxide/, (cited on Jan. 9, 2015).

[19] United States Environmental Protection Agency

http://www.epa.gov/airquality/carbonmonoxide/health.html, (cited on Jan. 9, 2015).

[20] R. Delmas, D. Serca & C. Jambert, Global inventory of NOx sources, Nutrient Cycling in Agroecosystems 48, pp. 51–60, 1997.

[21] United States Environmental Protection Agency,

http://www.epa.gov/airquality/nitrogenoxides/health.html, (cited on Jan. 9, 2015).

[22] United States Environmental Protection Agency,

http://www.epa.gov/airquality/sulfurdioxide/, (cited on Jan. 9, 2015).

[23] United States Environmental Protection Agency,

http://www.epa.gov/airquality/sulfurdioxide/health.html, (cited on Jan. 9, 2015).

[24] United States Environmental Protection Agency,

http://www.epa.gov/airquality/lead/, (cited on Jan. 9, 2015).

[25] United States Environmental Protection Agency,

http://www.epa.gov/airquality/lead/health.html, (cited on Jan. 9, 2015).

[26] U.S. Energy Information Administration,

http://www.eia.gov/cfapps/ipdbproject/IEDIndex3.cfm?tid=5&pid=53&aid=1, (cited on Jan. 9, 2015).

[27] Canada National Energy Board,

https://www.neb-one.gc.ca/nrg/ntgrtd/mrkt/archive/2011cndnnrgprcngtrndfct/cndnnrgprcngtrndfct-eng.html, (cited on Jan. 9, 2015).

[28] InvestmentMine,

http://www.infomine.com/investment/metal-prices/crude-oil/all/, (cited on Jan. 9, 2015).

[29] Willard W. Pulkrabek, Engineering fundamentals of the internal combustion engine (second edition), Pearson Education International, 2004.

[30] Richard Brittaine and NeBambi Lutaladio, Jatropha: A Smallholder Bioenergy Crop-The Potential for Pro-Poor Development, Integrated Crop Management Vol. 8, 2010.

[31] S.-Y. No. Inedible vegetable oils and their derivatives for alternative diesel fuels in CI engines: A review. Renewable and Sustainable Energy Reviews 2011, Volume 15, Issue 1, p. 131-149.

[32] K. Pramanik. Properties and use of jatropha curcas oil and diesel fuel blends in compression ignition engine. Renewable Energy 2003, Volume 28, Issue 2, p. 239-248.

[33] M. Senthil Kumar, A. Ramesh, B. Nagalingam. An experimental comparison of methods to use methanol and Jatropha oil in a compression ignition engine. Biomass and Bioenergy 2003, Volume 25, p. 309-318.

[34] D. Agarwal, A. K. Agarwal. Performance and emissions characteristics of Jatropha oil (preheated and blends) in a direct injection compression ignition engine. Applied Thermal Engineering 2007, Volume 27, Issue 13, p. 2314-2323.

[35] B. S. Chauhan, N. Kumar, Y. D. Jun, K. B. Lee. Performance and emission study of preheated Jatropha oil on medium capacity diesel engine. Energy 2010, Volume 35, Issue 6, p. 2484-2492.

[36] L. D. K. Nguyen, N. W. Sung, S. S. Lee, and H. S. Kim. Effect of split injection, oxygen enriched air and heavy EGR on soot emissions in a diesel engine. International Journal of Automotive Technology 2011, Volume 12, p. 339-350.

[37] M. Y. Kim, S. H. Yoon, and C. S. Lee. Impact of split injection strategy on the exhaust emissions and soot particulates from a compression ignition engine fueled with neat biodiesel. Energy & Fuel 2008, Volume 22, p. 1260-1265.

[38] R. Mobasheri, Z. Peng, S. M. Mirsalim. Analysis the effect of advanced injection strategies on engine performance and pollutant emissions in a heavy duty DI-diesel engine by CFD modeling. International Journal of Heat and Fluid Flow 2012, Volume 33, p. 59-69.

[39] D. Qi , M. Leick, Y. Liu, C. F. Lee. Effect of EGR and injection timing on combustion and emission characteristics of split injection strategy DI-diesel engine fueled with biodiesel. Fuel 2011, Volume 90, p.1884-1891.

[40] S. H. Park, S. H. Yoon, C. S. Lee. Effect of multiple-injection strategies of overall spray behavior, combustion and emissions reduction characteristics of biodiesel fuel. Applied Energy 2011, Volume 88, p. 88-98.

[41] C.Y. Choi, R.D. Reitz. An experimental study on the effects of oxygenated fuel blends and multiple injection strategies on DI diesel engine emissions. Fuel 1999, Volume 78, p.1303-1317.

[42] K. Yehliu, A. L. Boehman, O. Armas. Emissions from different alternative diesel fuels operating with single and split fuel injection. Fuel 2010, Volume 89, p. 423-437.

[43] R. J. Crookes, F. Kiannejad, and M. A. A. Nazha. Systematic assessment of combustion characteristics of biofuel and emulsions with water for use and diesel engine fuels. Energy Conversion and Management 1997, Volume. 38, p. 1785-1795.

[44] O. Armas, R. Ballesteros, F. J. Martos, J. R. Agudelo. Characterization of light duty diesel engine pollutant emissions using water -emulsified fuel. Fuel 84 (2005), p. 1011-1018.

[45] J. Ghojel, D. Honnery, K. Al-Khaleefi. Performance, emissions and heat release characteristics of direct injection diesel engine operating on diesel oil emulsion. Applied thermal engineering 2006, Volume 26, p. 2132-2141.

[46] R. Ochoterena, A. Lif, M. Nyden, S. Andersson, I. Denbratt. Optical studies of spray development and combustion of water-in-diesel emulsion and microemulsion fuels. Fuel 2010, Volume 89, p. 122-132.

[47] A. Maiboom, X. Tauzia. NOx and PM emissions reduction on an automotive HSDI diesel engine with water-in-diesel emulsion and EGR: An experimental study. Fuel 2011, Volume 90, p. 3179-3192.

[48] B. Fanz, P. Roth. Injection of a H_2O_2/water solution into the combustion chamber of a direct injection diesel engine and its effect on soot removal. Proceedings of the Combustion Institute 2000, Volume 28, Issue 1, p. 1219-1225.

[49] C. Born and N. Peters,. Reduction of soot emission at a DI diesel engine by additional injection of hydrogen peroxide during combustion. SAE Technical Paper 982676, 1998.

[50] K. S. Nagaprasad, D. Madhu. Effect of injecting hydrogen peroxide into diesel engine. International Journal of Engineering Sciences & Emerging Technologies 2012, Volume 2, Issue 1, p. 24-8.

[51] D. S-K. Ting, G. T. Reader. Hydrogen peroxide for improving premixed methane-air combustion. Energy 2005, Volume 30, Issues 2-4, p. 313-322.

[52] G. B. Chen, H. Li, T. S. Cheng, H. W. Hsu, Y. C. Chao. Effects of hydrogen peroxide on combustion enhancement of premixed methane/air flames. International Journal of Hydrogen Energy 2011, Volume 36, Issue 23, p. 15414-15426.

[53] M. C. Mulenga, D. S-K. Ting, G. T. Reader, and M. Zheng. The potential for reducing CO and NOx emissions from an HCCI engine using H_2O_2 addition. SAE Technical Paper 2003-01-3204.

[54] John B. Heywood. Internal Combustion Engine Fundamentals. Mc Graw-Hill 1988.

[55] M. F. J. Brunt, K. C. Platts. Calculation of heat release in direct injection diesel engines. SAE Technical Paper 1999-01-0187.

[56] A. K. Agarwal and L. M. Das. Biodiesel development and characterization for use as a fuel in compression ignition engines. J. Eng. Gas Turbines Power 2000, 123(2), p. 440-447.

[57] R. Altın, S. Çetinkaya and H. S. Yücesu. The potential of using vegetable oil fuels as fuel for diesel engines. Energy Conversion and Management 2001, Volume 42, Issue 5, p. 529–538.

[58] A. K. Agarwal, J. Bijwe and L. M. Das. Effect of biodiesel utilization of wear of vital parts in compression ignition engine. J. Eng. Gas Turbines Power 2003, 125(2), p. 604-611.

[59] Hemmerlein, N., Korte, V., Richter, H., and Schröder, G.. Performance, exhaust emissions and durability of modern diesel engines running on rapeseed oil. SAE Technical Paper 910848, 1991.

[60] C W Yu, S Bari, A Ameen. A comparison of combustion characteristics of waste cooking oil with diesel as fuel in a direct injection diesel engine. Proceedings of the Institution of Mechanical Engineers, Part D: Journal of Automobile Engineering 2002, Vol. 216, no. 3, p. 237-243.

[61] O.D. Hebbal , K.Vijayakumar Reddy, K. Rajagopal. Performance characteristics of a diesel engine with deccan hemp oil, Fuel 2006, Volume 85, Issues 14-15, p. 2187-94.

[62] A. S. Huzayyin, A.H. Bawady, M.A. Rady, A. Dawood. Experimental evaluation of diesel engine performance and emission using blends of jojoba oil and diesel fuel. Energy Conversion and Management 2004, Volume 45, Issues 13-14, p. 2093-2112.

[63] F. Lujaji, A. Bereczky, L. Janosi, Cs. Novak, M. Mbarawa. Cetane number and thermal properties of vegetable oil, biodiesel, 1-butanol and diesel blends. Journal of Thermal Analysis and Calorimetry 2010, Volume 102, no. 3, p. 1175-1181.

[64] J. N. Reddy, A. Ramesh. Parametric studies for improving the performance of a Jatropha oil-fuelled compression ignition engine. Renewable Energy 2006, Volume 31, Issue 12, p. 1994-2016.

[65] A. S. Ramadhas, S. Jayaraj, C. Muraleedharan. Use of vegetable oils as I.C. engine fuels-A review. Renewable Energy 2004, Volume 29, Issue 5, p. 727-742.

[66] B. S. Chauhan, N. Kumar, H. M. Cho. A study on the performance and emission of a diesel engine fueled with Jatropha biodiesel oil and its blends. Energy 2012, p. 616-622.

[67] M. Mofijur, H.H. Masjuki, M.A. Kalam, A.E. Atabani. Evaluation of biodiesel blending, engine performance and emissions characteristics of Jatropha curcas methyl ester: Malaysian perspective. Energy 2013, p. 879-887.

[68] T. Ganapathy, R. P. Gakkhar, K. Murugesan. Influence of injection timing on performance, combustion and emission characteristics of Jatropha biodiesel engine. Applied Energy 2011, Volume 88, p.4376~4386.

[69] C. Sayin, M. Gumus. Impact of compression ratio and injection parameters on the performance and emissions of a DI diesel engine fueled with biodiesel-

blended diesel fuel. Applied Thermal Engineering 2011, Volume 31, p.3182~3188.

[70] Y. Zhang and A. L. Boehman. Impact of biodiesel on NOx emissions in a common rail direct injection diesel engine. Energy & Fuels 2007, Volume 21, p.2003~2012.

[71] H.Z. Sheng, et al. The droplet group microexplosions in water-in-oil emulsion sprays and their effects on diesel engine combustion, Symposium (International) on Combustion 1994, Volume 25, Issue 1, p. 175-181.

[72] M. Nadeem et al. Diesel engine performance and emission evaluation using emulsified fuels stabilized by conventional and gemini surfactants. Fuel 2006, Volume 85, Issues 14-15, p. 2111-2119.

[73] A. Lif, K. Holmberg. Water-in-diesel emulsions and related systems. Advances in Colloid and Interface Science 2006, Volumes 123-126, 16, p. 231-239.